UNDERSTANDING THE ADAPTIVE ABILITY OF CORALS TO CHANGING ENVIRONMENTS

A DISSERTATION SUBMITTED TO THE GRADUATE DIVISION OF THE UNIVERSITY OF HAWAIʻI AT MĀNOA IN PARTIAL FULFILLMENT OF THE REQUIREMENTS FOR THE DEGREE OF

DOCTOR OF PHILOSOPHY

IN

MARINE BIOLOGY

MAY 2017

By

Kaho Hoshino Tisthammer

Dissertation Committee:

Robert Richmond, Chairperson

Cynthia Hunter

Peter Marko

Thomas Oliver

Robert Thomson

Keywords: *Porites lobata*, coral, population genetics, local adaptation, biomarkers, morphometrics

ACKNOWLEDGMENTS

My Advisor: Dr. Robert H. Richmond

My Committee: Dr. Cindy Hunter, Dr. Peter Marko, Dr. Thomas Oliver, Dr. Robert Thomson

Collaborators: Dr. Zac H. Forsman, Dr. Francois Seneca

Colleagues in the Richmond Lab:

Victoria Sindorf, Narrissa Spies, James Murphy, Austin Shelton, Jon Martinez, Luc Rougée, Lauren Wetzell, Sofia de la Sota, Sean Macduff, Aleka Lyman, Alia Irvine, Verena Hölzer, Alex Barkman, Laura Damiani, Keana Richmond

Funding:

Hawaii Department of Health, Marine Biology Graduate Program of the University of Hawaii at Manoa, Edmondson Research Fund, NOAA, NFWF

Special Thanks To:

Fenix Grange, Dr. Robert Toonen, Dr. Anthony Amend, Dr. Mahdi Belcaid, Dr. Brook Nunn

My Family:

My partner Michael Stiber, My daughter Ariel Tisthammer, My parents Hiroko and Satoshi Hoshino

ABSTRACT

Reduced water quality is a major local threat to coral reefs worldwide, and has caused severe declines in the health of coral reefs in Hawaii, especially the nearshore areas. The corals living in Maunalua Bay, Oahu are under continual stresses from sedimentation and toxicant laden runoff as a result of large-scale urbanization that has taken place in the last century. Despite prolonged exposure to these environmental stressors, some corals are able to thrive, suggesting selection (adaptation). My dissertation research investigated whether corals in the nearshore areas have genetically adapted to their reduced water quality environment. The first chapter analyzed the population genetic structure of *P. lobata*, which revealed clear genetic differentiation between the nearshore and offshore *P. lobata* populations in Maunalua Bay, as well as two reefs in West Maui. My second chapter investigated the phenotypic differences between the nearshore and offshore *P. lobata* genotypes, found in the first chapter, to determine if the observed genetic differentiation was formed by selection. The reciprocal transplant and common garden experimental results showed clear physiological and molecular response differences between the two genotypes, highlighting the stress resilient traits of the nearshore genotype and inherent differences in the metabolic state between the genotypes. The results from the first and second chapters, however, suggest this local adaptation might happen at the cost of genetic diversity.

The *Porites* corals are a notoriously difficult genus to identify correctly, due to their highly variable skeletal architecture and unresolved phylogeny. In order to assess the intraspecific morphological and genetic variations in *P. lobata*, morphometrics and genomic (RAD-seq) analyses were conducted in my third chapter. The morphometric data revealed significant groupings of skeletal characters between the geographic locations, and population genomic analysis also supported the strong geographical signature. There was a significant correlation between the morphological and the genetic distances, suggesting the genetic basis for the skeletal morphology of *P. lobata*.

Understanding the genetic basis of coral survival offers a critical insight into their adaptive ability, which is indispensable for protecting the essential reef-building corals from impending environmental and climate change.

TABLE OF CONTENTS

LIST OF TABLES

CHAPTER 1

CHAPTER 2

CHAPTER 3

LIST OF FIGURES

CHAPTER 1

CHAPTER 2

CHAPTER 3

LIST OF ABBREVIATIONS AND SYMBOLS

ADP	adenosine diphosphate
AMOVA	analysis of molecular variance
ANOVA	analysis of variance
ATP	adenosine triphosphate
BCA	bicinchoninic acid
bp	base pair
CaM	calmodulin
CDA	canonical discriminant analysis
CYP1A	cytochrome P450, family 1, member A1
DMSO	dimethyl sulfoxide
H2O2	hydrogen peroxide
HPR	horseradish peroxidase
HSD	honest significance difference
Hsp	heat shock protein
IBA	isolation by adaptation
IBC	isolation by colonization
IBD	isolation by distance
IFO	intermediate fuel oil
IgG	immunoglobulin G
kDa	kilo daltons
KML	Kewalo Marine Laboratory
LC-MS/MS	liquid chromatography tandem mass spectrometry
MANOVA	multivariate analysis of variance
MXR	multixenobiotic resistance protein
NTU	nephelometric Turbidity Units
PBST	phosphate buffered saline with Tween 20
PCA	principal component analysis
PCB	polychlorinated biphenyl

PCO	principal coordinate analysis
PCR	polymerase chain reaction
PGK	phosphoglycerate kinase
PPDF	photosynthetic photon flux density
PVDF	polyvinylidene difluoride
qPCR	quantitative PCR
RAD-seq	restriction site associated DNA sequencing
SDS-PAGE	sodium dodecyl sulfate - polyacrylamide gel electrophoresis
SOD	superoxide dismutase
w	weight

INTRODUCTION

Coral reefs are among the most biologically productive and diverse ecosystems in the world (Hoegh-Guldberg 2014; Birkeland 2015). They sustain the lives of millions of people through their economic, cultural, physical, biological, recreational and ecological services (Aswani *et al.* 2015). For example, coral reefs in Hawaii have been assessed a value of $9.7 billon, contributing $363.5 million in annual revenue to Hawaii's economy (Cesar & Van Beukering 2004). Another survey conducted by the National Oceanic and Atmospheric Administration shows that the Hawaiian coral reefs are valued at up to $33.6 billion (NOAA 2011). Coral reefs are also an integral part of Hawaiian culture; the people regard coral polyps as the first life to be created, as well as the origin of all life, according to 'Kumulipo,' the Hawaiian Hymn of Creation (Johnson, 1981). The Hawaiian culture grew intimately along with the coral reefs, both spiritually and practically. Corals in Hawaiian culture represent a multitude of resources, such as polishing device, building materials, cooking tools, poison for spear tips, and even the body form of a Hawaiian deity (Bennet *et al.* 2010; Gregg *et al.* 2015).

Despite their considerable values and functions, coral reefs worldwide have been severely impacted from anthropogenic activities (Wilkinson 2004; Hughes *et al.* 2010; Richmond & Wolanski 2011; Graham 2014). Studies have identified numerous global, as well as local stressors on coral reefs, yet the knowledge gap is still quite large between what we know about coral biology, and what is necessary for the effective conservation of these reefs. Much more information is needed on the basic functions of coral, their physiology and their biology in order to accurately predict their responses to impending climate and environmental changes, to develop strategies that mitigate future losses, and to reverse the current trends of deterioration (Aswani *et al.* 2015; Voolstra *et al.* 2015). For example, the genetic diversity within a location can provide adaptive capacity for a local stressor, which will help estimate how a coral population will respond to upcoming changes and/or restoration efforts. Currently, however, sparse information exists on the degree of genetic diversity within local populations to help estimate such capacity (Voolstra *et al.* 2015). My ultimate goal as a coral biologist is for my research to aid in coral reef conservation by contributing to filling these knowledge gaps. Building on this motivation, in my dissertation I investigated the genetic basis of the adaptive ability of corals to their changing environment.

The first two chapters of my dissertation focus on understanding local adaptation of corals at a small geographic scale in an ecological time scale. I use the lobe coral, *Porites lobata*, as a study species, since they are one of the most dominant scleractinian corals in Hawaii, where my dissertation research took place, and their robustness allows them to often thrive in marginal environments. Our nearshore marine environments are increasingly being exposed to a variety anthropogenic stressors, such as sedimentation, eutrophication, pollution, and overfishing. The central question for my research was to understand how some corals survive in such areas with high human influences.

In the first chapter, I analyze the small-scale population genetic structure of *Porites lobata* as a first step to understand the genetic basis for coral survival. Previously, population genetics of *P. lobata* was studied at a much larger scale. Baums *et al.* (2012) investigated the *P. lobata* genetic structure across the central Pacific using microsatellite markers, and Polato *et al*. (2010) assessed the genetic structure of *P. lobata* across the Hawaiian archipelago also using microsatellite markers. While the microsatellite markers used in these studies served well to understand the phylogeography of *P. lobata*, their results suggested that these markers would not provide a high enough resolution to understand small-scale genetic structure. Barshis *et al.* (2010) used nuclear and mitochondrial DNA markers to study genetic structure of *P. lobata* in Ofu Island, American Samoa. The genetic markers they used (ITS: internal transcribed spacer, CR: mitochondrial control region, and NAD5: mitochondrial NADH dehydrogenase subunit 5) showed genetic differentiation of *P. lobata* populations approximately five kilometers apart. Since the *P. lobata* populations I studied were located within a few hundred meters to a couple of kilometers of each other, I started my analysis with the DNA markers from Barshis *et al*. (2010). The ITS marker was successful in assessing the small scale genetic structure, but sequences of the mitochondrial markers (CR, NAD5) showed almost no variability among populations. I, therefore, developed new genetic markers to assess the small-scale population genetic structure of *P. lobata*. Out of the five sets of markers tested, the histone marker that spans from the H2A to the H4 region (H2) turned out to be a useful marker. The genetic structure of *P. lobata* from my primary study site off the island of Oahu, as well as two reefs off the island of Maui, were analyzed using H2. Since then, the H2 marker has been shared with coral researchers worldwide, and is producing promising results in understanding fine-scale genetic structure and evolutionary relationships of *Porites* corals. In Chapter 1, I was able to demonstrate that *P. lobata* in the

nearshore areas were genetically distinct from the offshore individuals. That such proximal populations were genetically differentiated without geographic barriers suggests the genetic structure was likely formed by isolation by adaptation (Orsini *et al.* 2013). Interestingly, the nearshore populations from Maui and Oahu were genetically closer to each other than to their respective offshore populations, suggesting the operation of independent, yet similar selective forces at both locations.

Based on the results from the first chapter, I tested the isolation by adaptation hypothesis (whether the genetic differentiation observed on Oahu was caused by selection) in the second chapter. Reciprocal transplant and common garden experiments were used to assess the differences in phenotypes between the 'nearshore' and the 'offshore' genotype corals. In these experiments, I analyzed molecular and physiological stress responses in order to capture sublethal effects. Cellular molecular biomarkers, assessed using biomedical research tools, have recently been proven effective in understanding the stress levels in corals (Downs *et al.* 2005; Richmond & Wolanski 2011; Downs *et al.* 2012). Traditional coral reef assessments have largely used mortality as an indicator, such as coral cover reductions and loss of individuals or species. Since mortality is not an adequate metric of health or stress level, molecular biomarkers, such as changes in protein expressions, enzymatic activity levels and gene expression levels, as well as DNA damage, have been successfully applied to measure coral stress responses (e.g. Downs *et al.* 2005; Seneca *et al.* 2009; Rougée 2011; Richmond 2011; Kenkel *et al.* 2011; Edge *et al.* 2013; Seveso *et al.* 2013; Seneca & Palumbi 2015; Murphy & Richmond 2016). Since proteins directly affect organismal physiology and hence represent the functional adaptations (Feder & Walser 2005; Tomanek 2011), I used protein biomarkers for assessing the response differences between the nearshore and offshore genotypes, in addition to physiological measurements. The field of coral molecular biomarker (ecotoxicology) is, however, still at an early stage (Tisthammer 2016), and no coral-specific antibodies are available commercially to analyze their protein expressions. Previous studies suggest many key biomarker proteins may be highly conserved across metazoans (e.g. Barshis *et al.* 2010; Seveso *et al.* 2016). Therefore, in search for usable antibodies, coral (*P. lobata*) protein sequences, translated from the transcriptomes (unpublished data, F. Seneca), were aligned with the sequences of commercially available antibodies (mostly made from vertebrates). Then potentially compatible antibodies were selected

and tested with coral protein extractions. Through this process, I was able to successfully use eight protein biomarkers for my dissertation research to show protein response differences between the two genotypes.

The trend, however, is now shifting to the '-omics' era, and we are currently exploring coral proteomics to more efficiently capture stress responses in corals. Coral samples, including those from the reciprocal transplant experiment in my dissertation, have been analyzed using ultra-sensitive liquid chromatography tandem mass-spectrometry (LC-MS/MS). Well over 1,000 proteins were identified from each sample, which further validated clear response differences between the two genotypes from the transplant experiment. Advantages of using the proteomic approach are paramount. The more traditional protein assays, such as the western blot, may still serve useful in screening initial response time, and in identifying response patterns and dosages, since little information is often available to accurately predict organismal response direction and timing when working with non-model organisms like corals.

By revealing clear response differences between the nearshore and offshore corals across multiple phenotypes, the results of the second chapter highlighted the differences in the metabolic state of the two genotypes, as well as the more stress resilient traits of the nearshore corals. The results therefore substantiated the genetic results, showing that the local adaptation in corals could occur in a much smaller scale than previously thought, and such adaptation may happen in a relatively short-time period. Much information is still needed to understand the causative effects of stressors and molecular responses, as well as how particular molecular phenotypes translate into stress resilience in coral genotypes. Proteomics holds a promising future in this regard, since proteomics can elucidate the cellular mechanisms of organism-level responses, by providing access to the entire protein pool.

Porites lobata is among the most studied, well-known coral species (Veron 2013), most likely due to its massive colony size and wide geographic range. In contrary to its popularity, the taxonomic state of *P. lobata* is not fully settled. Identification of *P. lobata,* and other certain *Porites* species, has proved challenging, as a result of their highly variable morphology and unresolved phylogeny. In 1977, Brakel published an article titled "Corallite variation in *Porites* and the species issues in corals." Almost 40 years later, we are still up against the same challenges. Although molecular genetics has contributed notably to the understanding of the

evolutionary history of corals, as well as to their biological and ecological functions (Fukami *et al.* 2008; Prada *et al.* 2014; Birkeland 2015), the "species problem" in corals still persists among many coral taxa, including the genus *Porites*. With the increasing number of threats corals are facing, this understudied field of coral systematics needs more attention, since misidentification of species can have potentially serious consequences. Species misidentification jeopardizes accurate data collection involving species distribution, plasticity, biological functions, and under or overestimation of taxonomic diversity (Vilgalys 2003; Forsman *et al.* 2009; Costa *et al.* 2015; Abecia *et al.* 2016), which may lead to incorrect predictions about responses to climate change, and loss of biological diversity. Species misidentifications are, indeed, reported at relatively high rates. For example, some of the reported misidentification rates are ~27% for freshwater mussels and ~20% for sharks, with an average of 2.7%–25.6% (Costa *et al.* 2015). Correct species identification is vital, especially for assessing population genetic structure. My concern for misidentification motivated me to investigate the range of corallite morphological variation in *P. lobata*, and the genetic basis for such variation using genomic data, and these results are summarized as my third chapter.

Using multivariate morphometric analysis and high throughput sequencing data, I was able to show a strong correlation between the corallite morphology and genetics in *P. lobata*, even with a limited number of samples. However, strong geographic clustering from the genomic and morphological data suggests that influence of local environment may also be strong. The skeletal morphological differences found between the nearshore and offshore genotypes on Oahu was especially intriguing, since it could indicate adaptive values to these morphological structures. A question remains regarding how much plasticity in corallite morphology corals may exhibit under different environmental conditions. The reciprocal transplant experiment, conducted in the second chapter, under the constraints of a limited transplant timeline, was not long enough to detect changes in skeletal morphology. A longer transplant experiment, as well as laboratory experiments, will be interesting next steps to explore the plasticity of skeletal morphology, and its adaptive values.

Our understanding of how coral populations adapt to changing environments is at an early stage (Edmunds & Gates 2008; Logan *et al.* 2013). Learning about the adaptive ability of corals is essential in today's world, where climate and environments are changing faster than at

any other time in the modern Earth's history. The work of my dissertation research provided significant insight into corals' short-term adaptive ability to changing environments by revealing how different genotypes responded to environmental stressors at the physiological and molecular levels, and showing the little-known population-level genetic diversity in the lobe coral. Through morphometric and genomic analyses, the genetic basis of skeletal morphology was revealed, which may also have adaptive functions. Understanding the genetic basis of stress tolerance in corals will allow more accurate predictions of the effects of climate change on coral reefs, and provide valuable tools for resource managers for making effective decisions about coral reef conservation. Examples include incorporating the maintenance of genetic diversity as a critical element in management policy (e.g. a marine protected area design), and using the resilient genotypes identified in the study for breeding, translocation, or migration programs for seeding future reefs.

REFERENCES

Abecia JED, Guest JR, Villanueva RD (2016) Geographical variation in reproductive biology is obscured by the species problem: a new record of brooding in Porites cylindrica, or misidentification? *Invertebrate Biology*, **135**, 58–67.

Aswani S, Mumby PJ, Baker AC *et al.* (2015) Scientific frontiers in the management of coral reefs. *Frontiers in Marine Science*, **2**.

Barshis DJ, Stillman JH, Gates RD, Toonen RJ, Smith LW, Birkeland C (2010) Protein expression and genetic structure of the coral *Porites lobata* in an environmentally extreme Samoan back reef: does host genotype limit phenotypic plasticity? *Molecular Ecology*, **19**, 140297–140297.

Baums IB, Boulay JN, Polato NR, Hellberg ME (2012) No gene flow across the Eastern Pacific Barrier in the reef-building coral *Porites lobata*. *Molecular Ecology*, **21**, 5418–5433.

Bennet S, Paulson J, Reynolds S (2010) Chapter 8: Hawaiian Culture. *Transcultural Nursing*.

Birkeland C (2015) Coral reefs in the Anthropocene. In: *Coral Reefs in the Anthropocene* (ed Birkeland C), pp. 1–15. Springer, Dordrecht.

Brakel WH (1977) Corallite variation in Porites and the species problem in corals. *Proceedings of Third International Coral Reef Symposium*, 457–462.

Cesar H, Van Beukering P (2004) Economic valuation of the coral reefs of Hawai'i. *Pacific Science*, **58**, 231–242.

Costa H, Foody G, Jiménez S, Silva L (2015) Impacts of Species Misidentification on Species Distribution Modeling with Presence-Only Data. *ISPRS International Journal of Geo-Information*, **4**, 2496–2518.

Downs CA, Fauth JE, Robinson CE, Curry R, Lanzendorf B, Halas JC, Halas J, Woodley CM (2005) Cellular diagnostics and coral health: Declining coral health in the Florida Keys. *Marine pollution bulletin*, **51**, 558–569.

Downs CA, Ostrander GK, Rougee L, Rongo T, Knutson S, Williams DE, Mendiola W, Holbrook J, Richmond RH (2012) The use of cellular diagnostics for identifying sub-lethal stress in reef corals. *Ecotoxicology*, **21**, 768–782.

Edge SE, Shearer TL, Morgan MB, Snell TW (2013) Sub-lethal coral stress: Detecting molecular responses of coral populations to environmental conditions over space and time. *Aquatic Toxicology*, **128-129**, 135–146.

Edmunds PJ, Gates RD (2008) Acclimatization in tropical reef corals. *Marine Ecology Progress Series*, **361**, 307–310.

Forsman ZH, Barshis DJ, Hunter CL, Toonen RJ (2009) Shape-shifting corals: molecular markers show morphology is evolutionarily plastic in Porites. *BMC Evolutionary Biology*, **9**, 45.

Fukami H, Chen CA, Budd AF, Collins A, Wallace C, Chuang Y-Y, Chen C, Dai C-F, Iwao K, Sheppard C, Knowlton N (2008) Mitochondrial and nuclear genes suggest that stony corals are monophyletic but most families of stony corals are not (Order Scleractinia, Class Anthozoa, Phylum Cnidaria). *PLoS ONE*, **3**, e3222.

Graham NAJ (2014) Habitat Complexity: Coral Structural Loss Leads to Fisheries Declines. *Current Biology*, **24**, R359–R361.

Gregg TM, Mead L, Burns JHR, Takabayashi M (2015) Puka Mai He Koʻa: The Significance of Corals in Hawaiian Culture. In: *Ethnobiology of corals and coral reefs* Ethnobiology. (eds Narchi NE, Price LL), pp. 103–115. Springer International Publishing, Switzerland.

Hoegh-Guldberg O (2014) ScienceDirectCoral reef sustainability through adaptation: glimmer of hope or persistent mirage? *Current Opinion in Environmental Sustainability*, **7**, 127–133.

Hughes TP, Graham NAJ, Jackson JBC, Mumby PJ, Steneck RS (2010) Rising to the challenge of sustaining coral reef resilience. *Trends in Ecology & Evolution*, **25**, 633–642.

Johnson, R. K. 1981. Kumulipo, The Hawaiian Hymn of Creation. Vol. 1. Top Gallant Publishing Co., LTD. Honolulu, HI. 188 pp.

Kenkel CD, Aglyamova G, Alamaru A *et al.* (2011) Development of Gene Expression Markers of Acute Heat-Light Stress in Reef-Building Corals of the Genus Porites (CR Voolstrag, Ed,). *PLoS ONE*, **6**, e26914.

Logan CA, Dunne JP, Eakin CM, Donner SD (2013) Incorporating adaptive responses into future projections of coral bleaching. *Global Change Biology*, **20**, 125–139.

Murphy JWA, Richmond RH (2016) Changes to coral health and metabolic activity under oxygen deprivation. *PeerJ*, **4**, e1956.

NOAA (2011) U.S. residents say Hawaii's coral reef ecosystems worth $33.57 billion per year. *National Oceanic and Atmospheric Administration, U.S. Department of Commerce*. http://www.noaanews.noaa.gov/stories2011/20111021_hawaii_coral.html

NOAA (2011) "U.S. residents say Hawaii's coral reef ecosystems worth $33.57 billion per year." National Oceanic and Atmospheric Administration, U.S. Department of Commerce. http://www.noaanews.noaa.gov/stories2011/20111021_hawaii_coral.html (October 2011).

Orsini L, Vanoverbeke J, Swillen I, Mergeay J, De Meester L (2013) Drivers of population genetic differentiation in the wild: isolation by dispersal limitation, isolation by adaptation and isolation by colonization. *Molecular Ecology*, **22**, 5983–5999.

Polato NR, Concepcion GT, Toonen RJ, Baums IB (2010) Isolation by distance across the Hawaiian Archipelago in the reef-building coral Porites lobata. *Molecular Ecology*, **19**, 4661–4677.

Prada C, DeBiasse MB, Neigel JE, Yednock B, Stake JL, Forsman ZH, Baums IB, Hellberg ME (2014) Genetic species delineation among branching Caribbean Porites corals. *Coral Reefs*, **33**, 1019–1030.

Richmond RH (2011) *Watersheds impacts on coral reefs in Maunalua Bay, Oahu, Hawaii (Progress Report FY 2010)*. HCRI Project Report.

Richmond RH, Wolanski E (2011) Coral research: past efforts and future horizons. In: *Corals Reefs: An Ecosystem in Transition* (eds Dubinsky Z, Stambler N), pp. 3–12. Coral Reefs: An ecosystem in transition, Springer Science.

Rougée L (2011) Expression and Activity of Xenobiotic Metabolizing Enzymes in the Reef Coral *Pocillopora damicornis*. Ph.D. Dissertation. University of Hawaii at Manoa.

Seneca FO, Palumbi SR (2015) The role of transcriptome resilience in resistance of corals to bleaching. *Molecular Ecology*, **24**, 1467–1484.

Seneca FO, Forêt S, Ball EE *et al.* (2009) Patterns of Gene Expression in a Scleractinian Coral Undergoing Natural Bleaching. *Marine Biotechnology*, **12**, 594–604.

Seveso D, Montano S, Strona G, Orlandi I, Galli P, Vai M (2013) Exploring the effect of salinity changes on the levels of Hsp60 in the tropical coral *Seriatopora caliendrum*. *Marine Environmental Research*, **90**, 96–103.

Seveso D, Montano S, Strona G, Orlandi I, Galli P, Vai M (2016) Hsp60 expression profiles in the reef-building coral *Seriatopora caliendrum* subjected to heat and cold shock regimes. . *Marine Environmental Research*, **119**, 1–11

Tisthammer, KH. 2016. Coral Molecular Biomarkers. Costal Wiki. http://www.coastalwiki.org/wiki/Coral_Molecular_Biomarkers.

Tomanek L (2011) Environmental Proteomics: Changes in the Proteome of Marine Organisms in Response to Environmental Stress, Pollutants, Infection, Symbiosis, and Development. *Annual Review of Marine Science*, **3**, 373–399.

Veron JEN (2013) Overview of the taxonomy of zooxanthellate Scleractinia. *Zoological Journal of Linnean Society*, **169**, 485–508.

Vilgalys R (2003) Taxonomic misidentification in public DNA databases. *New Phytologist* **160**, 4-5.

Voolstra CR, Miller DJ, Ragan MA (2015) The ReFuGe 2020 Consortium—using "omics" approaches to explore the adaptability and resilience of coral holobionts to environmental change. *Frontiers in Marine Science*, **2**:68.

Wilkinson C (2004) Status of coral reefs of the World: 2004. Volume 1. *Australian Institute of Marine Science*.

CHAPTER 1

Isolation by adaptation? Genetic structure is stronger across habitats than islands in the coral *Porites lobata* from Oahu and Maui

Kaho H. Tisthammer, Zac H. Forsman, Robert H. Richmond

ABSTRACT

Many marine organisms, including reef-building corals have traditionally been viewed as having vast interconnected 'open' populations. However, recent work has provided evidence for genetic structure along environmental gradients over smaller spatial scales than previously thought. Since corals in nearshore environments are increasingly exposed to reduced water quality, the lineage-scale population genetic structure of the lobe coral *Porites lobata* was analyzed to determine if genetic differentiation exists between offshore and nearshore sites in Hawaii. *P. lobata* populations from Maunalua Bay, Oahu and two reefs in West Maui were studied, where urbanization has caused serious decline in coral health in nearshore habitats. At both islands, using nuclear markers, we found clear genetic differentiation in *P. lobata* populations between offshore and nearshore sites ($F_{ST} = 0.0715 \sim 0.241$, $P < 0.001$). Additionally, nearshore corals showed overall lower genetic diversity, and a sign of population contraction was seen in Oahu but not in Maui. Pairwise F_{ST} analysis revealed no isolation by distance, but rather genetic similarity was stronger by habitat type than by geographic distance. Since there are no geographic barriers between the nearshore and offshore sites, the observed genetic partitioning may be maintained by selection of the genotypes that are more adapted to particular environmental conditions such as sedimentation and pollution ('isolation by adaption'). Nearshore populations from Oahu and Maui were also genetically closer, suggesting operation of similar selective forces at these locations. Understanding unexplored small-scale genetic diversity in corals will provide critical information for predicting the effects of climate and environmental changes on coral populations, since such diversity is responsible for their short-term adaptive responses.

INTRODUCTION

Coral reefs are centers of marine biodiversity and productivity that provide a variety of ecosystem services of substantial cultural and economic value to humankind, yet coral reefs worldwide are under serious threat as a result of human activities (Wilkinson 2008; Hughes *et al*. 2010; Graham 2014). Coral cover has declined over 50% in the past 100 years due to sedimentation, pollution, overfishing, disease outbreaks and climate change (Hughes *et al*. 2010; Richmond and Wolanski 2011; Graham 2014). Modern reef-building corals have persisted over a wide geographic range, with associated variations in climate and ocean conditions, since they first appeared during the Triassic Period approximately 250 million years ago (Stanley 2003). However, rates of current environmental change are orders of magnitude faster than those of ice age transitions (Hoegh-Guldberg *et al*. 2007). It is not clear if corals will be able to adapt quickly enough to survive the current rates of climate change (Donner *et al*. 2005; Hoegh-Guldberg 2012; Hoegh-Guldberg 2014). To predict how corals will respond to such variability, it is critical to understand their short-term adaptive abilities. Our understanding of how coral populations adapt to changing environments is its infancy (Edmunds and Gates 2008; Logan *et al*. 2013; Bay and Palumbi 2014), partly because little is known about the small-scale genetic diversity that is responsible for corals' plastic and short-term adaptive responses (Voolstra *et al*. 2015). Because lineage-scale adaptation originates from the standing genetic variation (Stapley *et al*. 2010), genetic diversity within a location can provide a scope for such adaptive abilities.

Many marine organisms, including reef-building corals, have traditionally been viewed as interconnected 'open' populations based on their planktonic larval stages and seeming lack of dispersal barriers in marine systems (Sanford and Kelly 2011). Indeed, many reef-building coral species have very large geographic distributions (Veron 2000). For example, the lobe coral *Porites lobata* (Dena,1846), is one of the most abundant and important reef-building corals in Hawaii and across its range spanning the Tropical Pacific Ocean from the Eastern Pacific to the Red Sea (Veron 2000). Colonies of *P. lobata* can live up to 1,000 years (Cole *et al*. 1993; Brown *et al*. 2009), and their planktonic larvae contain symbiotic algae with long dispersal potential (Richmond 1988), contributing to the perception of coral populations being well-mixed with high gene flow.

Recent advances in molecular technologies have started to provide a better understanding of genetic structure of coral populations. For example, genetic structure of *P. lobata* populations has been analyzed at both a regional, and ocean-wide scale. Baums *et al*. (2012) analyzed *P. lobata*'s genetic structure throughout the Pacific using nine microsatellite markers. They found that Eastern Pacific populations were highly distinct from the rest of the Pacific populations, concluding no recent gene flow between these regions. Also, Hawaiian populations were isolated from the rest of the Central Pacific, having a significant pairwise F_{ST} value as high as 0.27. At a regional scale, Polato *et al*. (2010) analyzed *P. lobata*'s population genetic structure across the Hawaiian archipelago. They found that the genetic structure followed the isolation by distance pattern, and the Hawaiian populations clustered into three main groups, reflecting the ocean currents and topology. Very little recent gene flow was found between the *P. lobata* populations from Johnston Atoll and the Hawaiian Islands.

Genetic patterns of corals at smaller spatial scales have remained understudied until recently, when several studies have found evidence for finer scale population structure than previously expected. For example, Bongaerts *et al*. (2010, 2011) showed strong genetic partitioning in the coral *Seriatopora hystrix* among depth gradients within a site, as well as among closely located sites in the Great Barrier Reef. Data from their field reciprocal transplant experiment, the authors suggested adaptive divergence. Barshis *et al*. (2010) studied thermal adaptation in *P. lobata* using populations from the back-reef and the fore-reef in American Samoa, separated by approximately 5 km. They found significant genetic differentiation between the two populations using nuclear and mitochondrial markers. Their reciprocal transplant experiment showed differential protein expression profiles between the two populations, suggesting the observed thermal tolerance had a genetic basis. Kenkel *et al*. (2013) also found a significant genetic subdivision between the inshore and offshore populations of *Porites astreoides* in the Florida Keys, separated by 7km. Their transcriptomic analysis showed higher thermotolerance of inshore corals than offshore corals, although whether such tolerance was due to adaptation or acclimatization was yet to be determined. Gorospe and Karl (2015) found a significant genetic cline in *Pocillopora damicornis* along a depth gradient within a 40 m diameter patch reef. Together with their size and age class analyses, depth was suggested as a

selective factor in post-recruitment processes. Local adaptation in marine organisms to micro-environmental variations (isolation by adaptation) is evidently more common than once thought (Sanford and Kelly, 2011; Bond *et al*. 2014), and corals do show varying degrees of physiological response and genetic differentiation over a relatively small area.

Nearshore marine habitats are increasingly exhibiting reduced water quality due to human activities (Wenger *et al*. 2015). In Maunalua Bay, Hawaii, Oahu, large-scale urbanization in adjacent watersheds over the last century has caused severe deterioration in the health of its coral reefs (Wolanski *et al*. 2009). There is an environmental gradient of toxicants and sedimentation from the mouth of the inner bay towards offshore. The corals in nearshore area are under chronic stress, and a previous survey showed significantly different cellular stress responses in the coral *P. lobata* along this gradient (Richmond 2011). Despite prolonged exposure to these stressors, some individual corals continue to thrive in the bay, suggesting these individuals may have adapted to withstand such stressors. Corals in Maunalua Bay provide an excellent system for studying small-scale, short-term adaptation since there are no physical barriers to the current movement between nearshore and offshore sites (Storlazzi *et al*. 2010; Presto *et al*. 2012) and nearshore development was well documented and started relatively recently. Similarly, the coral reefs off West Maui have experienced a dramatic decline in their coral cover from land-based anthropogenic impacts over the last several decades (Rodgers *et al*. 2015). Substantial deterioration in the health of West Maui's coral reefs has lead Honokowai and Wahikuli of West Maui to be designated as priority sites for conservation and management by the United States Coral Reef Task Force (USCRTF) and the State of Hawaii (Williams *et al*. 2014).

Based on the differences in water quality of nearshore and offshore environments, population genetic structures of *P. lobata* in Maunalua Bay, Oahu and Wahikuli and Honokowai, Maui were analyzed to determine if genetic partitioning exists between 'high-stress' nearshore site and 'low-stress' offshore site. At all locations, significant genetic structure of *P. lobata* was detected, which suggests that habitat type (micro environment) has stronger effects than geographic separation in forming *P. lobata*'s genetic structure at these locations. Since varying selective pressures can cause significant genetic structure in proximate populations, the observed patterns are likely caused by 'isolation by adaptation (IBA)' (Nosil *et al*. 2009).

MATERIALS AND METHODS

Coral Sampling

Small fragments of *P. lobata* tissue samples were collected from live colonies between February 2013 to May 2015 at the following sampling sites in Hawaii; a) 'Oahu'- nearshore and offshore sites at Maunalua Bay, Oahu (21.261~21.278°N, 157.711°W), b) Maui1 - nearshore and offshore sites off the Hanakao'o Beach Park, West Maui (Wahikuli, 20.95°N, 156.68°W), and c) Maui2 - nearshore, middle, and offshore sites off the Honokowai Beach Park, West Maui (Honokowai, 20.90°N, 156.69°W) (Fig. 1, Table 1). Samples from each sampling location will be referred to as a 'population' in this paper for clarification purposes, although they more likely represent subpopulations of a larger population. Samples were taken from coral colonies at least two meters apart at each site to avoid sampling the same genets, except at nearshore site of Maunalua Bay, where extensive monitoring has been conducted. At this site, all existing *P. lobata* colonies were tagged and GPS recorded, and some colonies sampled were less than two meters apart. After sampling, each coral colony was photographed and tagged to avoid resampling of the same colony. In addition, six *P. lobata* colonies were sampled from the Kewalo Basin ('Kewalo'), Oahu (21.292°N, 157.865°W) and from colonies growing in the flow through tank located at the Kewalo Marine Laboratory (University of Hawaii at Manoa). The collected tissue samples were either flash frozen in liquid nitrogen on shore and subsequently stored at -80 ℃, preserved in DMSO buffer (0.25M EDTA, 20% dimethyl sulfoxide, NaCl saturated, pH 7.5), or stored in 100% ethanol. Genomic DNA was extracted from each coral tissue sample using the Qiagen® DNeasy Blood & Tissue Kit.

PCR

For the samples from Oahu, the following three regions of coral host DNA were PCR-amplified: (1) ~ 400 bp coral mitochondrial region including the putative control region (CR), (2) ~1500 bp coral nuclear histone region spanning H2A to H4 (H2), and (3) ~ 700 bp coral nuclear ITS1-5.8S-ITS2 region (ITS). CR regions were amplified with primers CRf and CO3r (Vollmer & Palumbi, 2002) under the conditions described in Barshis *et al*. (2010). An approximately 1500-bp sequence of coral host nuclear DNA from the histone region that spans from H2A to H4 was amplified using the primers zH2AH4f (5'-

GTGTACTTGGCTGCYGTRCT -3') and zH4Fr (5'-GACAACCGAGAATGTCCGGT-3') under the following conditions: 96 °C for 2 min (one cycle), followed by 34 cycles consisting of 96 °C for 20 s, 58.5 °C for 20 s, and 72 °C for 90 s, and a final extension at 72 °C for 5 min. H2 amplifications (25 µl) consisted of 0.5 µl of DNA template, 0.2 µl of GoTaq® DNA Polymerase (Promega, Madison, WI), 5 µl of GoTaq® Reaction Buffer, 1.6 µl of 50mM $MgCl_2$, 2 µl of 10 mM dNTPmix, 1.6 µl of each 10mM primer, and nuclease-free water to volume. For samples with multiple bands, approximately 1500-bp PCR products were extracted from agarose gels after electrophoresis and purified using the UltraClean® 15 DNA Purification Kit (MO BIO Laboratories, Carlsbad, CA) according to the manufacturer's instruction. The rest of the PCR products were purified with UltraClean® PCR Clean-Up Kit (MO BIO Laboratories) and sequenced directly in both directions on the ABI 3730xl DNA Analyzer. The ITS regions were PCR amplified with primers ITSZ1 and ITSZ2 (Forsman *et al*. 2009) as follows: 95 °C for 7 min (1 cycle), followed by 35 cycles consisting of 94 °C for30s, 50°C for 30s and 70°C for 2 min, and a final extension at 72 °C for 1 min. Clone libraries were created for each PCR product using the pGEM®-Easy Vector System (Promega). Positive inserts were verified by PCR using SP6 and T7 primers, and plasmids (2–5 per library) were treated with UltraClean® 6 Minute Mini Plasmid Prep Kit (MO BIO Laboratories) and sequenced on an ABI-3130XL Genetic Analyzer sequencer. For the Maui samples, the H2 region was amplified and sequenced using the same method as described above.

Sequence Analyses

Resulting DNA sequences were aligned using Geneious® 6.1.8 (Biomatters Ltd., Auckland, New Zealand). Polymorphic sites within H2 regions were identified using Geneious® (Find Heterozygotes option) and by eye. Middle sections, as well as both ends of H2 were then trimmed to 1352 bp due to many having low quality and/or missing nucleotides. H2 was phased using the program PHASE 2.1 (Stephens *et al*. 2001) and SeqPHASE (Flot, 2010). The analysis of molecular variance (AMOVA) and other population genetic statistics were estimated in Arlequin 3.5 (Excoffier & Lischer, 2010) and TCS 1.21 (Clement *et al*. 2000). The global AMOVA with a weighted average over loci with permutation tests was used as implemented in Arlequin 3.5. For H2, both phased and non-phased sequences were run with AMOVA, which produced the same statistical results, and therefore only the results from the phased sequences

are presented here. Up to five coral ITS sequences were successfully cloned and sequenced per colony, and the entire data set was used for calculation of population statistics, treating each cloned sequence as a haplotype. This method of analysis was chosen since there was no difference in the outcomes between the consensus by inclusivity and the consensus by plurality, as in Barshis *et al*. (2010). To address the unequal sample sizes (28 vs 44) between the sites in Maunalua Bay, the analysis was repeated after resampling to the equal sample size (28) for 10 times.

Checking for Multi-Sampled Individuals

Most scleractinian corals are capable of reproducing asexually through various methods including fragmentation, polyp bailout, and asexual planulae production (reviewed in van Oppen *et al*. 2011). This potentially causes the same coral genets to be sampled multiple times in the field even if collected from separate colonies. Therefore, DNA sequences were inspected for possibility of multi-sampled individuals using H2. No two individuals from a single site shared the same haplotypes, and thus all sampled colonies were considered as separate individuals (genets).

Species Identification

Due to its high morphological plasticity, the genus *Porites* is notorious for its difficulties in distinguishing between its species (e.g. Veron 1995; Veron 2000; Forsman *et al*. 2009, 2015). Genetic delineation of some *Porites*, including *P. lobata*, has been challenging due to cryptic species and polymorphic or hybrid species complexes (e.g. Forsman *et al*. 2009; Prada *et al*. 2014). Although *Porites* corallites are small, irregular and can be highly variable, micro-skeletal (corallite) structures have been proposed to be more reliable for species identification, therefore, we examined the corallites of all collected samples to confirm our taxonomic identifications (Veron and Pichon 1982; Veron 2000), In Hawaii, the only *Porites* species with a similar colony morphology to *P. lobata* is *P. evermanni* (there are no records of *P. lutea* in Hawaii, although Fenner 2005 synonymized *P. evermanni* and *P. lutea*, they represent two distinct genetic clades; Forsman *et al*. 2009). *P. evermanni* is genetically distinct from *P. lobata*, and *P. lutea* (Forsman *et al*. 2009, Clade V) has a distinct corallite skeletal morphology.

RESULTS

Characteristics of Genetic Markers

Comparisons among the three types of genetic markers revealed that the non-coding nuclear marker ITS had the highest levels of genetic variability relative to the coding nuclear region H2 and the mitochondrial marker CR. The level of polymorphism in ITS was particularly high: 77 polymorphic sites were observed across the 707 bp (10.9%) including indels. Seventy six polymorphic sites across the1352 bp (5.6%) were observed in H2, and in CR only two sites were polymorphic in the 366 bp (0.55%). The total number of indels observed in ITS was 50, while H2 and CR did not contain any indels. In the ITS marker, there were four major indels with base pairs that were two or more, and the longest indel observed was 23 bp. Polymorphic sites were observed scattered throughout the maker length in both H2 and ITS (Fig. 2). In ITS, 33% of polymorphic sites were present in only one or two alleles, while in H2, 63% of polymorphic sites were present in one or two alleles. These results were reflected in a mean gene diversity of polymorphic sites that was more than twice the value in ITS (0.310 ± 0.192) compared to the value in H2 (0.140 ± 0.167).

Analysis of Genetic Structure and Patterns of Genetic Diversity

1. Oahu (Maunalua Bay)

The population genetic structure of *P. lobata* in Oahu (Maunalua Bay) was analyzed using three genetic markers. We obtained 70 ITS sequences, 43 H2 sequences (86 phased sequences), and 27 CR sequences (Table 2). The degree of genetic differentiation was estimated using AMOVA (Excoffier and Lischer 2010) between *P. lobata* from the 'high-stress' nearshore site and 'low-stress' offshore site. The AMOVA results using nuclear makers revealed clear genetic differentiation between the two sites (Table 2). The level of genetic differentiation between sites (F_{ST}) was significant for both ITS ($F_{ST} = 0.1918$, $P < 0.001$) and H2 ($F_{ST} = 0.0715$, $P < 0.001$). The mitochondrial marker (CR) did not detect a significant differentiation ($F_{ST} = 0.086$, $P = 0.148$), however this is likely due to low polymorphism (only two variable positions). The number of shared haplotypes (alleles) between the sites was also low. Out of 37 ITS haplotypes identified from the 70 total sequences (53%), only three (8%) were shared between the offshore

and nearshore sites. For H2, we obtained 54 unique haplotypes out of the 86 total phased sequences (63%), and only 5 sequences (9.3%) were shared between the sites (Table 3). The network analysis showed sequences clustering into three major groups in both ITS and H2; one dominated by the nearshore individuals, the second one dominated by the offshore individuals, and the last group with mixed origins (Fig. 3).

For the mitochondrial marker CR, three haplotypes were identified from 27 sequences (11%). All three haplotypes were present at both sites. Although the level of genetic differentiation was not significant, the frequency distributions of the three haplotypes showed a marginal difference between the sites (Chi-square test, $^2 = 4.8705$, df = 2, P = 0.0876). The most common haplotype was also most dominant at the nearshore site, while a second haplotype was the dominant haplotype in the offshore site (Fig. 4).

In addition to a strong genetic partitioning observed between the nearshore and offshore sites, the pattern of genetic diversity also differed between the sites; the degree of *P. lobata*'s genetic diversity was higher at the offshore site. Compared to the nearshore samples, the ITS marker from the offshore samples was almost double in the following three parameters; percent private alleles (pA), percent polymorphic sites (poly), and nucleotide diversity level (π) (Table 3). The resampling results confirmed that this was not an artifact of a larger sample size of the offshore samples, since the proportions of haplotype numbers, private alleles, and polymorphic sites, the number of indels, and π were all similar or higher after standardizing the offshore sample size (Table 3). The level of genetic diversity in H2 was also slightly higher in the offshore samples; the number of haplotypes, the number of private alleles, and the heterozygosity level were higher in the offshore samples (Table 3). The number of polymorphic sites and π in H2 were similar between the sites. In both markers at all sites, $\theta\pi$ (the expected heterozygosity estimated from the average π) was higher than θs (the theta estimated from the number of segregating sites), reflecting the recent trend of a population decline.

2. Maui

The population genetic structure of *P. lobata* at two locations from West Maui were analyzed using the H2 marker. A total of 49 sequences (98 phased sequences) were obtained, 22 from the site 'Maui1' (Wahikuli) and 27 from 'Maui2' (Honokowai). Significant genetic structure between *P. lobata* from the nearshore and offshore sites was also found at Maui1 (F_{ST} =

0.241, P < 0.001) (Table 4a). At Maui2, where samples were collected from three sites ('nearshore', 'middle', and 'offshore'), *P. lobata* showed a more complex pattern of genetic structure. Although the overall AMOVA did not show significant structure at Maui2 (F_{ST} = 0.057, P = 0.238, Table 4b), pairwise comparison revealed significant genetic differentiation between the offshore and the middle sites (F_{ST} = 0.143, P = 0.003). No significant structure was found between the offshore and nearshore sites, or the middle and nearshore sites at Maui2 (see Oahu vs. Maui, pairwise comparison). To compare the Maui1 and Maui2 populations, the AMOVA was conducted by pooling all individuals from different sites within a location. The results revealed significant structure (F_{ST} = 0.0634, P < 0.001) between the locations (Fig. 5).

P. lobata populations from the two Maui locations had a relatively similar level of genetic diversity in terms of the number of haplotypes, the number of private alleles, and π. Maui2 samples had a higher proportion of polymorphic sites (3.6%) than Maui1 (1.8%), which primarily came from the Maui2 nearshore samples (Table 5). However, the proportion of homozygous individuals was also higher in Maui2 (22%) than Maui1 (4.8%), which reduced the observed heterozygosity (Ho) in Maui2 to 0.741, as opposed to 0.955 in Maui1 The theta estimators revealed that the population in Maui2 is expanding but not in Maui1.

3. Oahu vs. Maui

The population genetic structure of *P. lobata* was assessed between Oahu and Maui using H2. The AMOVA detected a significant structure between the pooled Oahu and pooled Maui populations (F_{ST} = 0.0589, P < 0.001). Adding the six *P. lobata* individuals from Kewalo to the Oahu samples also resulted in a significant F_{ST} value (0.0445, P <0.001) between Oahu and Maui. The patterns of genetic diversity were relatively similar between Oahu and Maui. The number of total alleles, the number of private alleles, and π were marginally higher for the pooled Oahu population. However, the proportion of homozygous individuals (hz) was lower for the pooled Maui population (16.3% vs. 23.5% in Oahu), and thus the Maui population had a higher observed heterozygosity (H_O, 0.837 vs. 0.755 in Oahu). The theta estimators indicated a population contraction for the Oahu population ($\theta\pi - \theta_S$), while the Maui population showed a sign of population expansion, primarily due to the Maui2 population (Table 5).

Pairwise F_{ST} values were estimated for all combinations in Arlequin based on the H2 marker. The results revealed that the offshore populations from Oahu, Maui1, and Maui2 were

genetically closer to each other than their respective nearshore/middle populations (Table 6). The nearshore populations from Oahu and Maui1 were also genetically closer to each other than to their respective offshore populations. The pairwise analysis also highlighted the unique pattern of the nearshore and middle populations at Maui2. The nearshore Maui2 population turned out to be genetically closer to the offshore populations in general; its F_{ST} values were significant from other nearshore populations (Oahu and Maui1), but not from other offshore populations. The Maui2 middle population was genetically distinct from all other, except for the nearshore Maui2. Figure 5 depicts the overall separation of the offshore individuals across geographic locations from the nearshore Oahu and Maui1 populations, with the unique Maui2 middle population clustering into one group. Based on the pairwise analysis, the seven populations compared in our study were grouped into three main genetic clusters (Fig. 6).

DISCUSSION

Porites lobata is one of the most dominant scleractinian coral species in Hawaii, and is known for its robustness; for example, *P. lobata* shows a high tolerance for sedimentation (Stafford-Smith 1993) and bleaching (Levas *et al*. 2013), and a colony can recover from partial mortality due to tissues residing deep within the perforate skeleton, a phenomenon referred to as the 'Phoenix effect' (Roff *et al*. 2014). At the nearshore site of Maunalua Bay, the suspended sediment concentration (SSC) periodically exceeds several hundred mg/L, and the run-off water introduces toxicants such as benzo[a]pyrene, benzo[k]fluoranthene, phenanthrene and alpha-chlordane (Richmond, 2009, Wolanski *et al*. 2009, Storlazzi *et al*. 2010). The detailed information on temperature, salinity and turbidity gradients across the bay are available in Storlazzi *et al* (2010). In such unfavorable conditions, *P. lobata* often dominates the coral community, and provides an opportunity to investigate patterns of genetic structure and gene flow between these different sites.

Genetic Markers

In order to analyze small-scale population genetic structure, selecting appropriate genetic markers is critical. Several mitochondrial (Vollmer and Palumbi 2002; Concepcion *et al*. 2009;

Kitahara *et al*. 2010) and nuclear (Forsman *et al*. 2006; Polato *et al*. 2010; Baums *et al*. 2012; Prada *et al*. 2014; Hellberg *et al*. 2016) markers have been developed, including microsatellites, for *P. lobata*. Since the mitochondrial genomes of scleractinian corals are known to evolve slowly (Shearer *et al*. 2002) and the mitochondrial genome of *P. lobata* exhibits very little sequence variability (< 0.02% was polymorphic) (Tisthammer *et al*. 2016), the short mitochondrial markers were expected to be unsuitable for studying fine scale population structures. Although Barshis *et al.* (2010) were able to show a significant genetic partitioning using two mitochondrial markers (CR and NAD) between the back-reef and the fore-reef *P. lobata* populations in American Samoa, our results suggest that the CR region would not be an efficient marker to assess a small-scale population genetic structure, since we only observed two polymorphic sites in our data, even though it is one of the most rapidly evolving regions of the coral mitochondrial genome. High polymorphism in the ITS marker is a desirable trait, yet sequencing of ITS requires time-consuming cloning, and analyzing the multi-copy gene poses analytical challenges, as it deviates from a standard diploid model. Attempts have been made to conduct genetic analysis using ITS by a) treating each sequence as a haplotype (inclusivity), b) making a consensus sequence per individual (consensus by plurality), or c) using a hierarchal PERMANOVA. In this study, we ran AMOVA using ITS by both a) and b) methods, which produced the same statistical outcome, and hence, the results from inclusivity (a) are presented in this paper. To create markers that allow direct sequencing post PCR, we designed several sets of new primers, and H2 was proven to be a useful marker for population genetic study in *P. lobata*. The sequence variability was lower than ITS, but high enough to detect the population differentiation. H2 does not have any indels, which added analytical simplicity when compared to ITS as well.

The ITS sequence variability of *P. lobata* was much higher than that of *Porites panamensis* from the Eastern Pacific populations. *P. panamensis* showed only two sequence variants per individual (Saavedra-Sotelo *et al*. 2013), while *P. lobata* from Maunalua Bay showed up to four sequence variants per individual. The number of sequence variants per individual in *P. lobata* may be much higher since only up to five clones per individual were successfully sequenced in this study, and previously up to eight sequence variants per individual were observed (Barshis *et al*. 2010). The total number of polymorphic positions was also higher in *P. lobata* than *P.*

panamensis; within the comparable 555 bp region, we found 26 polymorphic positions in *P. lobata*, while 15 polymorphic positions were reported in *P. panamensis*. The lower level of genetic variability in *P. panamensis* may be related to its limited geographic distribution (found only in the Eastern Pacific), since endemic species and geographically restricted populations often show a reduced level of genetic diversity (Hamrick *et al*. 1992; Frankham 1997).

Small-Scale Genetic Structure in Oahu (Maunalua Bay)

P. lobata from the nearshore and offshore sites in Oahu (Maunalua Bay) showed significant genetic differentiation using ITS and H2. The distance between the sites is less than two kilometers, and there are no apparent geographic barriers between the sites, suggesting selection is the cause of the observed genetic partitioning. In the bay, surface currents primarily flow west due to the prevailing trade-winds (offshore to nearshore). The below surface current movement seems to be more complex, and is generally towards the east (nearshore to offshore) with the presence of small eddies, at least during the summer (Presto *et al*. 2012). Eddies would increase the larval retention time in the summer spawning season, especially for *Porites* species that produce neutrally buoyant gametes (Hunter 1988). The water movement in the bay therefore suggests no dispersal barrier between the sites, supporting selection as a primary force of the observed genetic structure. Local genetic adaptation has increasingly been viewed as an important driver in establishing population genetic structure in nature. Isolation by adaptation (IBA) (e.g. Nosil *et al*. 2009) or isolation by colonization (IBC, or monopolization) (e.g. De Meester *et al*. 2002) are the two key processes that emphasize the role of selection in forming the genetic structure, in contrast to the neutral process of isolation by distance (IBD) (Orsini *et al*. 2013). Ecological theory predicts that the two processes, IBA and IBC, will result in different distributions of genetic variation across landscapes (see Fig. 1 of Orsini *et al*. 2013). In reality, a combination of processes contributes to structuring genetic variation, and pinpointing the possible underlying processes may be difficult. In the case of *P. lobata* populations from Maunalua Bay, the observed structure could have been formed by IBC with local adaptation, as opposed to IBA, since the nearshore population has likely undergone a population bottleneck after large-scale urbanization began half a century ago, mimicking a colonization event and causing founder effects. The deteriorated water and substrate qualities at the nearshore environment likely have limited new recruitments (Puritz and Toonen, 2011) and placed the population under strong local selection.

Investigating additional loci, especially those under selection (Orsini *et al*. 2013), and additional locations along the environmental gradient, will help further understand the processes driving the observed structures. A reciprocal transplant experiment conducted by the authors would also help elucidate the role of selection in driving the observed pattern.

Small-Scale Genetic Structure in West Maui

Coral cover in West Maui has been showing steady decline, likely due to chronic localized anthropogenic stressors and low herbivore populations over the last several decades. Its nearshore populations especially appear to be suffering from land-based sources of pollution, as their coral cover declines were faster than at deeper areas away from land-derived materials (Rodgers *et al*. 2015). Our study revealed significant genetic structure from West Maui's *P. lobata* populations. This structure was observed from approximately 10 individuals per site, which suggests the presence of a relatively strong force of either selection, gene flow barriers or both. Especially at Maui1, clear genetic differentiation was observed between offshore and nearshore sites that were merely 200 meters apart. Marked differences in water quality existed at this location due to its topography: A stream drains just north of the nearshore site, creating a visibly milky water body perpendicular to the coastline. This milky run-off is pushed southward by prevailing currents (Fig. 8). The nearshore site is located inside the milky water body, and is directly affected by the terrestrial run-offs, while the offshore site is located outside of the milky water. Therefore, reduced water quality in the nearshore habitat may have contributed to forming the observed genetic structure through selection (IBA). This structure may have been further strengthened by gene-flow barriers created by the unique local current pattern.

The genetic structure of Maui2 populations did not follow the same patterns we observed in Oahu and Maui1. Maui2's nearshore population turned out to be genetically closer to the offshore populations from all three locations than the other nearshore populations. The Maui2 middle population was genetically highly distinct from all other populations. However, the sample size at Maui2 was small, and we cannot effectively speculate the causes of observed patterns at this point. Increasing the sample size, as well as obtaining environmental and geographic characteristics, at Maui2 will help better understand *P. lobata*'s genetic structure at this location.

Oahu and Maui - Genetic Structure and Geographic Scale

The isolation by distance theory (IBD) predicts that the degree of genetic differentiation increases with geographic distance due primarily to dispersal limits (e.g. Orsini *et al*. 2013). IBD does not take into account environmental changes and hence, the associated selection/local adaptation. IBA, on the other hand, results in a pattern where genetic distance increases as ecological distance increases, but not with geographic distance for most loci (Orsini *et al*. 2013). The pattern we observed in *P. lobata*'s genetic structure showed an absence of IBD. Comprehensive environmental parameters are not available to estimate ecological distance among all of our study sites. However, the pairwise F_{ST} values across sites (Table 6, Fig. 7) revealed that the offshore populations are genetically closer to each other, and the nearshore populations are also genetically closer to each other (except for Maui2). This suggests a possibility of correlation between habitats and genetic distance, thus indicating IBA (or a combination of the processes that involve local adaptation). It is particularly interesting to find the genetic similarity between the nearshore populations from the two separate bays (Oahu and Maui1), which have been exposed to similar environmental changes, with currently having high turbidity and high sedimentation. This implies that similar selective force may be operating at both locations, and these coral populations may be selected for their local conditions independently from their standing genetic variations.

Since the island of Oahu has been heavily developed for a longer time period than the island of Maui, we expected Oahu's coral populations to have lower overall genetic diversity, suffering from prolonged exposure to the nearshore reduced water quality. The pattern of genetic diversity was, however, relatively similar between Oahu and Maui populations, which gives hope that corals in Oahu are still potentially maintaining a relatively high level of genetic diversity. Also it is promising for conservation efforts that Maui's *P. lobata* populations have not shown signs of population contraction, which is apparent in the Oahu population. Since then, severe bleaching that occurred in late 2015 due to El Niño caused high mortality on Maui's coral populations (up to 70%, Sparks et al. 2016), and therefore the population status has likely changed in Maui. Our results are from geographically limited sample locations. Incorporating larger sample locations from around the islands will reveal a more comprehensive pattern of *P. lobata*'s genetic diversity, which will provide useful insights for coral conservation efforts.

CONCLUSIONS

Our results show that corals do exhibit small-scale genetic structure, and habitat types appear to have a stronger effect in forming such genetic structure than geographic distances in the coastal areas. Genetic similarity found in Oahu and Maui1's nearshore populations suggest that the observed genetic structure maybe governed more by local adaptation, along with small-scale water movements (isolation by resistance, Thomas *et al*. 2015) than previously assumed. Without thorough samplings at a small-scale, we could easily overlook important local genetic diversity, and may mistakenly conclude that populations are uniform across the landscape. Being able to predict the effects of climate and environmental change on coral populations is paramount to ensuring their survival, yet remains difficult, partly because so little is known about the small-scale genetic diversity that provides variability for short-term adaptive responses. Our results have provided an important insight into answering such questions. Degradation of the nearshore environment around Oahu and Maui may have contributed to a loss of genetic diversity. The loss of genetic diversity could, in turn, reduce adaptive capacity for future environmental changes, including ocean warming and acidification. Further understanding of the genetic basis of stress tolerance in corals will allow us to more accurately estimate the effects of climate change on coral reefs, and will provide valuable tools for resource managers for making effective decisions about coral reef conservation.

ACKNOWLEDGEMENTS

We thank the following people for assistance in collecting corals: M. Stiber, V. Sindorf, F. Seneca, J. Murphy, J. Martinez, A. Lyman, K. Richmond, V. Hölzer, N. Spies, and A. Irvine. Special thanks to T. Oliver and R. Toonen for their support and advice. Coral samples were collected under the Hawaii Division of Aquatic Resources, Special Activity Permit 2013-26 & 2015-06. Financial support came from the National Fish and Wildlife Foundation (Grant Number 34413), the Hawaii Department of Health (MOA 13-502), and the NOAA Coral Reef Ecosystem Studies Program (NA09NOS4780178).

REFERENCES

Barshis DJ, Stillman JH, Gates RD, *et al* (2010) Protein expression and genetic structure of the coral *Porites lobata* in an environmentally extreme Samoan back reef: does host genotype limit phenotypic plasticity? *Molecular Ecology* **19**, 140297–140297.

Baums IB, Boulay JN, Polato NR, Hellberg ME (2012) No gene flow across the Eastern Pacific Barrier in the reef-building coral *Porites lobata*. *Molecular Ecology* **21**, 5418–5433.

Bay RA, Palumbi SR (2014) Multilocus Adaptation Associated with Heat Resistance in Reef-Building Corals. *Current Biology* **24***,*1–5.

Bird CE, Karl SA, Smouse PE, Toonen RJ (2011) Detecting and measuring genetic differentiation. In: Held C, Koenemann S, Schubart CD (eds.) *Crustacean Issues 19: Phylogeography and Population Genetics in Crustacea*. CRC Press , Boca Raton, FL, pp 31–55.

Bond MH, Crane PA, Larson WA, Quinn TP (2014) Is isolation by adaptation driving genetic divergence among proximate Dolly Varden char populations*? Ecology & Evolution* **4**, 2515–2532.

Bongaerts P, Riginos C, Hay KB, van Oppen MJH, Hoegh-Gouldberg O, Dove S (2011) Adaptive divergence in a scleractinian coral: physiological adaptation of *Seriatopora hystrix* to shallow and deep reef habitats. BMC *Evolutionary Biology* **11**, 303.

Bongaerts P, Riginos C, Ridgway Sampayo EM, van Oppen MJH, Englebert N, Vermeulen F, Hoegh-Gulderg O (2010) Genetic Divergence across Habitats in the Widespread Coral *Seriatopora hystrix* and Its Associated Symbiodinium. *PLoS ONE* **5**, e10871. doi: 10.1371/journal.pone.0010871.t001

Brown DP, Basch L, Barshis D, Forsman ZH, Fenner D, Goldberg, J (2009) American Samoa's island of giants: massive *Porites* colonies at Ta'u island. *Coral Reefs* **28**, 735–735.

Clement M, Posada D, Crandall KA (2000) TCS: a computer program to estimate gene genealogies. *Molecular Ecology* **9**, 1657–1659.

Cole JE, Fairbanks RG, Shen GT (1993) Recent Variability in the Southern Oscillation: Isotopic Results from a Tarawa Atoll Coral. *Science* **260**, 1790–1793.

Concepcion GT, Polato NR, Baums IB, Toonen RJ (2009) Development of microsatellite markers from four Hawaiian corals: *Acropora cytherea*, *Fungia scutaria*, *Montipora capitata* and *Porites lobata*. *Conservation Genetic Resources* **2**, 11–15.

Donner SD, Skirving WJ, Little CM, *et al* (2005) Global assessment of coral bleaching and required rates of adaptation under climate change. *Global Change Biology* **11**, 2251–2265.

Edmunds PJ, Gates RD (2008) Acclimatization in tropical reef corals. *Marine Ecology Progress Series* **361**, 307–310.

Excoffier L, Lischer HEL (2010) Arlequin suite ver 3.5: a new series of programs to perform population genetics analyses under Linux and Windows. *Molecular Ecology Resources* **10**, 564–567.

Excoffier L, Smouse PE, Quattro JM (1992) Analysis of molecular variance inferred from metric distances among DNA haplotypes: application to human mitochondrial DNA restriction data. *Genetics* **131,** 479–491.

Flot JF (2010) SeqPHASE: a web tool for interconverting PHASE input/output files and FASTA sequence alignments. *Molecular Ecology Resources* **10**, 162–166.

Forsman ZH, Hunter CL, Fox GE, Wellington GM (2006) Is the ITS region the solution to the "species problem" in corals? Intragenomic variation and alignment permutation in *Porites*, *Siderastrea* and outgroup taxa. *Proceedings of the 10th international coral reef symposium* **1**, 14–23.

Forsman Z, Wellington GM, Fox GE, Toonen RJ (2015) Clues to unraveling the coral species problem: distinguishing species from geographic variation in *Porites* across the Pacific with molecular markers and microskeletal traits. *PeerJ* **3**, e751. doi: 10.7717/peerj.751/supp-1

Frankham R (1997) Do island populations have less genetic variation than mainland populations? *Heredity* **78**, 311–327.

Graham NAJ (2014) Habitat Complexity: Coral Structural Loss Leads to Fisheries Declines. *Current Biology* **24**, R359–R361.

Hamrick JL, Godt M, Sherman-Broyles SL (1992) Factors influencing levels of genetic diversity in woody plant species. In: Adams WT, Strauss SH, Copes DL, Griffin AR (eds) *Population genetics of Forestry Trees*. Springer,

Hellberg ME, Prada C, Tan MH, Forsman ZH, Baums IB (2016) Getting a grip at the edge: recolonization and introgression in eastern Pacific *Porites* corals. *Journal of Biogeography* **43**, 2147-2159.

Hoegh-Guldberg O, Mumby PJ, Hooten AJ, *et al* (2007) Coral Reefs Under Rapid Climate Change and Ocean Acidification. *Science* **318**, 1737–1742.

Hoegh-Guldberg O (2012) The adaptation of coral reefs to climate change: Is the Red Queen being outpaced? *Scientia Marina* **76**, 403–408.

Hoegh-Guldberg O (2014) Coral reef sustainability through adaptation: glimmer of hope or persistent mirage? *Current Opinion in Environmental Sustainability* **7**, 127–133.

Hughes TP, Graham NAJ, Jackson JBC, *et al* (2010) Rising to the challenge of sustaining coral reef resilience. *Trends in Ecology & Evolution* **25**, 633–642.

Hunter CL (1988) Genotypic diversity and population structure of the Hawaiian reef coral, *Porites compressa*. Ph.D. Dissertation. University of Hawaii at Manoa.

Kenkel CD, Goodbody-Gringley G, Caillaud D, *et al* (2013) Evidence for a host role in thermotolerance divergence between populations of the mustard hill coral (*Porites astreoides*) from different reef environments. *Molecular Ecology* **22**, 4335–4348.

Kitahara MV, Cairns SD, Stolarski J, *et al* (2010) A Comprehensive Phylogenetic Analysis of the Scleractinia (Cnidaria, Anthozoa) Based on Mitochondrial CO1 Sequence Data. *PLoS ONE* **5**, e11490. doi: 10.1371/journal.pone.0011490.s002

Levas SJ, Grottoli AG, Hughes A, *et al* (2013) Physiological and Biogeochemical Traits of Bleaching and Recovery in the Mounding Species of Coral *Porites lobata*: Implications for Resilience in Mounding Corals. *PLoS ONE* **8**, e63267. doi: 10.1371/journal.pone.0063267.t006

Logan CA, Dunne JP, Eakin CM, Donner SD (2013) Incorporating adaptive responses into future projections of coral bleaching. *Global Change Biology* **20**, 125–139.

Polato NR, Concepcion GT, Toonen RJ, Baums IB (2010) Isolation by distance across the Hawaiian Archipelago in the reef-building coral *Porites lobata*. *Molecular Ecology* **19**, 4661–4677.

Presto KM, Storlazzi CD, Logan JB, *et al* (2012) Coastal Circulation and Potential Coral-larval Dispersal in Maunalua Bay, Oahu, Hawaii -Measurements of waves, Currents, Temperature, and salinity June-September 2010. U.S. Geological Survey Open-File Report 2012-1040.

Richmond RH (1988) Competency and dispersal potential of planula larvae of a spawning versus a brooding coral. *Proceedings of the 6th International Coral Reef Symposium* **2**, 827–831.

Richmond RH (2011) Watersheds impacts on coral reefs in Maunalua Bay, Oahu, Hawaii (Progress Report FY 2010). HCRI Project Report.

Richmond RH, Wolanski E (2011) Coral research: past efforts and future horizons. In: Dubinsky Z, Stambler N (eds) *Corals Reefs: An Ecosystem in Transition*. Springer Science, pp 3–12.

Rodgers KS, Jokiel PL, Brown EK, *et al* (2015) Over a Decade of Change in Spatial and Temporal Dynamics of Hawaiian Coral Reef Communities. *Pacific Science* **69**, 1-13.

Roff G, Bejarano S, Bozec Y-M, *et al* (2014) *Porites* and the Phoenix effect: unprecedented recovery after a mass coral bleaching event at Rangiroa Atoll, French Polynesia. *Marine Biology* **161**, 1385–1393.

Saavedra-Sotelo NC, Calderon-Aguilera LE, Reyes-Bonilla H, *et al* (2013) Testing the genetic predictions of a biogeographical model in a dominant endemic Eastern Pacific coral (*Porites panamensis*) using a genetic seascape approach. *Ecology and Evolution* **3**, 4070–4091.

Sanford E, Kelly MW (2011) Local Adaptation in Marine Invertebrates. *Annu Rev Marine Sci* **3**, 509–535.

Seneca FO, Forêt S, Ball EE, *et al* (2009) Patterns of Gene Expression in a Scleractinian Coral Undergoing Natural Bleaching. *Marine Biotechnology* **12**, 594–604.

Shearer TL, van Oppen MJH, Romano SL, Wörheide G (2002) Slow mitochondrial DNA sequence evolution in the Anthozoa (Cnidaria). *Molecular Ecology* **11**, 2475–2487.

Sparks R, Stone K, White D, Ross M (2016) Maui and Lanai Monitoring Report, Decemer 2015. Department of Land and Natural Resources, Division of Aquatic Resources, Maui Office.

Stafford-Smith MG (1993) Sediment-rejection efficiency of 22 species of Australian scleractinian corals. *Marine Biology* **115**, 229–243.

Stanley GD Jr (2003) The evolution of modern corals and their early history. *Earth-Science Reviews* **60**, 195–225.

Stapley J, Reger J, Feulner PGD, *et al* (2010) Adaptation genomics: the next generation. *Trends in Ecology & Evolution* **25**, 705–712.

Stephens M, Smith NJ, Donnelly P (2001) A new statistical method for haplotype reconstruction from population data. *American Journal of Human Genetics* **68**, 978–989.

Storlazzi CD, Presto KM, Logan JB, Field ME (2010) Coastal Circulation and Sediment Dynamics in Maunalua Bay, Oahu, Hawaii. USGS Open-File Report 2010-1217.

Thomas L, Kennington WJ, Stat M, *et al* (2015) Isolation by resistance across a complex coral reef seascape. *Proceedings of the Royal Society B: Biological Sciences* **282**, 20151217.

Tisthammer KH, Forsman ZH, Sindorf VL, Massey TL, Bielecki CR, Toonen JR (2016) The complete mitochondrial genome of the lobe coral *Porites lobata* (Anthozoa: Scleractinia) sequenced using ezRAD. *Mitochondrial DNA Part B*, **1**, 1–3.

van Oppen MJH, Souter P, Howells EJ, *et al* (2011) Novel Genetic Diversity Through Somatic Mutations: Fuel for Adaptation of Reef Corals? *Diversity* **3**, 405–423.

Veron JEN (1995) Corals in space and time. Cornell University Press, Ithaca

Veron JEN (2000) *Corals of the World*. Australian Institute of Marine Science and CRR Qld Pty Ltd.

Veron J (2013) Overview of the taxonomy of zooxanthellate Scleractinia. *Zoological Journal of Linnean Society* **169,** 485–508.

Veron JEN, Pichon M (1982*) Scleractinia of Eastern Australia. Part IV Family Poritidae*. Australian Institute of Marine Science and Australian National University Press, Miami, FL.

Vollmer SV, Palumbi SR (2002) Hybridization and the evolution of reef coral diversity. *Science* **296**, 2023–2025.

Voolstra CR, Miller DJ, Ragan MA (2015) The ReFuGe 2020 consortium-Using "omics" approaches to explore the adaptability and resilience of coral holobionts to environmental change. *Frontiers in Marine Science* **2**:68. doi: 10.3389/fmars.2015.00068

Wenger AS, Williamson DH, da Silva ET, *et al* (2015) Effects of reduced water quality on coral reefs in and out of no-take marine reserves. *Conservation Biology* **20**, 142–153.

Wilkinson C (2008) Status of coral reefs of the world: 2008. Global Coral Reef Monitoring Network and Reef and Rainforest Research Centre, Townsville, Australia.

Williams I, Vargas B, White D, Callender T (2014) West Maui Wahikuli & Honokowai Priority watershed Area Reef Condition Report December 2014. Scientific Report: Hawaii Division of Aquatic Resources, Ridge 2 Reef Initiative, NOAA, Coral Reef Conservation Program.

Wolanski E, Martinez JA, Richmond RH (2009) Quantifying the impact of watershed urbanization on a coral reef: Maunalua Bay, Hawaii. *Estuarine, Coastal and Shelf Science* **84**, 259–268.

DATA ACCESSIBILITY

All DNA sequences have been deposited in GenBank (ITS: Accession# KY493091- KY493160, H2: Accession# KY502280 – KY 502376, CR: Accession# KY502373-KY502375).

TABLES

Table 1. Approximate distance between the sampling sites and locations.

Sampling Sites	Approximate Distance
Oahu: Nearshore - Offshore	2 km
Maui1: Nearshore - Offshore	300 m
Maui2: Nearshore - Offshore	680 m
Maui2: Middle – Offshore	580 m
Maui1 – Maui2	5.6 km
Oahu - Maui	113 km

Table 2. AMOVA results of *P. lobata* from Oahu (Maunalua Bay).

	Source of Variation	Variance components	% Variance	F_{ST}
ITS	Between populations	2.27	19.18	**0.1918*****
(n=70)	Within populations	9.56	80.82	
H2	Between populations	0.29	7.15	
(n=43)	Within populations	1.30	31.88	**0.0715*****
	Within individuals	2.49	60.96	
CR	Between populations	0.034	8.49	0.08595
(n=20)	Within populations	0.370	91.5	(P = 0.148)

Table 3. Population genetic statistics of *P. lobata* from Oahu (Maunalua Bay): Sample size (n), number of haplotypes (A), number of private haplotypes (pA), number of polymorphic sites (poly), mean overall gene diversity ($D_A \pm$ SD), mean gene diversity for polymorphic sites only ($D_P \pm$ SD), observed heterozygosity (H_O), expected heterozygosity (He), number of indels (i), number of homozygous individuals (hz), nucleotide diversity ($\pi \pm$ SD), theta estimator 1 ($\theta\pi$: expected heterozygosity at a nucleotide position estimated from the mean π), theta estimator 2 (Watterson estimator, θs). *Standardized values to the minimum sample size of 28.

	ITS (707 bp)									
Sites	n	A	pA	poly	D_A	D_P	i	π	θπ	θs
Oahu Nearshore	28	13 (46%)	10 (36%)	45 (6.4%)	1.0 ± 0.009	0.259 ±0.182	31	0.0167 ±0.009	11.64 ±5.44	3.60 ±1.45
Oahu Offshore	42	27 (64%)	24 (57%)	70 (10%)	1.0 ± 0.005	0.343 ±0.192	50	0.0340 ±0.017	24.03 ±10.78	6.04 ±2.06
Oahu Offshore*	(28)	21.7 (78%)	19.3 (69%)	65.2 (9.2%)			48.5	0.0337 ±0.017	23.7 ±11.96	5.37 ±2.00
	H2 (1352 bp)									
	n	A	pA	poly	Ho	He (D_A)	D_P	hz	π	θπ	θs
Oahu Nearshore	22 (44)	28 (64%)	23 (52%)	27 (2.0%)	0.773	0.965	0.120 ±0.151	5 (23%)	0.00553 ±0.003	7.483 ±3.96	6.207 ±2.09
Oahu Offshore	21 (42)	31 (74%)	26 (62%)	27 (2.0%)	0.810	0.977	0.162 ±0.179	4 (19%)	0.00558 ±0.003	7.554 ±4.00	6.275 ±2.12
	CR (366 bp)									
	n	A	pA	poly	D_A	D_P		π	θπ	θs
Oahu Nearshore	13	3 (23%)	0 (0%)	2 (0.5%)	1.0 ± 0.0302	0.282 ±0.000		0.00154 ±0.0015	0.5641 ±0.551	0.6445 ±0.485
Oahu Offshore	14	3 (21%)	0 (0%)	2 (0.5%)	0.45 ± 0.0270	0.451 ± 0.124		0.0056 ±0.003	0.9011 ±0.747	0.6289 ±0.474

Table 4. AMOVA results of *P. lobata* from Maui: (a) Maui1 (Nearshore vs. Offshore Sites), and (b) Maui2 (Nearshore, Middle vs. Offshore Sites).

a.	Source of Variation	Variance components	% Variance	F_{ST}
H2	Between populations	0.794	20.3	
	Within populations	0.568	14.5	**0.241*****
	Within individuals	2.55	65.1	

b.	Source of Variation	Variance components	% Variance	F_{ST}
H2	Between populations	0.177	5.74	
	Within populations	1.457	47.31	0.057 (P = 0.238)
	Within individuals	1.446	46.96	

Table 5. Population genetic statistics of *P. lobata* from Oahu and Maui. See Table 2 for symbols and abbreviations.

	H2 (1352 bp)									
	n	A	pA	poly	hz	Ho	He	π	θπ	θs
Maui1	22 (44)	31 (70%)	24 (55%)	24 (1.8%)	1 (4.5%)	0.955	0.969	0.0050 ±0.003	6.780 ±3.62	5.5717 ±1.89
Maui2	27 (54)	32 (59.3%)	25 (46%)	49 (3.6%)	7 (26%)	0.741	0.948	0.0043 ±0.002	5.798 ±3.13	10.095 ±3.07
Maui (pooled)	49 (98)	56 (57.1%)	43 (44%)	52 (3.8%)	8 (16.3%)	0.837	0.961	0.00479 ±0.0025	6.473 ±3.42	10.083 ±2.78
Oahu	43 (86)	54 (62.8%)	42 (49%)	35 (2.6%)	9 (20.9%)	0.791	0.974	0.00597 ±0.0031	7.844 ±4.08	6.964 ±2.06
Oahu (pooled)	49 (98)	61 (62.2%)	48 (49%)	36 (2.7%)	12 (24.5%)	0.755	0.976	0.00596 ±0.0031	7.856 ±4.08	6.981 ±2.02

Table 6. Pairwise F_{ST} values for all populations from Oahu and Maui. The values were estimated using AMOVA in Arlequin with 5000 permutations. Below diagonal = F_{ST} values, Above diagonal = P-Values. The aster risks refer to the level of statistical significance. N: Nearshore, O: Offshore, M: Middle site.

	Oahu N	Maui1 N	Oahu O	Maui1 O	Maui2 O	Maui2 N	Maui2 M
Oahu N	-	0.2252	0.0000	0.0000	0.0000	0.0000	0.0000
Maui1 N	0.0071	-	0.0000	0.0000	0.0000	0.0000	0.0000
Oahu O	**0.0791****	**0.1155*****	-	0.1712	0.1622	0.0631	0.0000
Maui1 O	**0.1806*****	**0.2458*****	0.0108	-	0.1081	0.3874	0.0180
Maui2 O	**0.1687*****	**0.1896*****	0.0125	0.0290	-	0.1892	0.0090
Maui2 N	**0.2001*****	**0.2416*****	0.0416	0.0024	0.0235	-	0.0000
Maui2 M	**0.3730*****	**0.4985*****	**0.1540*****	**0.0885***	**0.1636****	**0.0719*****	-

FIGURES

Figure 1. Maps of sampling locations.

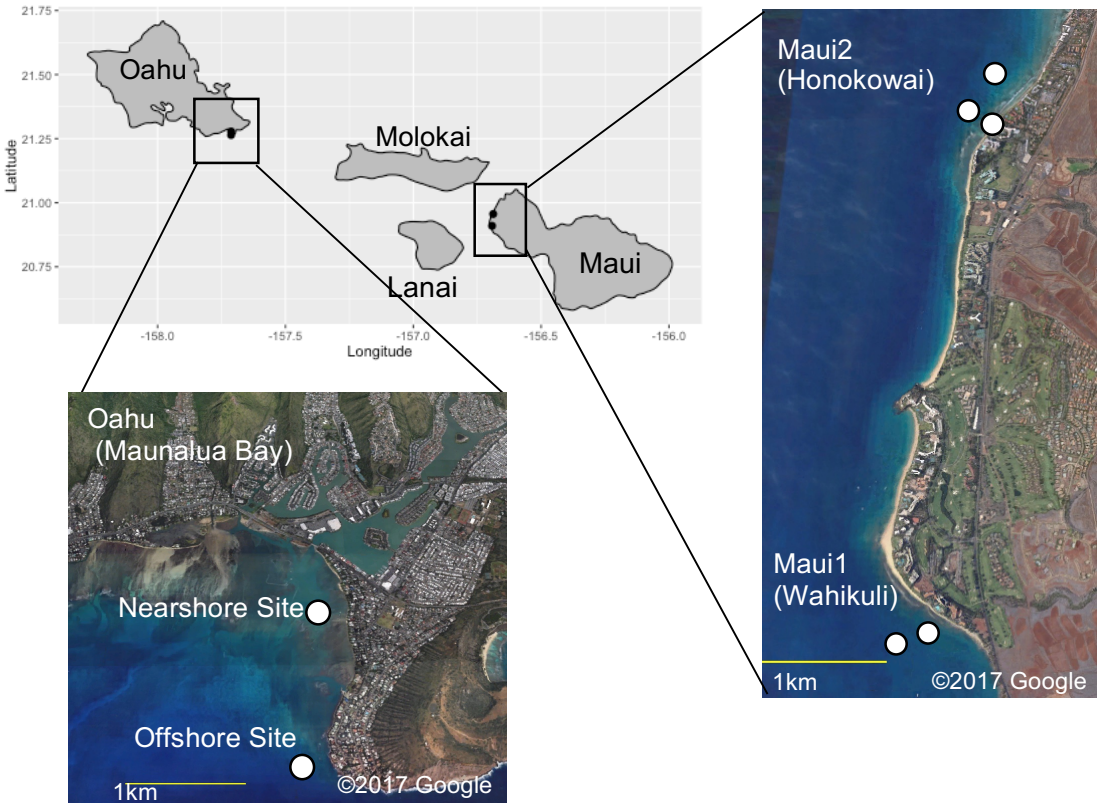

Figure 2. Locations of polymorphic sites across the genetic markers and their frequencies: (a) ITS and (b) Histone2 markers.

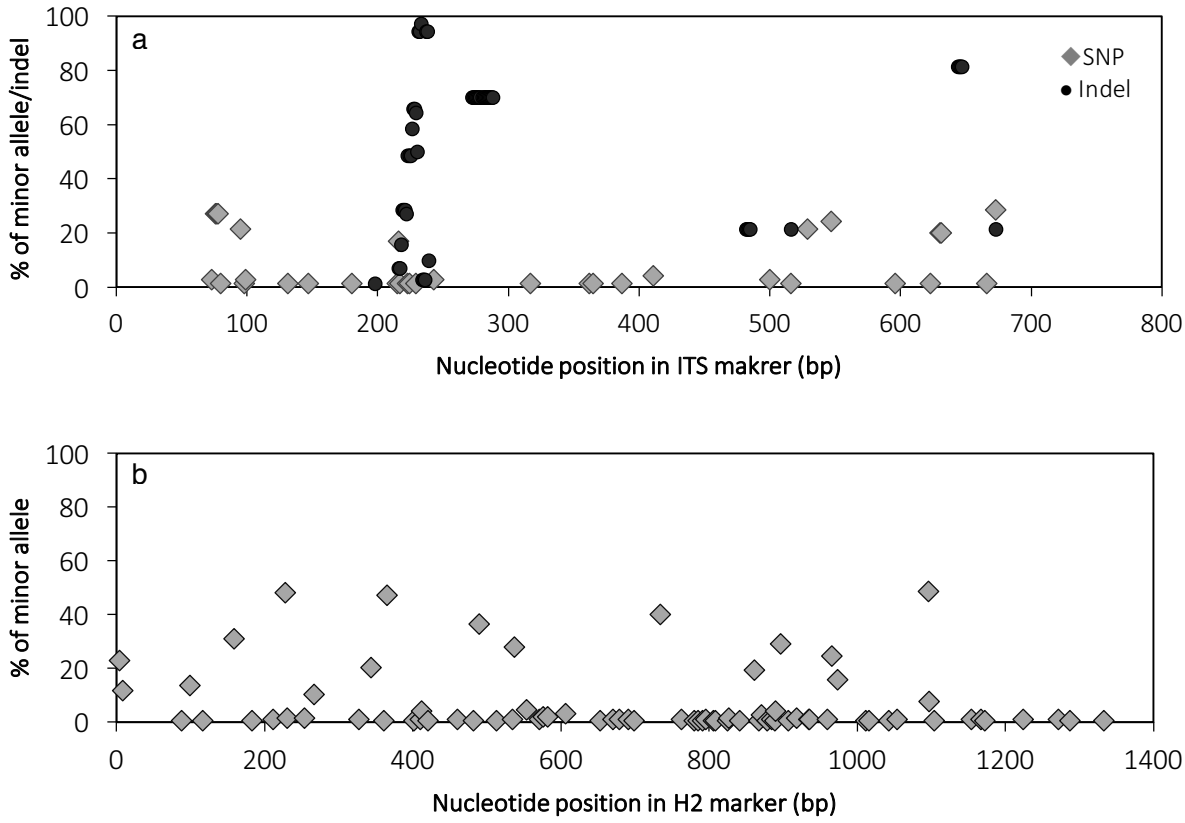

Figure 3. Diagrams of neighbor-net tree networks generated by SplitsTree v.4.14.2 for Oahu (Maunalua Bay) *P. lobata* populations, based on (a) ITS and (b) H2. Pie charts represent the proportion of sequences in each cluster.

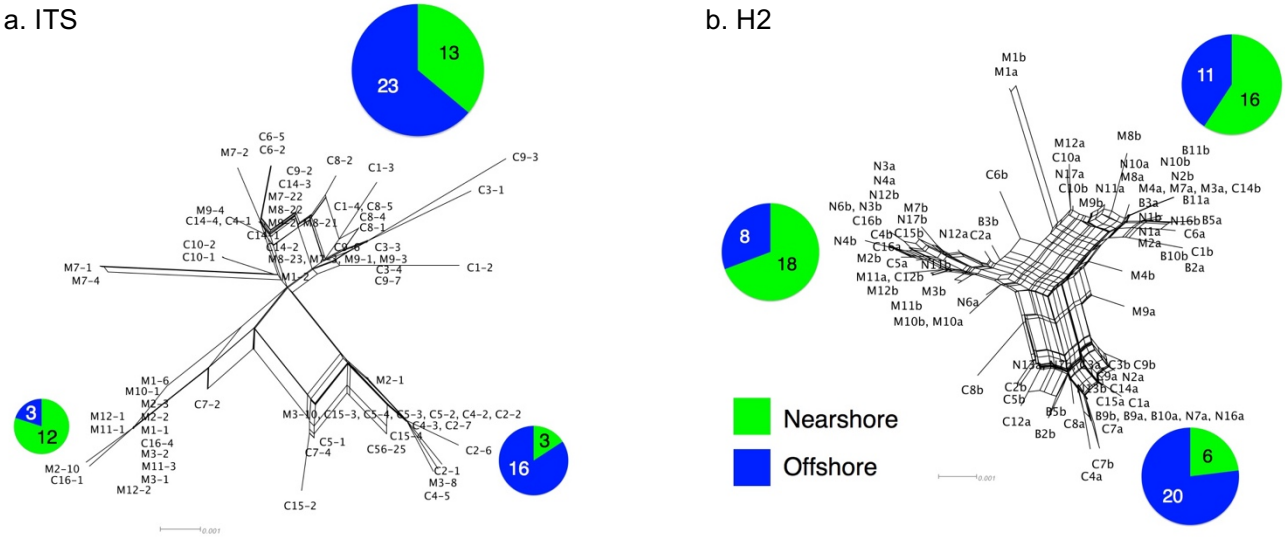

Figure 4. Haplotype network using the mitochondrial putative control region (CR) for the Oahu (Maunalua Bay) *P. lobata* populations.

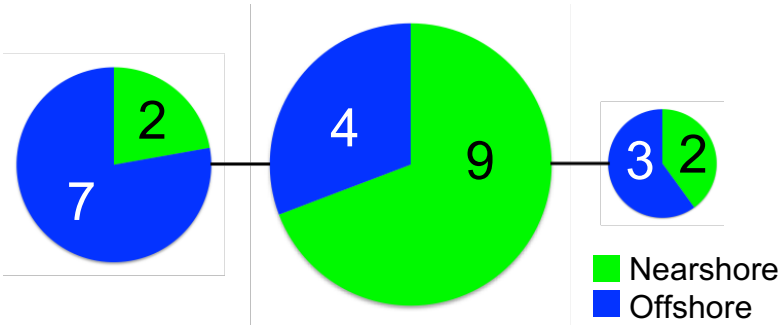

Figure 5. Summary of F_{ST} values between and within locations (Images ©2017 Google).

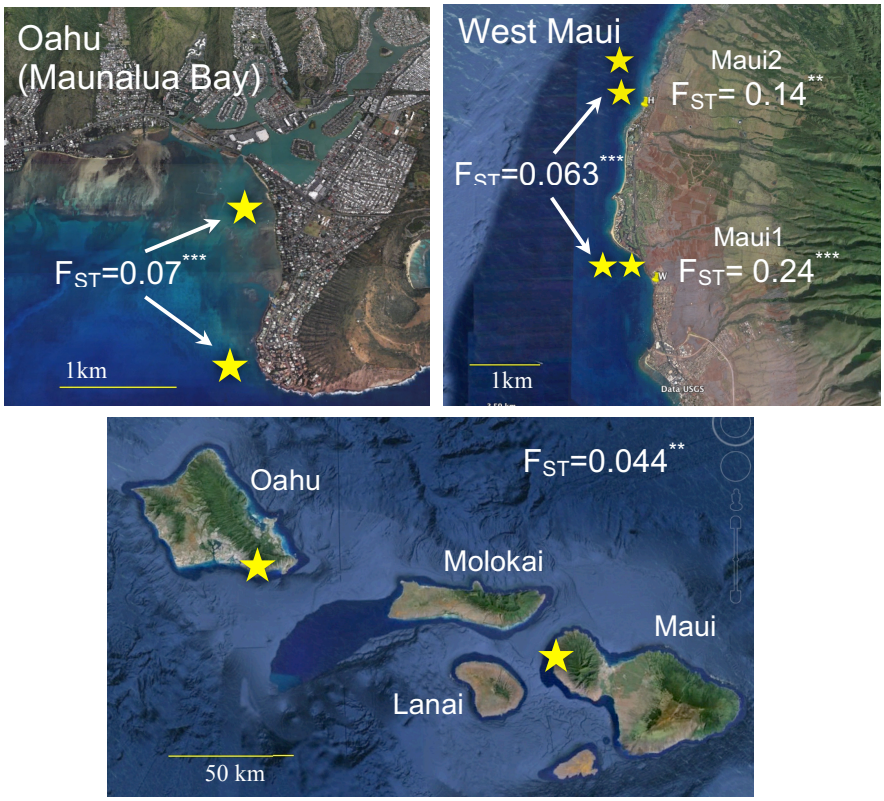

Figure 6. Diagrams of neighbor-net tree networks generated by SplitsTree v.4.14.2 for Oahu and Maui *P. lobata* populations based on phased H2 sequences. Colors are based on genetic clusters: Blue colors represent offshore populations, green colors represent the two genetically close, nearshore populations. The pie charts show the proportion of sequences present in each group.

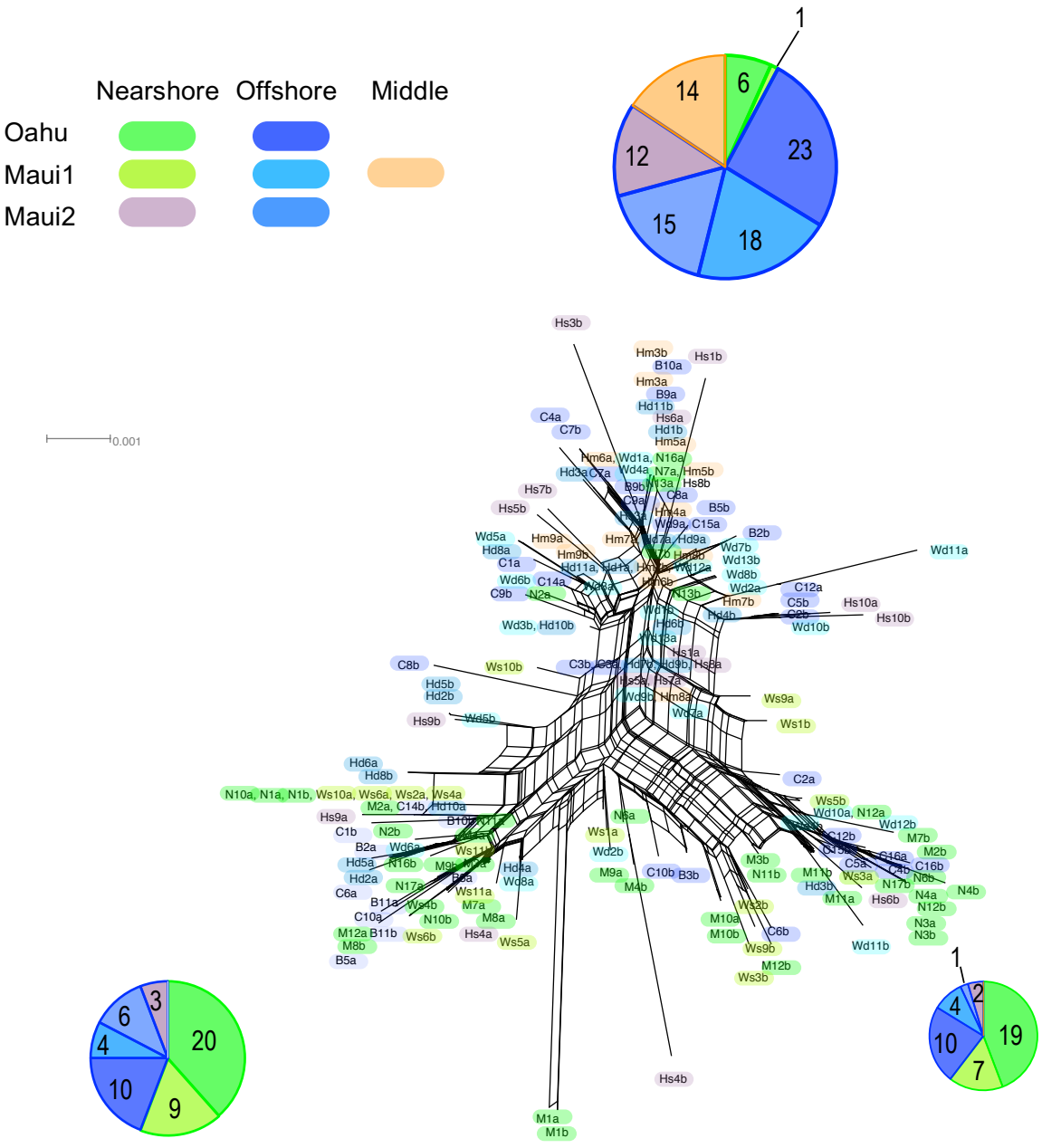

Figure 7. Diagram illustrating genetic connectivity of *P. lobata* populations. Solid arrows connect populations without significant genetic differentiation (non-significant F_{ST} values, Table 6), while dotted arrows represent populations with significant genetic differentiation (significant F_{ST} values). Colors corresponds to those of Fig. 6.

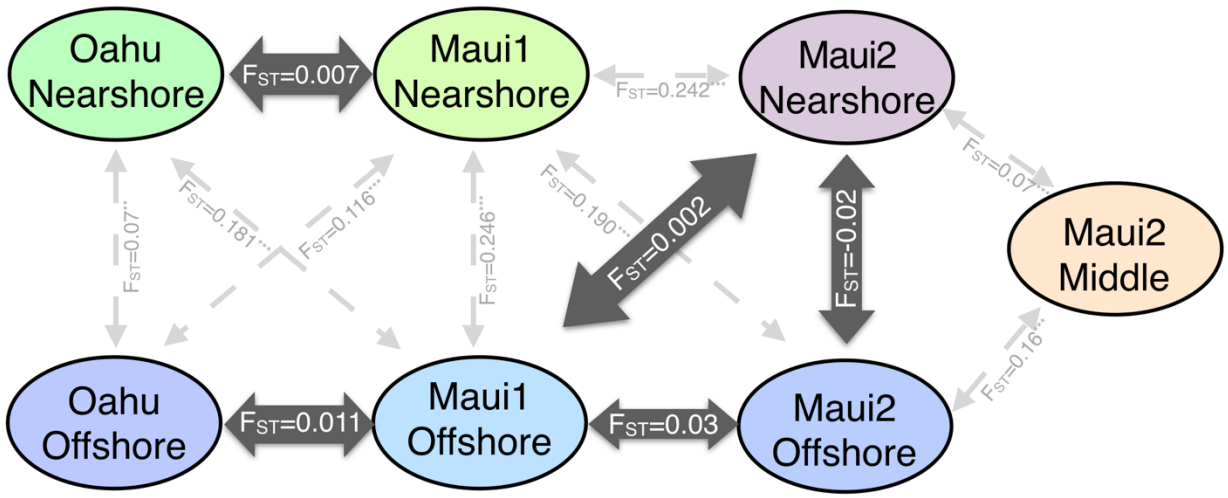

Figure 8. Map of Maui1 (Wahikuli) sampling location.

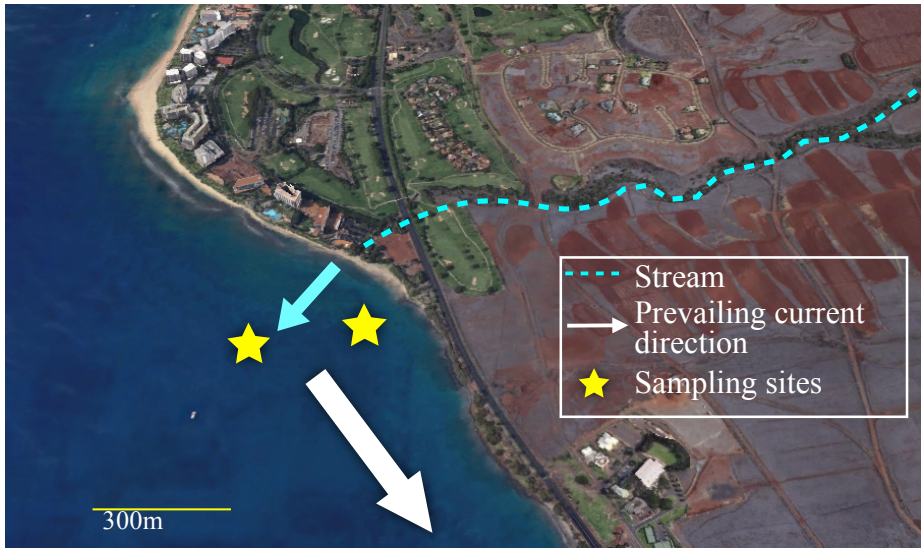

CHAPTER 2

Physiological and Molecular Responses Show Local adaptation of the lobe coral *Porites lobata* to the Nearshore Environment

Kaho H Tisthammer, Francois Seneca, & Robert H Richmond

ABSTRACT

Corals in nearshore marine environments are increasingly facing reduced water quality, which is the major local threat to coral reefs in Hawaii. Corals surviving in such conditions may have adapted to withstand sedimentation, pollutants, and other environmental stressors. Our previous studies revealed that the lobe coral (*Porites lobata*) populations at a high-stress nearshore site and a low-stress offshore site of Maunalua Bay, Hawaii had significantly different stress-induced protein expression profiles, as well as clear genetic differentiation. To understand whether selection is driving the observed genetic partitioning, a 30-day reciprocal transplant experiment and a common-garden experiment were conducted using the nearshore and offshore colonies of *P. lobata* from Maunalua Bay. Stress-related physiological and molecular responses were compared between the two genotypes. Physiological responses (tissue layer thickness, tissue lipid content, and short-term growth rates) all showed differences between the genotypes, revealing more stress resilient traits in the nearshore genotype. Cellular protein responses by Western blot analysis also highlighted the inherent differences in the metabolic state between the two genotypes. Our results of response differences across multiple phenotypes suggest that the observed genetic partitioning was due to local adaptation. This study also highlighted *P. lobata*'s potential ability to adapt relatively quickly to environmental change since the bay's environmental deterioration started within the last century. Such short-term adaptation, however, appeared to be responsible for a decrease in genetic diversity of the nearshore *P. lobata* population, which raises a concern for their future adaptive capacity since corals' ability to evolve under environmental stressors depends upon their underlying genetic diversity,

INTRODUCTION

Coral reefs are one of the most productive ecosystems on the plant, and are often called the rainforests of the ocean due to their complexity and biological diversity (Reaka-Kudla 1997). Coral reefs provide important benefits, not only to the incredibly diverse species that inhabit them, but also to hundreds of millions of people (Conservation-International 2008; Wilkinson 2008). Coral reef ecosystems worldwide are, however, highly threatened by local and global stressors as a result of human activities; coral cover around the world has declined over 50% in the past 100 years, if not more (Hughes *et al.* 2010; Richmond & Wolanski 2011; Graham 2014). Rates of current environmental change are orders of magnitude faster than those of ice age transitions (Hoegh-Guldberg *et al.* 2007), so the fate of coral reefs will ultimately depend on whether corals and their ecosystems can adequately adapt (with physiological and ecological modifications) to such rapid environmental changes. Understanding coral's short-term adaptive ability is critical in order to accurately predict the future of coral reefs. Climate change, a global stressor which causes elevated sea surface temperature and changes in water chemistry, is viewed as the dominant threat to coral reefs; however, localized anthropogenic stressors, such as overfishing, pollution, and coastal development, also play significant roles in the decline of coral reefs (Aswani *et al.* 2015; Morgan *et al.* 2016). Because coral reefs experiencing multiple stressors have a lower ecosystem resilience (West & Salm 2003; Carilli *et al.* 2009; Richmond & Wolanski 2011; Kennedy *et al.* 2013; Ban *et al*. 2014), understanding the effects of local stressors and coral's adaptability to such stressors is vital as global level stressors continue to increase.

Nearshore marine habitats are increasingly facing reduced water quality due to human actions (Wenger *et al.* 2015), and reduced water quality is one of the major local threats to coral reefs, especially in Hawaii. The health of coral reefs in Maunalua Bay, Oahu has deteriorated due to large-scale urbanization that began in the last century (Wolanski *et al.* 2009). The corals in Maunalua Bay, especially in the nearshore areas, are under chronic stress from sedimentation and toxicant/pollutant laden terrestrial runoff (Richmond 2011). Despite prolonged exposure to these stressors, some individual corals continue to survive in the bay, suggesting these individuals may have acclimatized or adapted to withstand such stressors. A physiological survey showed that the cellular stress responses in the lobe coral *Porites lobata* differed between

those growing in the nearshore area exposed to reduced water quality and colonies from the relatively clean offshore area. The levels of stress-induced proteins, such as multixenobiotic resistance proteins, cytochromes P450, and heat shock proteins, were correspondingly elevated in corals from the nearshore site, compared to those from the offshore site (Richmond 2011) (Fig. 1). Population genetic structure analysis also revealed a clear genetic differentiation between the nearshore and offshore populations in Maunalua Bay (Tisthammer et al. 2017). Because the distance between the two sites is small (< 2 km), with no apparent barriers (Presto *et al.* 2012), the results suggest the possibility of local selection as the driving force of the observed genetic partitioning (Tisthammer et al. 2017).

Based on these results, we tested whether the observed genetic differentiation between the nearshore population ('nearshore genotype') and the offshore population ('offshore genotype') in *P. lobata* at Maunalua Bay was due to local adaptation, using reciprocal transplant and common garden experiments. *P. lobata* in Maunalua Bay offers a unique opportunity to study the coral's short-term adaptability at a population level, since the environmental change at the bay has been well-documented, and the bay's physical and chemical water properties have been characterized. The species *P. lobata* also allows us to assess coral host's adaptive abilities, as opposed to that of its endosymbiotic zooxanthellae, since *P. lobata* primarily harbors *Symbiodinium* Clade C15 (LaJeunesse *et al.* 2004; Smith *et al.* 2008; Barshis *et al.* 2010; Fabina *et al.* 2012) which is vertically transmitted with high fidelity (Fabina *et al.* 2012). No shuffling of *Symbiodinium* in *P. lobata* has been reported, to our knowledge. We focused on the physiological and cellular stress response differences in the two *P. lobata* genotypes, asking whether the nearshore genotype had higher tolerance to reduced water quality than the offshore genotype. Our goal was to capture the response difference between the two genotypes using key stress-related proteins, and physiological responses, rather than to understand the causal effects of particular biomarker proteins and stressors. Assessing tissue layer thickness, tissue lipid content, growth rate, and stress-related protein expression profiles of *P. lobata,* we observed clear response differences between the two genotypes; the nearshore genotype displayed more resilient physiological traits (tissue thickness, growth rate), and the patterns of stress-induced protein expressions differed markedly.

MATERIALS AND METHODS

Sample Collection and Reciprocal Transplant Experiment

Five individual *P. lobata* colonies, previously tagged and genotyped, were selected as source colonies from the nearshore and offshore sites for the reciprocal transplant experiment. All samples were identified as *P. lobata* through colony morphology, corallite skeletal morphology, and sequence analysis of Histone2 marker (Tisthammer *et al*. 2017). Sequence analysis confirmed that all of them belonged to the Clade I of *Porites* phylogeny (Forsman *et al.* 2009).

Up to ten small fragments (approximately 1.5 cm in diameter) from each source colony were collected using tin snips or chisel and hammer, from the upward facing surface on April 15, 2015. One sample was immediately frozen on shore using liquid nitrogen and another was fixed in 10% Z-fix in filtered seawater for baseline data. Half of the remaining coral fragments from each colony were cross-transplanted to the other location, and the remaining half were back-transplanted to their original location, for 30 days (Fig. 2) Temperature profiles were measured by deploying a data logger (HOBO®, Onset Computer, Bourne, MA) at each site. Extensive chemical and physical data of Maunalua Bay's sediments and water were referenced from previous studies (Richmond 2009; Storlazzi *et al.* 2010; Presto *et al.* 2012). On May 15, 2015, the coral samples were retrieved from the experiment sites, and one fragment of each source colony at each location was flash frozen on site using liquid nitrogen and stored at -80℃ at the Kewalo Marine Laboratory (KML), University of Hawaii at Manoa, for protein analyses. The other source colony fragments were fixed in Z-fix for physiological assays.

Tissue Layer Thickness & Tissue Lipid Content Assessment

The coral fragments preserved in Z-fix were rinsed with distilled water and dried at room-temperature overnight. All coral fragments were then cut in half vertically, and the thickness of the exposed tissue layer was measured to the nearest 0.01 mm using a digital caliper. Ten measurements were taken from each specimen, to account for the variability within a sample, and the results were compared among treatments using nested 2-way ANOVA (testing the effects of genotype, transplant-site, and interaction), followed by Tukey HSD post hoc test.

The dried coral fragments were then used to analyze the total tissue lipid content of holobionts using the modified method of Stimson (1987). The dried samples were first decalcified in ~10% hydrochloric acid. The decalcified samples were then rinsed with distilled

water, and placed in 50 mL polypropylene centrifuge tubes containing an adequate volume of chloroform-methanol (2:1) for over 24 hours for lipid extraction. The solvent-extract solution was decanted into a pre-weighed glass beaker through a coarse paper filter, and the filter and remaining tissues were rinsed with additional fresh chloroform-methanol solvent. The solvent was evaporated at 55°C, and the remaining extracts were weighted to the nearest 0.1 mg. The remaining tissues were dried completely at room temperature and weighed to the nearest 0.1 mg. The total lipid content is expressed as percent lipid per dried tissue (w/w). The results were compared among treatments using 2-way ANOVA, followed by Tukey HSD test, as in the tissue layer thickness results.

Cellular Protein Assessment Using Western Blot

The frozen coral fragments were pulverized using a chilled mortar and a pestle. Proteins (the S9 post-mitochondrial fraction of coral protein) were then extracted and quantified using the bicinchoninic acid (BCA) assay as described in Murphy and Richmond (2016). Equal amounts of protein aliquots (35-45 µg) were separated by SDS-PAGE on 10% polyacrylamide gels. The resulting gels were transferred onto PVDF membranes (EMD Millipore, Billerica, MA) using a wet transfer system (Mahmood & Yang 2012). Correct protein transfer was confirmed by staining the membranes by Ponceau S Solution (Biotium, Fremont, CA), as well as staining the gels with Coomassie Brilliant Blue R-250 to visualize the leftover proteins. For each blot, 22.5-45 µg of HeLa Whole Cell Lysate (Santa Cruz Biotechnology, Dallas, TX) was included as an internal control for signal differences across blots and quantification. The membranes were blocked in 5% non-fat dry milk (Carnation, Los Angeles, CA), and incubated with the following primary antibodies overnight at 4℃: anti-Ig-1 (SOD1) antibody (IgG rabbit clone, sc-11407, Santa Cruz Biotechnology, 1:2500 dilution), anti-catalase antibody (IgG rabbit clone, sc-50508, Santa Cruz Biotechnology, 1:1000 dilution), anti-Ferrochelatase antibody (IgG rabbit clone, sc-99138, Santa Cruz Biotechnology, 1:1000 dilution), anti-cytochrome P450, family 1, member A1 (CYP1A) antibody (IgG rabbit clone, sc-20772, Santa Cruz Biotechnology, 1:1000 dilution), anti-phosphoglycerate kinase 1/2 (PGK) antibody (IgG mouse clone, sc-166432, Santa Cruz Biotechnology, 1:500 dilution), anti-calmodulin (CaM) antibody (IgG rabbit clone, sc-5537, Santa Cruz Biotechnology, 1:500 dilution), anti-transgelin antibody (IgG rabbit clone, sc-50446, Santa Cruz Biotechnology, 1:1000 dilution), anti-actin antibody (IgG goat clone, sc-1615, Santa

Cruz Biotechnology, 1:2000 dilution) and anti-Hsp60 antibody (IgG mouse clone, ADI-SPA-807, Enzo Life Sciences, 1:2000 dilution equivalent).

The blots were washed in phosphate buffered saline with Tween 20 (PBST) four times, and incubated in either an HPR (horseradish peroxidase) conjugated goat anti-rabbit secondary antibody (sc-2004, Santa Cruz Biotechnology, 1:5000 dilution), an HPR-conjugated goat anti-mouse secondary antibody (sc-2005, Santa Cruz Biotechnology, 1:5000 dilution), or an HPR - conjugated bovine anti-goat secondary antibody (sc-2350, Santa Cruz Biotechnology, 1:5000 dilution) for one hour at room temperature. Blots were again washed four times in PBST, and binding was visualized with the WesternSure® PREMIUM Chemiluminescent Substrate on the C-DiGit® Blot Scanner (LI-COR Biosciences, Lincoln, NB).

Band signal (net-intensity) quantification was performed using Image Studio™ Software (LI-COR Biosciences). Each image was defined using a rectangle, an ellipse, or a customized shape and the background was subtracted using the Median method. Blots were run with different combinations of treatment samples, and normalized using the overlapping samples to compare across membranes. Data were expressed as the mean ± standard deviation of the means (SEM). Two-way ANOVA, followed by Tukey HSD test for pair-wise comparison of means was performed for all normalized net intensity values obtained from different groups of samples to assess significant differences.

Common Garden Experiment

Five coral fragments were collected from the nearshore and offshore sites in Maunalua Bay. The live coral fragments were transported back to KML and further divided into six small nubbins of approximately 2 cm^2 per sample, and glued to a ceramic tile with marine epoxy and a tag indicating the source colony and site. The 30 nubbins from each site were then placed in an outdoor flow-through seawater tank at KML with a temperature logger. The coral nubbins were left in the tank for three weeks for healing, and then the buoyant weight of each nubbin was measured weekly for 11 weeks to the nearest 0.01g using a digital scale (Ohaus SPX222, Parsippany, NJ). The coral nubbins were placed randomly in the tank every week to eliminate the tank effect. The average % gain of five individuals relative to their initial weights was log transformed and analyzed using ANOVA.

RESULTS

During the 30-day reciprocal transplant experimental period, there were no storms, and precipitation was minimal. Mortality, partial mortality, and bleaching were not observed in the experimental coral nubbins, other than losing several nubbins that detached from the tiles. The temperature fluctuation was larger for the nearshore site; the maximum and minimum seawater temperatures during the experimental period were 28.6 ℃ and 23.8 ℃ for the nearshore site, and 27.7 ℃ and 24.4 ℃ for the offshore site (Fig. S1). The average temperature was 25.4 ℃ at the nearshore site and 24.4 ℃ at the offshore site. The maximum light intensity was 159.31 photosynthetic photon flux density (PPDF) (8611.2 Lux) at the nearshore site and 395.08 PPDF (21355.7 Lux) at the offshore site (Fig. S1).

Physiological Responses

1. Tissue Thickness

The average tissue layer thicknesses of coral samples were compared among the four treatments (two genotypes x two transplant sites, [genotype][transplant-site] NN, NO, OO, ON). The results of ANOVA (Table 1) showed significant genotype, transplant-site, and interaction effects. Tukey HSD test revealed that the offshore genotype transplanted to the nearshore site (ON) had a significantly thinner tissue thickness, compared to the rest of the treatments (Tukey HSD P-value < 0.001) (Fig. 3a). No other treatments resulted in significantly different tissue thickness.

2. Lipid Content

The average total lipid contents were compared among the four treatments, as in the tissue thickness comparison. The offshore genotype had a marginally higher average lipid content when transplanted to the nearshore site (ON) than to the offshore site (OO) (Tukey HSD, $p = 0.059$). The nearshore genotype showed very little difference in lipid content between the sites (Fig. 3b). The 2-way ANOVA showed no genotype or transplant-site effects, but resulted in a significant interaction between the genotype and site (Table 2).

Protein Response

1. Antibody Recognition

The following antibodies recognized the presence of the targeted protein biomarkers in the coral homogenate extracts; anti-SOD1, anti-ferrochelatase, anti-PGK, anti-Hsp60, anti-catalase, anti-CaM, anti-CYP1A, anti-transgelin, and anti-actin (Fig. S2). The protein expression levels were compared among the treatments. The results revealed clear differences in expression patterns of the six biomarker proteins between the nearshore and offshore genotypes, and the results fell into either of the two following patterns; 1) only one genotype showing the transplant effect, and 2) the overall expression levels differing between the two genotypes, regardless of the transplant site.

2. Pattern 1: Transplant effects present in only one genotype

Three biomarker proteins, SOD1, Ferrochelatase and PGK, from Western analysis exhibited the pattern in which one of the genotypes showed a significant transplant-site effect, while the other genotype showed no such response. The polyclonal antibody anti-SOD1 recognized an approximately 15 kDa band, slightly smaller than 17 kDa of the HeLa whole cell lysate (Fig. S2a). There was a significant transplant-site effect on SOD1 expressions ($F = 8.59$, $df = 1$, $P =$ Table S1 $= 0.0098$), and Tukey HSD test revealed significant downregulation of SOD1 only in the nearshore genotype transplanted to the offshore site (NO), compared to the nearshore site (NN) ($P = 0.036$, Table S2). The offshore genotype showed no difference in SOD1 expression level between the transplant-sites (Tukey HSD, $P = 0.690$) (Fig. 4a). For ferrochelatase, the polyclonal antibody produced approximately 70 kDa and 40 kDa bands, which were assumed to be the homodimer and the monomer of ferrochelatase, respectively (Fig. S2b). The monomer bands were faint and therefore not used for quantification. In ferrochelatase (homodimer), significant genotype, transplant-site, and interaction effects were observed ($F = 4.66$, $df = 1$ $P = 0.047$; $F = 9.36$, $df = 1$, $P = 0.0075$; $F = 5.31$, $df = 1$, $P = 0.035$, Table S1b). The pairwise comparison revealed that only the nearshore genotype showed significant upregulation when transplanted to the offshore site (NO) (Tukey HSD, $P = 0.0282$, Table S2), while the expression levels in the offshore genotype did not differ between the transplant-sites, as in SOD1 (Tukey HSD, $P = 0.9996$) (Fig. 4b). The monoclonal antibody anti-PGK produced an

approximately 45 kDa band, which was almost the same size as the band of the HeLa lysate (Fig. S2c). For PGK, a significant transplant-site effect was observed ($F = 8.82$, $df = 1$, $P = 0.009$, Table S1c), but the pattern was reversed, and slight upregulation was observed in the offshore genotype transplanted to the nearshore site (Tukey HSD, $P = 0.0854$, Table S2), but not in the nearshore genotype (Fig. 4c).

3. Pattern 2: Genotypic difference in the overall expression level

The second pattern of protein biomarker responses observed from the Western analysis highlighted the genotype differences in the protein expression levels. Three proteins, Hsp60, Catalase, and CaM-binding protein, followed this pattern, showing no genotypic differences in transplant effect (direction of change), but differences in the overall expression levels. The monoclonal antibody anti-Hsp60 recognized an approximately 60 kDa band, the same size as the band from the HeLa whole cell lysate (Fig. S2d). The 2-way ANOVA revealed that there were significant differences in the expression level of Hsp60 between the transplant-sites ($F=9.670$, $df = 1$, P-value = 0.00674), as well as between the genotypes ($F=5.648$, $df = 1$, P-value = 0.0303) (Fig. 4d, Table S1d). In both genotypes, Hsp60 was upregulated at the nearshore site compared to the offshore site, and the offshore genotype had a consistently higher expression level than the nearshore genotype.

The polyclonal antibody anti-catalase recognized an approximately 60 kDa band, slightly smaller than 67 kDa of the HeLa whole cell lysate (Fig. S2e). Similar to Hsp60, the 2-way ANOVA revealed that there were significant differences in the expression level of catalase between the transplant-sites ($F=9.4$, $df =1$, P-value = 0.007), as well as between the genotypes ($F=11.5$, $df =1$, P-value= 0.0035, Table S1e). Catalase was upregulated at the offshore site in both genotypes, and the expression level was consistently higher in the offshore genotype than in the nearshore genotype (Fig. 4e). The polyclonal antibody anti-CaM recognized an approximately 14 kDa band, as well as a band of approximately 55 kDa (Fig. S2f). The 14 kDa band was assumed to be calmodulin or calmodulin-like 2 (CALML3) protein, which was slightly smaller than the 17 kDa of CaM in the HeLa whole cell lysate. The 55 kDa band was assumed to be one of the calmodulin binding proteins. The Western analysis of CaM (14 kDa bands) did not yield clear, consistent results, on which to perform quantitative analysis, and only the 55 kDa

CaM-binding protein was used for quantification. A significant difference in the expression level was observed between the genotypes (F=8.767, P-value = 0.00875) (Fig. 4f), while no difference was observed between the transplant-sites in both genotypes (F=1.302, P-value = 0.2697, Table S1f).

4. No Difference

The protein biomarker CYP1A, as well as actin, showed no significant difference between the transplant-sites and genotypes (Fig. 5). The polyclonal antibody anti-CYP1A recognized an approximately 60 kDa band, and the polyclonal antibody anti-actin recognized a 43 kDa band, the expected size of actin. The protein expression levels were assessed using 2-way and 1-way ANOVA with Tukey HDR tests, but no significant difference was observed among treatments (Table S1g, h, Table S2). However, did we notice a consistent lack of expression of CYP1A in one of the offshore individuals (Fig. S2g, O1-individual), while the rest of the individuals had bands at approximately 60 kDa.

Short-Term Growth Rate

The average growth rate of *P. lobata,* measured using buoyant weight, differed significantly between the nearshore and offshore genotypes. The nearshore genotype corals grew on average 5.57% of their initial weight over 11 weeks (August to October, 2016), while the offshore genotypes grew 2.57% (Fig. 6, ANOVA, F = 13.09, p = 0.0068, Table 3). During the experimental period, the maximum tank water temperature was 29.95 ℃ and the minimum temperature was 24.55 ℃, with an average of 27.93 ℃. The maximum light intensity was 2141.08 PPFD (115,734.1 Lux), and the daytime average was 53.40 PPFD (2886.3 Lux). The shade cover was placed over the tank during the experimental period, except for one weekend when a hurricane was approaching. Eliminating the days without the shade cover resulted in the maximum light intensity of 815.65 PPFD (44089.2 Lux), with a daytime average of 41.31PPFD (2232.8 Lux).

DISCUSSION

Physiological Response Differences Between the Genotypes

The reciprocal transplant experiment revealed physiological response differences between the nearshore and offshore genotypes. The difference was clearly seen in the tissue layer thickness of *P. lobata*. The transplantation caused a significant reduction in the average tissue layer thickness only in the offshore individuals transplanted to the nearshore site (ON). The tissue layer thickness of *Porites* is known to be reduced by sedimentation and other environmental stressors (Barnes & Lough 1999; Rotmann & Thomas 2012), which was observed in the offshore genotype in this study. The nearshore genotype, however, did not show any difference in tissue thickness between the transplant sites. Sedimentation (measured as turbidity or suspended sediment concentration [SSC]) is one of the biggest environmental parameters that differ between nearshore and offshore sites. Mean turbidity differs an order of magnitude between the sites, with 150-180 Nephelometric Turbidity Units (NTU) at the nearshore site, and 12-50 NTU at the offshore site (Nov. '08, Feb. '09, Strolazzi et al 2010). SSCs also showed the most difference (orders of magnitude) between the sites, especially during and after a storm (Richmond, 2011). High turbidity at the nearshore site can also be inferred from its extremely low light intensity level (Fig. S2). Therefore, the observed difference in the tissue layer thickness probably is due to sedimentation stress, which thereby reflects higher resiliency of the nearshore genotype to sedimentation stress.

Contrary to our initial expectation that environmental stress might reduce the total tissue lipid content in corals, the offshore genotype transplanted to the nearshore site showed an increase in tissue lipid content, while the nearshore genotype did not show any change in lipid content between the transplant sites. High sedimentation is known to alter corals' metabolism by increasing the energy gains from heterotrophic sources (Anthony & Fabricius 2000; Fabricius 2005; Baumann *et al.* 2014). A study by Seemann *et al.* (2012) showed that the coral *Stylohora subseriata* transplanted to a eutrophic, nearshore site had increased lipid content, possibly through an increase in both phototrophic and heterotrophic feeding. However, *Porites* species appear to lack an ability to increase their feeding rate to meet their daily metabolic energy requirements through heterotrophy; no increase in the feeding rate was observed in *Porites cylindrica* exposed to increased suspended particles and shading, and less than 10% of its energy

budget was met heterotrophically in this experiment. *Goniastrea retiformis*, on the other hand, doubled their feeding rate and fully compensated their daily metabolic energy requirements in the same experiment (Anthony & Fabricius 2000). *Porites compressa* and *P. lobata* also did not increase their feeding rate after bleaching, thus their lipid content decreased significantly, while colonies of *Montipora capitata* and *M. verrucosa* showed a substantial increase in heterotrophically acquired carbon and maintained/recovered their lipid content after bleaching (Grottoli *et al.* 2004; 2006). These observations suggest that it was unlikely that the offshore genotype increased its lipid content through increased heterotrophic feeding, but more studies will be needed to uncover the reasons behind the observed phenomenon.

Additionally, comparing lipid content before and after the transplant experiment revealed that lipid content of the offshore genotype increased significantly after the experiment at both sites, while the nearshore genotype showed no difference between before and after the experiment (Fig. S3). One explanation may be due to reproduction (although this does not explain the transplant response difference between the offshore and nearshore sites in the offshore genotype); *P. lobata* is gonochoric spawner with its peak in June and July (Richmond & Hunter 1990), and the experiment took place during the pre-reproductive season of April to May. Oku *et al.* (2003) reported that lipid content in *Goniastrea aspera* showed seasonal variations, with higher content in summer and lower in winter. Lipid biosynthesis was therefore suggested to be linked to oocyte development, as well as light intensity and temperature (Oku *et al.* 2003). The sex of the source colonies used in our experiments are unknown. Identifying the sex of *Porites* colonies is extremely difficult, as visible oocyte or spermary development needs to be captured in histological analysis. However not all tissues contain oocytes or spermaries, and not all colonies are reproductively active (Oliver, T. Pers. comm.; Tortolero-Langarica *et al.* 2016). It is possible that the offshore samples had more female colonies than the nearshore samples, resulting in differences in lipid content. Another possibility is that reproductive activities were suppressed in the nearshore individuals due to higher environmental stress. Still little is known about 1) interspecific and intraspecific variability, as well as seasonal changes in lipid content in corals, 2) specific sources of lipid carbon, and 3) heterotrophic plasticity in corals. Available information suggests that lipid metabolism differed substantially from species to species, and even from colony to colony (e.g. Anthony:2000uk; Teece:2011ir; Hinrichs *et al.* 2013), which

makes it difficult to draw a precise conclusion from our results. If the sex ratio of source colonies was equal between the sites, only then would the two genotypes showed different responses to transplanting in terms of lipid content. In this case, this may reflect the differences in life history strategy between the two genotypes, investing in lipid storage *vs*. growth or tissue growth.

Protein Expression Differences Between the Genotypes

In six out of the eight biomarker proteins analyzed in this study, a clear response difference was observed between the nearshore and offshore genotypes; the transplant effect was observed in one genotype but not the other in three proteins (SOD1, Ferrochelatase, and PGK), and the differences in the overall expression levels between the two genotypes were observed in other three proteins (Hsp60, catalase, and CaM-binding protein) (Fig. 4). The direction of the changes (up- or down-regulation) and the responding genotype varied for these biomarker proteins, and are likely to be protein specific. We do not have enough knowledge to predict how these proteins may respond to different environmental stressors, especially in a field experiment where corals experience multiple stressors. Therefore, our objective was to assess the response differences of stress-related proteins between the genotypes. Our results highlighted the genetic differences for the observed molecular responses, although precisely how these differences translate to resilient traits from environmental stressors has yet to be determined.

Implications of biomarker proteins

SOD1 is the primary enzyme involved in cellular antioxidant activity. It converts the oxygen radical ($\cdot O_2^-$) to H_2O_2 (Fig. 7), and is often upregulated with exposure to oxidative stress. This trend was observed in the nearshore genotype at the nearshore site, but not in the offshore genotype (Fig. 4a). The results suggest that the ability of the nearshore genotype to upregulate SOD1 at a greater extent in a stressful environment may be contributing to its resilience. Catalase is another important antioxidant enzyme involved in the breakdown of H_2O_2 (Fig. 7). Although studies have reported a correlation between the enzymatic activities of SODs and catalase under some conditions in marine invertebrates (e.g. Maria & Bebianno 2011), the expression levels (abundance) of these proteins may not always show a strong correlation (Tomanek 2014). In this study, the expression levels of catalase were not correlated to the expression levels of SOD1. Also, no correlation of SOD1 and catalase was observed in another experiment using *P. lobata*

(Tisthammer, unpublished data). This discrepancy may be due to an extremely rapid turnover rate of catalase (Nicholls *et al.* 2000); an increase in stress does not necessarily result in an increase in catalase expression levels, but will result in an increase in SOD1. Based on our results, we speculate that SOD1 and catalase expressions do not necessarily correlate in corals. It is also likely that corals rely more on other redundant antioxidant pathways to reduce H_2O_2, such as glutathione peroxidase (Fig. 7). The initial results from our proteomic analysis using liquid chromatography tandem mass spectrometry (LC-MS/MS) of the same experimental samples validated the directions and trends of SOD1 and catalase (unpublished data). The detailed proteomic analysis currently underway will provide finer resolution as to the relationships between the antioxidant enzymes, as well as other metabolic pathways involved in environmental stress responses.

Ferrochelatase is an enzyme involved in the terminal stage of the heme biosynthetic pathway in all cells (Ferreira *et al.* 1995). Studies have reported that the expressions of ferrochelatase in corals increased when exposed to stressors, such as exposure to the antifouling paint ingredient Irgarol in *Madracis mirabilis* (Downs & Downs 2007) and IFO -180 fuel oil in *Pocillopora damicornis* (Rougée *et al.* 2006). However, gene expressions of ferrochelatase in *Acropora millepora* was significantly downregulated under macroalgal exposure (Shearer *et al.* 2012), and ferrochelatase expression and porphyrin metabolism in general, were significantly downregulated in *P. damicornis* at a field site where a landfill was the source of PCBs and other contaminant exposures (Downs *et al.* 2012). Therefore, response direction of ferrochelatase appears to be stress-specific, and how the ability to up- or down-regulate ferrochelatase translates into corals' resilience is unclear at this point. PGK is an enzyme that catalyzes the formation of ADP to ATP in glycolysis, as well as converts ATP back to ADP (Campbell, 1996). Only the offshore genotype showed significant upregulation of PGK at the nearshore site (Fig. 4c). This may suggest enhanced metabolic activities in the offshore genotype at the nearshore site. In summary, both Ferrochelatase and PGK had clear response differences between the genotypes, which suggests that both enzymes are effective biomarkers for stress response in corals. However, further studies will be needed to understand more precise roles of ferrochelatase and PGK in stress response and adaptive traits in corals.

The offshore genotype had higher expressions of Hsp60 than the nearshore genotype at both sites. This trend was also confirmed by our proteomic analysis results, as significant

upregulation of Hsp60 in the offshore genotype, compared to the nearshore genotype at the nearshore site, indicating the stress level experienced by the offshore genotype was likely higher than the nearshore genotype. CaM-binding protein had an opposite trend from Hsp60, where the nearshore genotype had higher expressions than the offshore genotype at both sites. The size of the CaM-binding protein was approximately 55 kDa, but the nature of this protein is unknown. A family of 60 kDa CaM-binding proteins in plants is reported to be involved in abiotic and biotic stress responses (Wan *et al.* 2012), including induction of defense responses (Ali *et al.* 2003) and positive regulations of plant immunity (Truman *et al.* 2013). The CaM-binding protein of corals may have similar functions. CaM itself is a highly conserved, small messenger protein that binds and regulates a suite of different protein targets. CaM of approximately 14 kDa was observed in our Western blot analysis, and the pattern of its expressions was similar to the CaM-binding protein. Our proteomic analysis also confirmed this pattern. We know little about how CaM or CaM-binding proteins respond to environmental stressors in corals, but our results highlighted the genotype differences in their responses. In summary, the three proteins, Hsp60, catalase, and CaM-binding protein, showed differences in overall expression levels between the genotypes, suggesting that the two genotypes' metabolic states may be inherently different. Simple generalizations of protein expression patterns cannot be made since the responses are highly protein-specific, but there does seem to be a genetic-basis for the observed protein responses.

Regarding the xenobiotic response protein, CYP1A, neither genotype showed significant changes in its expression. The previous survey (Richmond, 2011) resulted in a detection of significant upregulation of biomarker proteins involved in xenobiotic metabolism (CYP1A, MXR) in corals collected from the nearshore site. Therefore, we predicted CYP1A would be upregulated at the nearshore site. The offshore genotype appeared to show slight upregulation of CYP1A at the nearshore site (Fig. 5), yet the inter-sample variability was too high to detect a significance difference. The proteomic analysis produced similar results of no significant differences in CYP1A between the genotypes or the sites. This may be explained by the fact that there was almost no precipitation during the experimental period, and thus the run-off introducing pollutants and toxicants could have been minimal. Further proteomic analysis should reveal the state of other xenobiotic proteins between the genotypes. The expression levels of

actin did not show any difference between the sites or genotypes, confirming the equal loading of the protein samples.

Growth Rate Comparison

The short-term growth rate clearly highlighted the phenotypic difference between the two genotypes (Fig. 7). The nearshore genotype had a significantly higher growth rate than the offshore genotype in a common garden setting. The experiment was conducted in a flow through tank at the Kewalo Marine Laboratory, where seawater was taken from the Kewalo Channel during the experimental period. Kewalo Basin receives several discharges that introduce terrestrial runoff, as well as has a marina that introduces boat fuels. The water quality from the channel was therefore probably closer to that of the nearshore site in Maunalua Bay than the offshore site. Also the temperature range that corals experienced during the experimental period was 3.4℃, with a maximum daily temperature range of 2.97℃. The daily fluctuation was closer to the range observed at the nearshore site during the reciprocal experiment period (2.83℃ daily max) than the offshore site (2.14 daily max). The common garden setting hence created conditions closer to the nearshore site of Maunalua Bay, and the faster growth in the nearshore genotype highlighted the resilient traits of the nearshore genotype to excel under such environmental conditions.

CONCLUSIONS

At Maunalua Bay, Hawaii, a steep environmental gradient exists from the mouth of the bay toward offshore in a relatively short distance (~2 km), and the corals in the area show a strong genetic partitioning between the nearshore and offshore sites. Our study showed that phenotypic differences exist between the nearshore and offshore genotypes. The physiological traits assessed in our study revealed more resilient traits of the nearshore genotype in an environment with reduced water quality; the nearshore corals showed no reduction in their tissue layer thickness at the nearshore site, and grew faster in the common-garden setting under poor water quality. The molecular responses indicated inherent differences in the metabolic state between the two genotypes, as well as how they handle the environmental stresses. These response differences across multiple phenotypes suggest that the deteriorated water and substrate

qualities in the nearshore environment likely subjected the nearshore corals to selection, causing local adaptation. This local adaptation observed in our study may have emerged in a relatively short period of time, as the most drastic environmental changes at the bay occurred in the last century, suggesting selection on standing genetic variations as a mechanism behind the observed local adaptation. Correspondingly, our previous genetic study showed a reduction in genetic diversity of *P. lobata* at the nearshore site, indicating the nearshore population underwent bottleneck after the large-scale development. At a time in the planet's modern history when the environment is changing more rapidly than ever, corals may not be able to tolerate such a challenge, while also losing their genetic diversity to a myriad of local stressors.

ACKNOWLEDGEMENTS

We thank V. Sindorf for field assistance. Special thanks to J. Martinez and T. Oliver for their support and advice. Coral samples were collected under the Hawaii Division of Aquatic Resources, Special Activity Permit 2015-06. Financial support came from the National Fish and Wildlife Foundation (Grant Number 34413), the Hawaii Department of Health (MOA 13-502), and the NOAA Coral Reef Ecosystem Studies Program (NA09NOS4780178).

REFERENCES

Ali GS, Reddy VS, Lindgren PB, Jakobek JL, Reddy ASN (2003) Differential expression of genes encoding calmodulin-binding proteins in response to bacterial pathogens and inducers of defense responses. *Plant molecular biology*, **51**, 803–815.

Anthony K, Fabricius K (2000) Shifting roles of heterotrophy and autotrophy in coral energetics under varying turbidity. *Journal of experimental marine biology and ecology*, **252**, 221–253.

Aswani S, Mumby PJ, Baker AC *et al.* (2015) Scientific frontiers in the management of coral reefs. *Frontiers in Marine Science*, **2**.

Ban SS, Graham NAJ, Connolly SR (2014) Evidence for multiple stressor interactions and effects on coral reefs. *Global Change Biology*, **20**, 681–697.

Barnes DJ, Lough JM (1999) Porites growth characteristics in a changed environment: Misima Island, Papua New Guinea. *Coral Reefs*, **18**, 213–218.

Barshis DJ, Stillman JH, Gates RD *et al.* (2010) Protein expression and genetic structure of the coral Porites lobata in an environmentally extreme Samoan back reef: does host genotype limit phenotypic plasticity? *Molecular Ecology*, **19**, 140297–140297.

Baumann J, Grottoli AG, Hughes AD, Matsui Y (2014) Photoautotrophic and heterotrophic carbon in bleached and non-bleached coral lipid acquisition and storage. *Journal of Experimental Marine Biology and Ecology* **461**:469–478.

Campbell NA (1996) *Biology*. Benjamin/Cummings Publishing Company, Menlo Park, California.

Conservation-International (2008) *Economic Values of Coral Reefs, Mangroves, and Seagrasses: A Global Compilation*. Center for Applied Biodiversity Science, Conservation International, Arlington, CA.

Carilli JE, Norris RD, Black BA, Walsh SM, McField M (2009) Local stressors reduce coral resilience to bleaching. *PLoS ONE*, **4**, e6324.

Downs C, Downs A (2007) Preliminary Examination of Short-Term Cellular Toxicological Responses of the Coral *Madracis mirabilis* to Acute Irgarol 1051 Exposure. *Archives of environmental contamination and toxicology*, **52**, 47–57.

Downs CA, Ostrander GK, Rougée L *et al.* (2012) The use of cellular diagnostics for identifying sub-lethal stress in reef corals. *Ecotoxicology*, **21**, 768–782.

Fabina NS, Putnam HM, Franklin EC, Stat M, Gates RD (2012) Transmission Mode Predicts Specificity and Interaction Patterns in Coral-Symbiodinium Networks (SCA Ferse, Ed,). *PLoS ONE*, **7**, e44970.

Fabricius KE (2005) Effects of terrestrial runoff on the ecology of corals and coral reefs: review and synthesis. *Marine pollution bulletin*, **50**, 125–146.

Ferreira G, Franco R, Lloyd S *et al.* (1995) Structure and Function of Ferrochelatase. *Journal of Bioenergetics and Biomembranes*, **27**, 221–229.

Forsman ZH, Barshis DJ, Hunter CL, Toonen RJ (2009) Shape-shifting corals: molecular markers show morphology is evolutionarily plastic in Porites. *BMC Evolutionary Biology*, **9**, 45.

Graham NAJ (2014) Habitat Complexity: Coral Structural Loss Leads to Fisheries Declines. *Current Biology*, **24**, R359–R361.

Grottoli AG, Rodrigues LJ, Juarez C (2004) Lipids and stable carbon isotopes in two species of Hawaiian corals, *Porites compressa* and *Montipora verrucosa*, following a bleaching event. *Marine Biology*, **145**, 621–631.

Grottoli AG, Rodrigues LJ, Palardy JE (2006) Heterotrophic plasticity and resilience in bleached corals. *Nature*, **440**, 1186–1189.

Hinrichs S, Patten NL, Allcock RJN *et al.* (2013) Seasonal variations in energy levels and metabolic processes of two dominant *Acropora* species *(A. spicifera* and *A. digitifera*) at Ningaloo Reef. *Coral Reefs*, **32**, 623–635.

Hoegh-Guldberg O, Mumby PJ, Hooten AJ *et al.* (2007) Coral Reefs Under Rapid Climate Change and Ocean Acidification. *Science*, **318**, 1737–1742.

Hughes TP, Graham NAJ, Jackson JBC, Mumby PJ, Steneck RS (2010) Rising to the challenge of sustaining coral reef resilience. *Trends in Ecology & Evolution*, **25**, 633–642.

Kennedy EV, Perry CT, Halloran PR *et al.* (2013) Avoiding coral reef functional collapse requires local and global action. *Current Biology*, **23**, 912–918.

LaJeunesse T, Thornhill D, Cox E *et al.* (2004) High diversity and host specificity observed among symbiotic dinoflagellates in reef coral communities from Hawaii. *Coral Reefs,* **23**, 596–603.

Mahmood T, Yang P-C (2012) Western blot: Technique, theory, and trouble shooting. *North American Journal of Medical Sciences*, **4**, 429–434.

Maria VL, Bebianno MJ (2011) Antioxidant and lipid peroxidation responses in *Mytilus galloprovincialis* exposed to mixtures of benzo(a)pyrene and copper. *Comparative Biochemistry and Physiology, Part C*, **154**, 56–63.

Morgan KM, Perry CT, Smithers SG, Johnson JA, Daniell JJ (2016) Evidence of extensive reef development and high coral cover in nearshore environments: implications for understanding coral adaptation in turbid settings. *Scientific Reports*, 1–10.

Nicholls P, Fita I, Loewen PC (2000) Enzymology and structure of catalases. In: *Advances in Inorganic Chemistry* Advances in Inorganic Chemistry. pp. 51–106. Elsevier.

Oku H, Yamashiro H, Onaga K, Sakai K, Iwasaki H (2003) Seasonal changes in the content and composition of lipids in the coral *Goniastrea aspera*. *Coral Reefs*, **22**, 83–85

Presto KM, Storlazzi CD, Logan JB, Reiss TE, Rosenberger KJ (2012) Coastal Circulation and Potential Coral-larval Dispersal in Maunalua Bay, Oahu, Hawaii -Measurements of

waves, Currents, Temperature, and salinity June-September 2010. U.S. Geological Survey Open-File Report 2012-1040.

Reaka-Kudla ML (1997) The Global Biodiversity of Coral Reefs: A Comparison with Rain Forests. In: *Biodiversity II: Understanding and Protecting Our Biological Resources* (eds Wilson EO, Wilson DE, Reaka-Kudla ML), pp. 83–108. Joseph Henry Press, Washington, D.C.

Richmond RH (2009) Watersheds impacts on coral reefs in Maunalua Bay, Oahu, Hawaii. HCRI Project Progress Report FY2008.

Richmond RH (2011) Watersheds impacts on coral reefs in Maunalua Bay, Oahu, Hawaii. HCRI Project Report. FY 2010

Richmond RH, Hunter CL (1990) Reproduction and recruitment of corals: Comparisons among the Caribbean, the Tropical Pacific, and the Red Sea. *Marine Ecology Progress Series*, **60**, 185–203.

Richmond RH, Wolanski E (2011) Coral research: past efforts and future horizons. In: *Corals Reefs: An Ecosystem in Transition* (eds Dubinsky Z, Stambler N), pp. 3–12. Coral Reefs: An ecosystem in transition, Springer Science.

Rotmann S, Thomas S (2012) Coral Tissue Thickness as a Bioindicator of Mine-Related Turbidity Stress on Coral Reefs at Lihir Island, Papua New Guinea. *Oceanography*, **25**, 52–63.

Rougée L, Downs CA, H RR, Ostrander GK (2006) Alteration of normal cellular profiles in the scleractinian coral (Pocillopora damicornis) following laboratory exposure to fuel oil. *Environmental toxicology and chemistry*, **25**, 3181–3187.

Seemann J, Sawall Y, Auel H, Richter C (2012) The Use of Lipids and Fatty Acids to Measure the Trophic Plasticity of the Coral Stylophora subseriata. *Lipids*, **48**, 275–286.

Shearer TL, Rasher DB, Snell TW, Hay ME (2012) Gene expression patterns of the coral Acropora millepora in response to contact with macroalgae. *Coral Reefs*, **31**, 1177–1192.

Smith LW, Wirshing HH, Baker AC, Birkeland C (2008) Environmental versus genetic influences on growth rates of the corals *Pocillopora eydouxi* and *Porites lobata* (Anthozoa: Scleractinia) 1. *Pacific Science*, **62**, 57–69.

Stimson JS (1987) Location, quantity and rate of change in quantity of lipids in tissue of Hawaiian hermatypic corals. *Bulletin of Marine Science*, **41**, 889–904.

Storlazzi CD, Presto KM, Logan JB, Field ME (2010) *Coastal Circulation and Sediment Dynamics in Maunalua Bay, Oahu, Hawaii*. USGS Open-File Report 2010-1217.

Tisthammer, K, Forsman Z, Richmond R (2017) Isolation by adaption? Genetic structure is stronger across habitats than islands in the coral Porites lobata from Oahu and Maui. Manuscript in preparation.

Tomanek L (2014) Proteomics to study adaptations in marine organisms to environmental stress. *Journal of Proteomics*, **105**, 92–106.

Tortolero-Langarica J de JA, Cupul-Magaña AL, Carricart-Ganivet JP, Mayfield AB, Rodríguez-Troncoso AP (2016) Differences in Growth and Calcification Rates in the Reef-Building Coral *Porites lobata*: The Implications of Morphotype and Gender on Coral Growth. *Frontiers in Marine Science*, **3**, 3019.

Truman W, Sreekanta S, Lu Y *et al.* (2013) The CALMODULIN-BINDING PROTEIN60 family includes both negative and positive regulators of plant immunity. *Plant Physiology*, **163**, 1741–1751.

Wan D, Li R, Zou B *et al.* (2012) Calmodulin-binding protein CBP60g is a positive regulator of both disease resistance and drought tolerance in Arabidopsis. *Plant Cell Reports*, **31**, 1269–1281.

Wenger AS, Williamson DH, da Silva ET *et al.* (2015) Effects of reduced water quality on coral reefs in and out of no-take marine reserves. *Conservation Biology*, **20**, 142–153.

West JM, Salm RV (2003) Resistance and resilience to coral bleaching: implications for coral reef conservation and management. *Conservation Biology*, **17**, 956–967.

Wilkinson C (2008) *Status of coral reefs of the world: 2008*. Global Coral Reef Monitoring Network and Reef and Rainforest Research Centre, Townsville, Australia.

Wolanski E, Martinez JA, Richmond RH (2009) Quantifying the impact of watershed urbanization on a coral reef: Maunalua Bay, Hawaii. *Estuarine, Coastal and Shelf Science*, **84**, 259–268.

Table 1. ANOVA results of tissue layer thickness of *P. lobata*, comparing between the nearshore and offshore colonies, as well as between the nearshore and offshore sites of Maunalua Bay.

	Df	Mean Sq	F value	Pr(>F)
Genotype	1	3.336	44.90	**2.57e-10*** **
Transplant-site	1	2.132	28.70	**2.56e-07*** **
Interaction	1	1.399	18.84	**2.37e-05*** **

Table 2. ANOVA results of tissue lipid content of *P. lobata*, comparing between the nearshore and offshore genotypes, as well as between the nearshore and offshore sites of Maunalua Bay.

	Df	Mean Sq	F value	Pr(>F)
Genotype	1	0.01543	2.179	0.1594
Transplant-site	1	0.01706	2.409	0.1402
Interaction	1	0.03305	4.668	**0.0462***

Table 3. ANOVA results of the average short-term grow rate of *P. lobata* from the common-garden experiment, comparing between the nearshore and offshore genotypes of Maunalua Bay.

	Df	Mean Sq	F value	Pr(>F)
Genotype	1	1.4904	13.09	**0.00681 ****

Figure 1. a) Biomarker sampling sites in Maunalua Bay from the study of Richmond (2011), and b) results of canonical correlation analysis of biomarkers (stress-induced cellular proteins) of *P. lobata* (Richmond, 2011). The site names (A, B, and C) and their colors in (a) correspond to those in (b). 'a' is the nearshore site, and 'c' is the offshore site in this study.

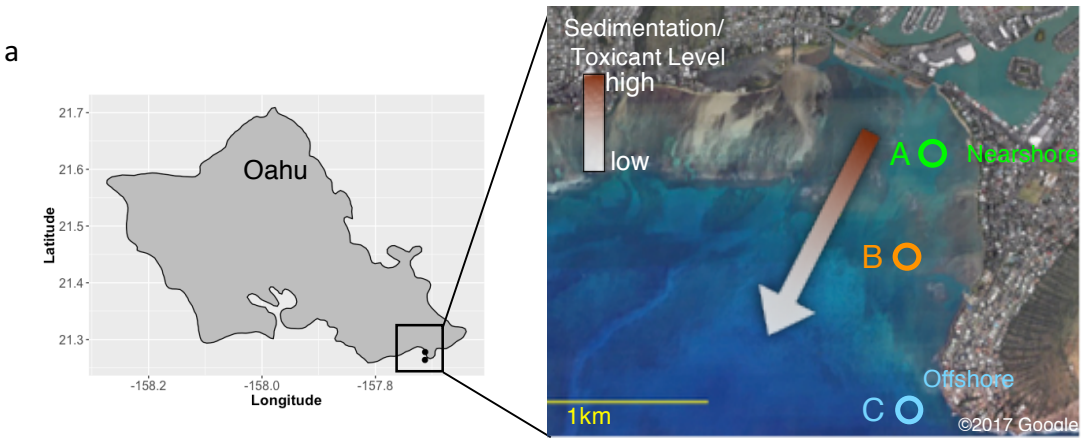

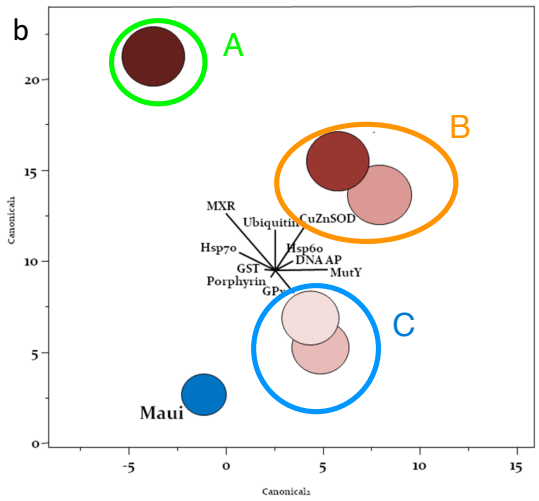

Figure 2. Diagram of the reciprocal transplant experimental design (a), and pictures of the experiment in the field (b: Nearshore Site, c: Offshore Site).

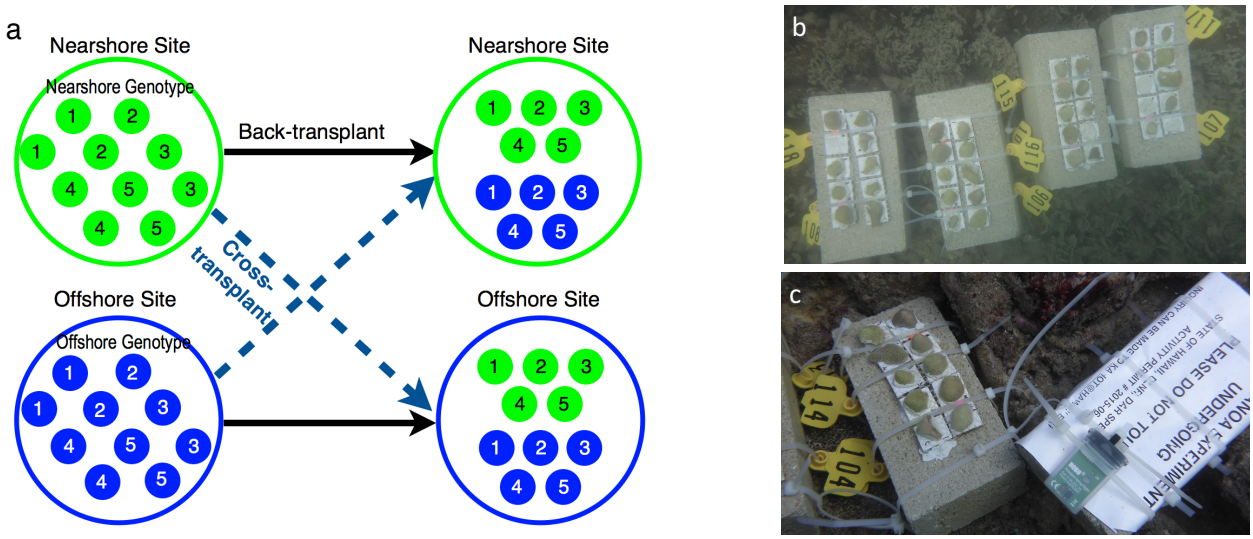

Figure 3. Results of the 30-day reciprocal transplant experiment I: a) Tissue layer thickness (mm) measurements of *P. lobata*, and b) tissue lipid content (%) of *P. lobata* holobiont. Arrows show the direction of transplanting. Different letters indicate a statistically significant difference.

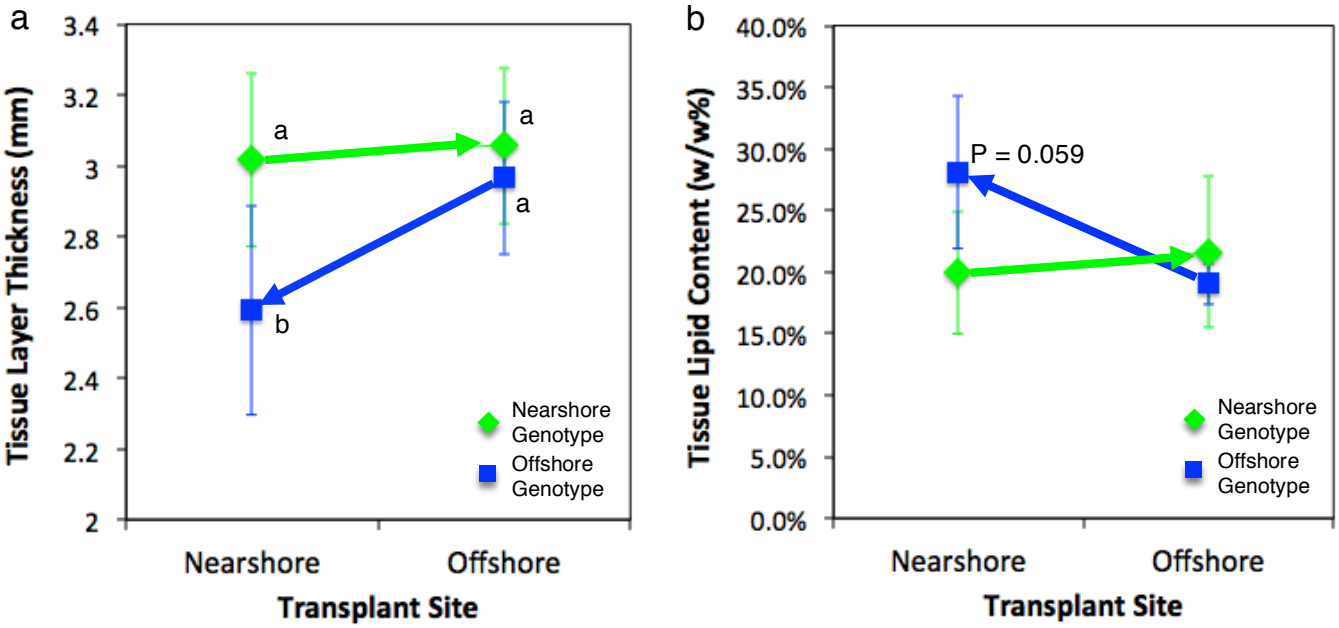

Figure 4. Results of the reciprocal transplant experiment II: the biomarker protein expressions of *P. lobata*. (a) ~ (c) - Pattern1: Transplant effects present in only one genotype, (d) ~ (f) Pattern 2: Genotypic difference in the overall expression level.

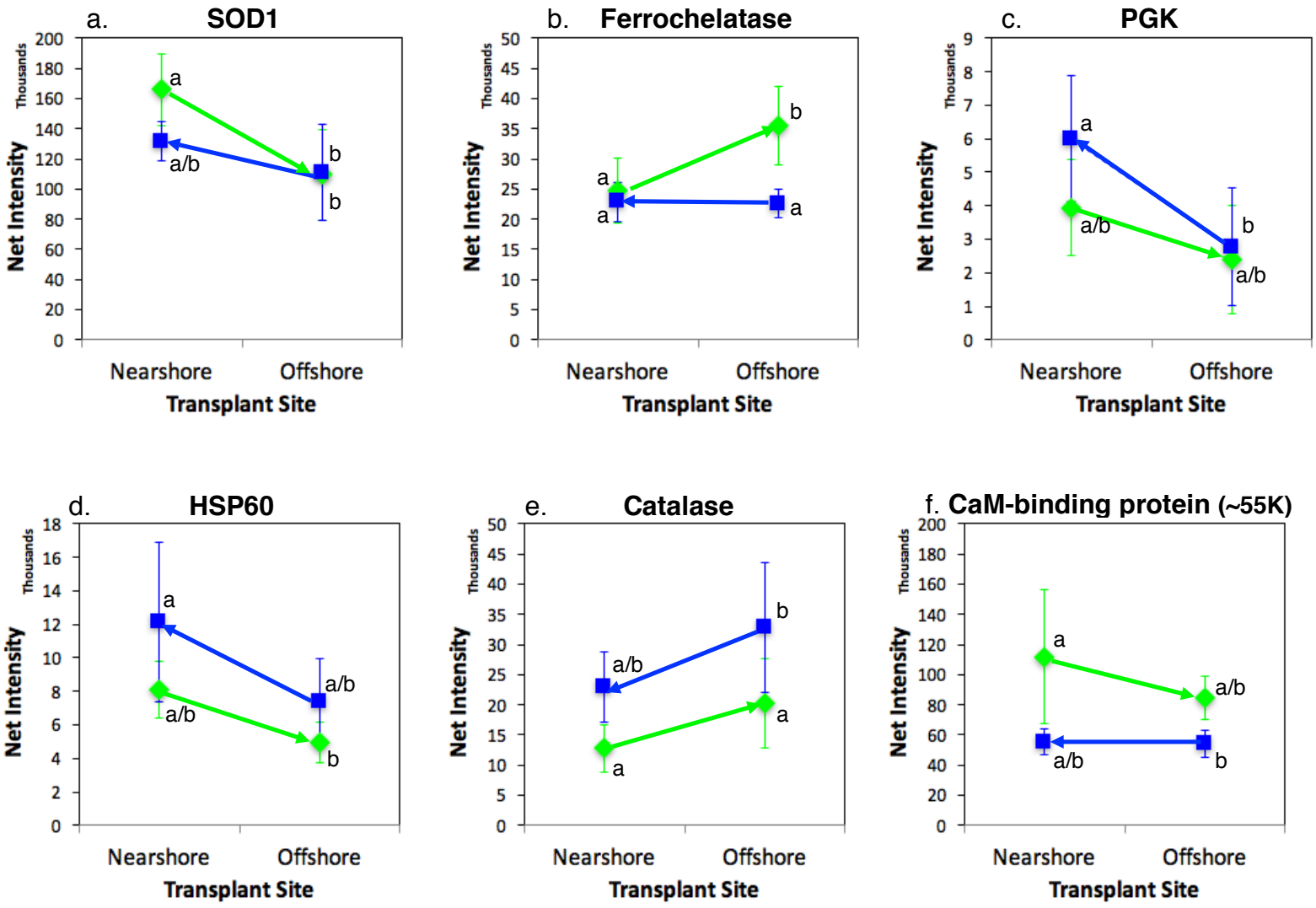

Figure 5. Results of the reciprocal transplant experiment III: CYP450 expressions.

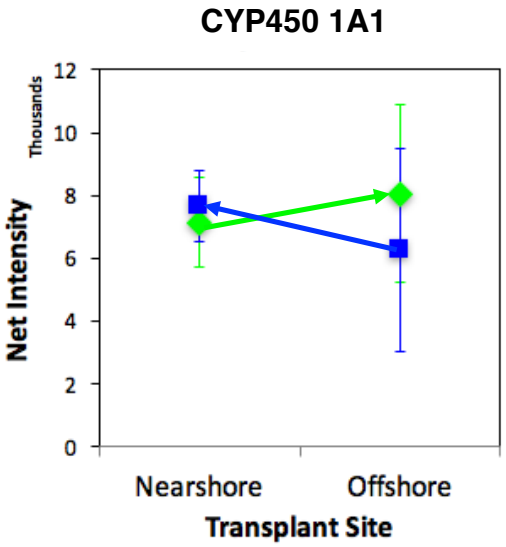

Figure 6. Short-term growth rate of two genotypes of *P. lobata* in a common-garden setting. The error bars denote standard error.

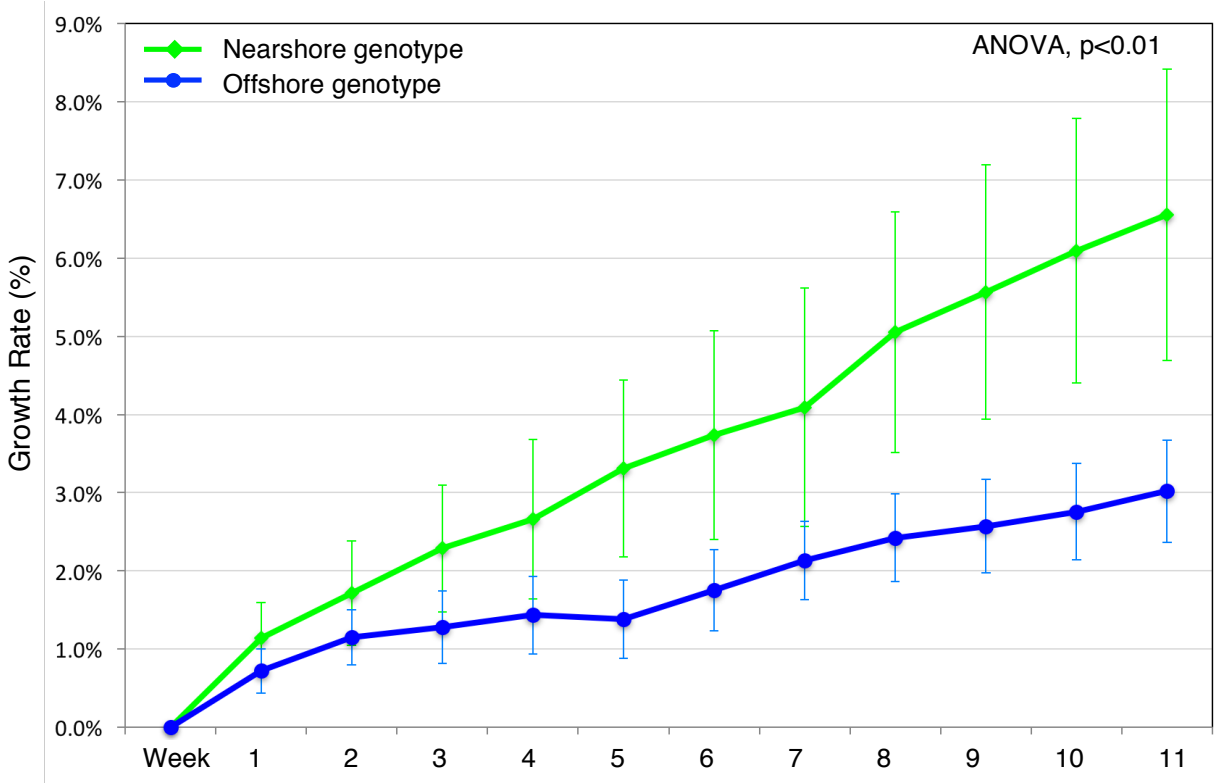

Figure 7. Diagram of oxidative stress response pathway. SOD= superoxide dismutase, GSH = glutathione (reduced), GSSG = oxidized glutathione, GPX = glutathione peroxidase, Trx=Thioredoxin

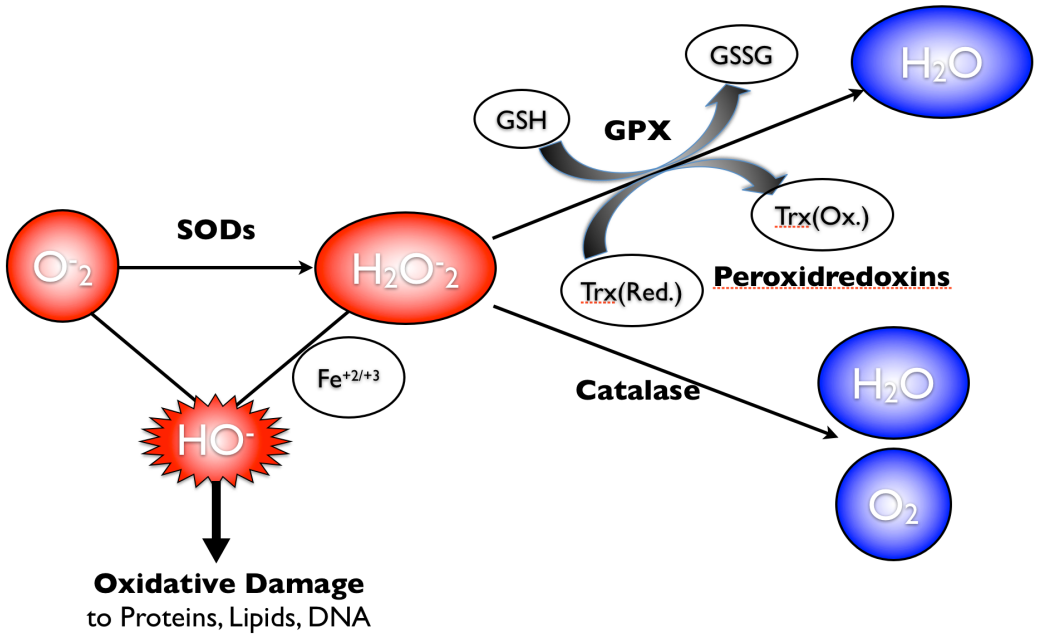

Table S1. ANOVA tables of protein expression results of the reciprocal transplant experiment of *P. lobata* colonies.

a. SOD1	Df	Mean Sq	F value	Pr(>F)
Genotype	1	1.341e+09	1.547	0.23155
Transplant-site	1	7.450e+09	8.592	**0.00979 ****
Interaction	1	1.613e+09	1.860	0.19149

b. Ferrochelatase	Df	Mean Sq	F value	Pr(>F)
Genotype	1	273229908	9.357	**0.0075 ****
Transplant-site	1	135933361	4.655	**0.0465 ***
Interaction	1	154897103	5.305	**0.0350 ***

c. PGK	Df	Mean Sq	F value	Pr(>F)
Genotype	1	2434263	0.508	0.48617
Transplant-site	1	42177687	8.806	**0.00907 ****
Interaction	1	9280664	1.938	0.18297

d. Hsp60	Df	Mean Sq	F value	Pr(>F)
Genotype	1	44096112	5.648	**0.03030 ***
Transplant-site	1	75506599	9.670	**0.00674 ****
Interaction	1	3009241	0.370	0.55198

e. Catalase	Df	Mean Sq	F value	Pr(>F)
Genotype	1	6.906e+08	11.5	**0.00347 ****
Transplant-site	1	5.645e+08	9.4	**0.00700****
Interaction	1	46562075	0.765	0.39483

f. CaM	Df	Mean Sq	F value	Pr(>F)
Genotype	1	9.556e+09	8.767	**0.00875 ****
Transplant-site	1	1.419e+09	1.302	0.26970
Interaction	1	1.218e+09	1.126	0.30444

g. CYP1A	Df	Mean Sq	F value	Pr(>F)
Genotype	1	2022945	0.161	0.694
Transplant-site	1	291829	0.023	0.881
Interaction	1	6839703	0.543	0.472

g. Actin	Df	Mean Sq	F value	Pr(>F)
Genotype	1	46601239	2.538	0.131
Transplant-site	1	246968	0.013	0.909
Interaction	1	31758213	1.730	0.207

Table S2. Results of Tukey HSD Test for six protein biomarker expressions, following one-way ANOVA of four treatments. O = Offshore, N = Nearshore. Symbols 'ON' represent [Genotype(Origin)][Destination] = offshore corals transplanted to Nearshore Site.

	SOD1		Ferrochelatase		PGK	
	diff	p adj	diff	p adj	diff	p adj
ON-OO	20639.87	0.68976	351.83	0.99959	4266.80	**0.03251***
NO-OO	-1583.33	0.99977	12958.22	**0.00783***	664.65	0.96239
NN-OO	54976.68	**0.04195***	2178.22	0.91838	2206.65	0.40924
NO-ON	-22223.19	0.63957	12606.38	**0.00965***	-3602.15	0.08133
NN-ON	34336.82	0.29009	1826.38	0.94937	-2060.15	0.46675
NN-NO	56560.0	**0.03555***	-10780.0	**0.02823***	1542.00	0.68639

	Hsp60		Catalase		CaM	
	diff	p adj	diff	p adj	diff	p adj
ON-OO	-2426.54	0.59530	-13677.25	0.05933·	1238.35	0.99992
NO-OO	4751.33	0.07891	-14804.05	**0.03825***	28108.86	0.54572
NN-OO	725.46	0.97716	-22378.05	**0.00173****	60561.82	**0.04540***
NO-ON	7177.87	**0.00925****	-1126.80	0.99563	26870.51	0.58096
NN-ON	3152.00	0.38324	-8700.80	0.32591	59323.46	0.05090·
NN-NO	-4025.87	0.15920	-7574.00	0.44121	32452.95	0.42745

	CYP1A		Actin	
	diff	p adj	diff	p adj
ON-OO	1411.18	0.92130	2742.49	0.74486
NO-OO	1805.66	0.85138	-532.66	0.99720
NN-OO	877.66	0.97900	2830.66	0.72652
NO-ON	394.48	0.99799	3275.15	0.63046
NN-ON	-533.52	0.99508	5573.15	0.20923
NN-NO	-928.00	0.97537	-2298	0.83086

Table S3. Pairwise comparison (ANOVA) results of tissue lipid content of *P. lobata*, comparing before and after the experiment, as well as between the nearshore and offshore genotypes before the experiment.

Treatments		F	P
Before-After comparison	N→N	0.16	0.7
	N→O	0.424	0.533
	O→O	29.75	**0.00061**
	O→N	22.22	**0.00151**
Before samples	N vs O	0.781	0.403

Figure S1. Temperatures and light intensity during the reciprocal transplant experiment of the nearshore and offshore sites of Maunalua Bay.

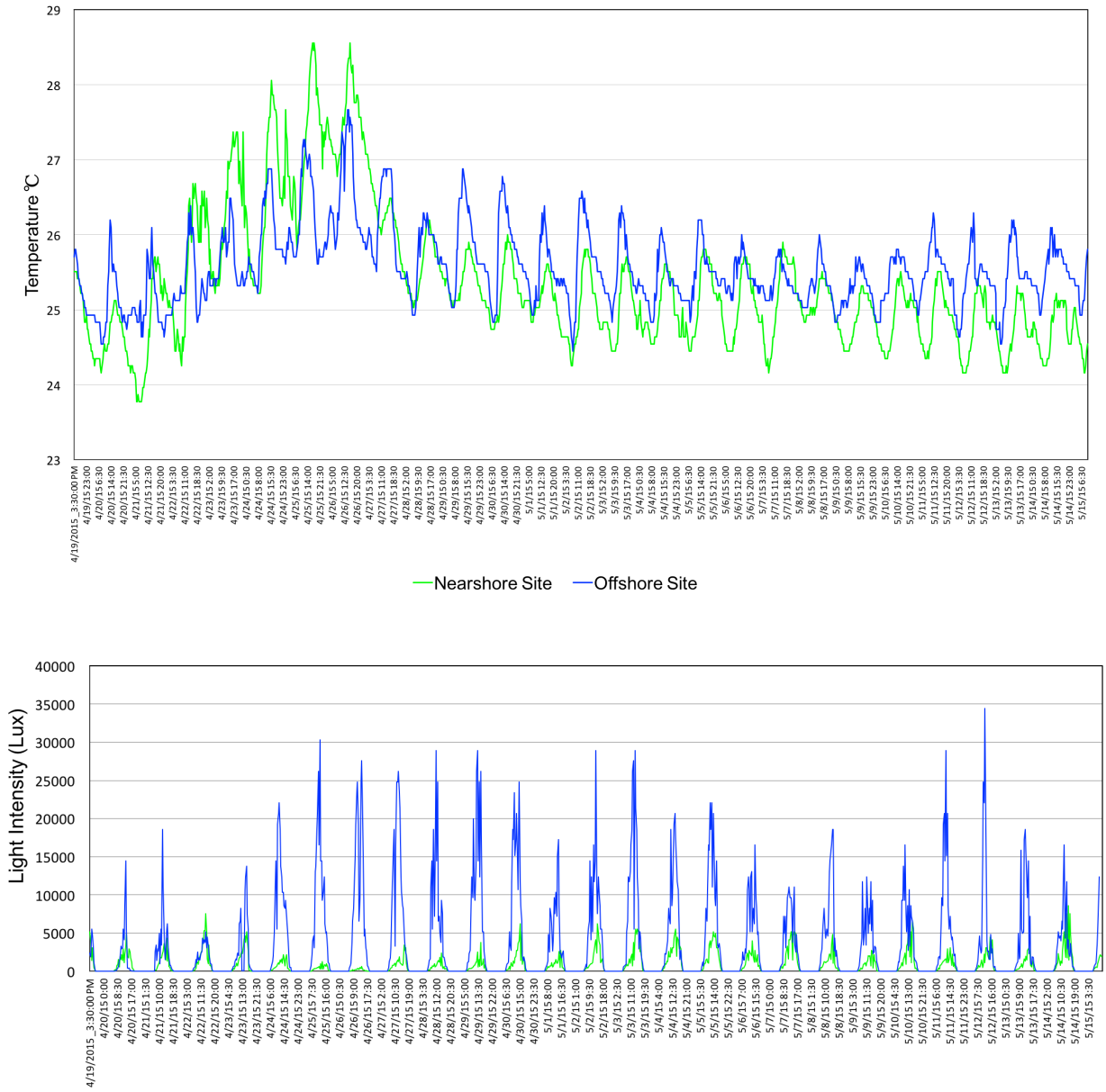

Figure S2. Images of western blots of antibodies on coral protein extractions.

a.SOD1

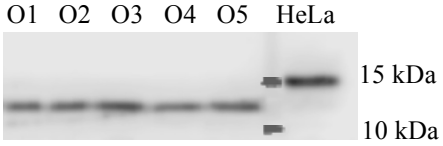

b. Ferrochelatase

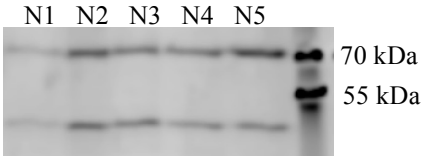

c. PGK

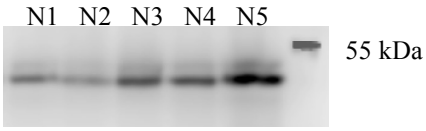

d. Hsp60

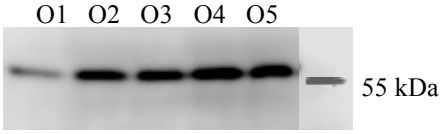

e. Catalase

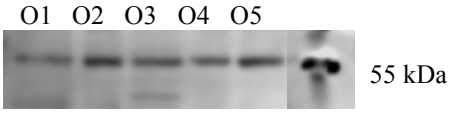

f. CaM

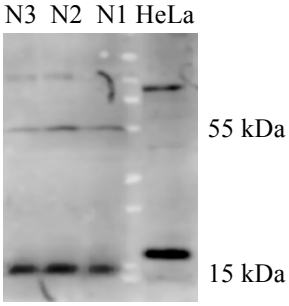

g. CYP1A

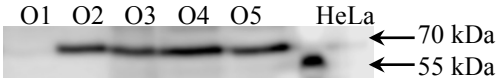

h. Actin

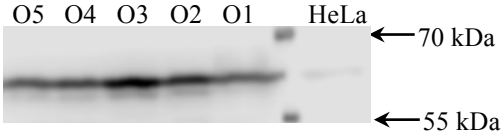

Figure S3. Tissue lipid content of *P. lobata* before and after the reciprocal transplant experiment in Maunalua Bay. Different letters indicate statistical significant difference. N = nearshore, O=offshore. Arrows point the transplant direction; e.g. N→N indicates Nearshore Genotype transplanted to Nearshore Site.

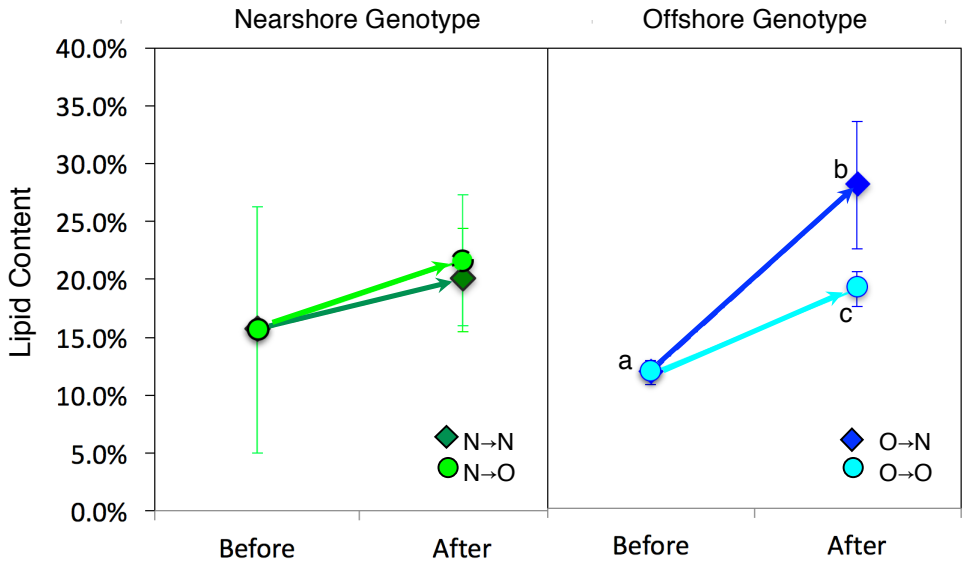

Chapter 3

Corallite skeletal morphological variation in Hawaiian *Porites* and its genetic basis

Kaho H Tisthammer and Robert H Richmond

ABSTRACT

Due to their high morphological plasticity and complex evolutionary history, the species boundaries of reef-building corals are poorly understood. The skeletal structures of corals have traditionally been used for species identification, but these structures can be highly variable, and currently we lack knowledge regarding the extent of morphological variation that defines a species. *Porites* species are notorious for their taxonomic difficulties, both morphologically and genetically, and currently there are several unresolved species complexes in the Pacific. Despite its ubiquitous presence and broad use in coral research, *Porites lobata* belongs to one such unresolved species complex. To understand the degree of intraspecific variation in skeletal morphology, a large number of corallites from the massive Hawaiian *Porites* species (*P. lobata* and *P. evermanni*) were examined. Selected samples from different populations were then quantitatively analyzed, using multivariate morphometrics. Genetic contributions to morphological differences were assessed by exploring correlations between morphology and genetics, using approximately 18,000 loci generated from the restriction site associated DNA sequencing. Our observations revealed high intraspecific variation in *Porites* corallite morphology. Much of their variation appeared to be determined genetically, since significant correlation was found between the morphological and genetic distances. The unique morphological characters observed from the population under environmental stress suggest that they have adaptive values, but how such traits increase their fitness, and how much plasticity they can occur remain to be determined by future studies. Relatively simple morphometric analyses used in our study can be useful in clarifying the existing ambiguity in skeletal architecture, thus contributing to resolving species issues in corals.

INTRODUCTION

Species are a fundamental unit of biological classification (de Queiroz 2007). However, species delimitation has been a controversial topic in evolutionary biology (e.g. de Queiroz 1998). In the most general sense, biological species are defined based on reproductive isolation, such as "a group of populations that have the potential to interbreed in nature (Campbell, 1996)." However, due to notable challenges arising from complex and diverse biological reproductive systems, morphology has been the default for classifying species: The traditional Linnaean taxonomy classifies a species based primarily on its morphological characters. Although this morphology-based taxonomy has worked well for the past 300 years, its limitations are increasingly forcing biologists to migrate towards DNA-based taxonomy and phylogenetics (Dunn 2003; Tautz *et al*. 2003). These new molecular approaches have greatly advanced our understanding of the ecological and evolutionary processes involved in the origin and maintenance of biodiversity (Yang & Rannala 2012). However, DNA-based taxonomy has its own limitations (Valentini *et al*. 2009; Ahrens *et al*. 2016), resulting in discordance between morphology-based and DNA-based taxonomies.

Reef-building corals (Scleractinia) are one such taxon with taxonomic confusion, otherwise known as 'the species problem.' Coral reefs are centers of biodiversity (Selkoe *et al*. 2016), and over 800 reef-building coral species are currently described (Carpenter *et al*. 2008). However, the species boundaries of most reef building corals are poorly defined due to their high phenotypic plasticity and their complex evolutionary history (Knowlton 2000; Stat *et al*. 2012; Bosch & Miller 2016). Because colony morphology is extremely variable (Todd 2008), the skeletal architecture of the corallite (the structure associated with individual polyps, Fig. 1), rather than the colony, has been used as a more reliable metric for coral taxonomic distinctions (Brakel 1977; Veron 2000). Yet, in many genera this still does not solve the problem since corallites can be small, irregular and/or highly variable between and even within colonies. Geographic variation in morphology also adds confusion (Veron 2000). These traits of corals have caused widespread disparity between morphology-based taxonomy and molecular phylogeny (e.g. Fukami *et al*. 2004b; Forsman *et al*. 2009; Huang *et al*. 2009; Stat *et al*. 2012; Prada *et al*. 2014; Arrigoni *et al*. 2016); for example, recent genetic studies have revealed 1) some morphospecies to be a single species (Eytan *et al*. 2009; Stefani *et al*. 2011; Pinzón *et al*. 2013), 2) an assumed single species with multiple colony forms to be separate species (Fukami *et*

al. 2004a), and 3) multiple populations of an assumed single species to be cryptic species (Baums *et al*. 2005; Warner *et al*. 2015). Genetic delineation of reef-building corals has also been extremely challenging in some genera due to their slow rates of mitochondrial molecular evolution (Romano and Palumbi 1997; van Oppen *et al*. 1999), hybridization (e.g. Vollmer & Palumbi 2002; Hellberg *et al*. 2016), reticulate evolution (e.g. Veron 1995; Richards *et al*. 2013), and/or incomplete lineage sorting due to recent speciation (Miller & van Oppen 2003; Willis *et al*. 2006).

Presently, consensus has not been reached regarding the scale of genetic and morphological variation for many reef building corals that define a species (Stat *et al*. 2012). A new classification system is needed to understand coral species boundaries, which are key to recording and mapping patterns of biodiversity, understanding the ecological and evolutionary processes involved in speciation, predicting future changes, and determining appropriate conservation strategies. The Endangered Species Act has so far listed 20 coral species as threatened in 2014, and three coral species as endangered in 2015. Evaluating extinction risk for coral species continues to be challenging, as taxonomic uncertainty hinders the determination of species ranges, population sizes, and management actions (Brainard *et al*. 2011).

The genus *Porites* (Link, 1804) of Scleractinian corals occurs in tropical regions throughout the world, with the earliest fossil record from the Eocene (Veron 2000). Certain *Porites* species, such as *P. lobata*, have an especially extensive geographic distribution, throughout the Indo-Pacific Ocean from the Red Sea to the eastern Pacific. Despite its ubiquitous presence in the world, the genus *Porites* is among the most taxonomically challenging corals (Brakel 1977; Veron 2000; 2013). Over 50 *Porites* species are currently described (Veron 2000), but genetic studies on *Porites* are revealing unresolved species complexes, as well as cryptic species (Forsman *et al*. 2009; Forsman *et al*. in review). *P. lobata* falls into the 'Clade I' species complex (Forsman *et al*. 2009), containing a mixture of endemic, rare, and cosmopolitan corals (*P. lobata*, *P. compressa* [endemic], *P. cylindrical*, *P. duerdeni*, *P. pukoensi*s [rare], *P solida*, *P. annae*, & *P. lutea*) with various colony morphologies. Although some *Porites* species appear to have distinct skeletal characters, which can aid in species identification, information is lacking regarding the extent of intra- and interspecific skeletal plasticity. This is partly because the skeletal characters are often summarized from a small set of samples without statistical analysis (Jameson 1995).

In order to more efficiently use corallite skeletal characters in species identification, quantitative assessment of corallite structures is essential. Corallite morphology between populations of *P. lobata* was investigated to capture the intraspecific skeletal variability using morphometrics. Our previous studies have identified clear genetic differentiation between *P. lobata* from the nearshore and offshore sites of Maunalua Bay, Oahu, Hawaii (Tisthammer *et al*, 2017a). These nearshore and offshore *P. lobata* showed differences in their physiological and molecular responses to stress exposure, leading us to conclude that selection has driven the nearshore corals to adapt to their high-stress environment. We used these populations as a study platform, and tested whether and how the skeletal structures of the two genotypes differed. Also, over 100 *Porites* corallite samples were observed to capture the degree of variability. Lastly, the degree of genetic contribution to the corallite skeletal variation was explored using the genomic data by assessing the relationship between the morphological and genetic distances in selected *P. lobata* samples.

MATERIALS AND METHODS

Sample Collection

Samples of *P. lobata* used in morphometric and genomic analyses were collected from the offshore site in Maunalua Bay, Oahu (21.26 N, 157.71 W), the nearshore site in Maunalua Bay, Oahu (21.27 N, 157.71 W), and Kewalo Basin, Oahu (21.29 N, 157.86 W). For general corallite observations, *Porites* samples collected from Maunalua Bay, Kewalo and West Maui were used (Fig. 2). Samples were collected under the State of Hawaii Special Activity Permit (SAP 2013-26). Samples were either flash frozen in liquid nitrogen and stored at -80 °C, stored in 100% ethanol, or stored in DMSO buffer. For morphometric analysis, nine nearshore samples, seven offshore samples, and one Kewalo sample were used (Table 1). For genomic analysis, five nearshore samples, two offshore samples, one Kewalo sample, and one *P. evermanni* sample were used. Tree analysis was run with an additional 12 *Porites* samples, processed previously for phylogenomic analysis of *Porites*. The collection locations are listed in Table 1 of Forsman *et al*. (2017).

Corallite Observation

Corallite micro-skeletal characters were observed under a stereomicroscope, based on published morphological descriptions of the species (Veron and Pichon 1982; Weil 1992; Veron 2000; Ketchum and Reyes 2001; Forsman *et al*. 2015) (e.g. Fig. 3). Variability in skeletal characters were recorded for two species, *P. lobata* and *P. evermanni*, with a similar colony-level morphology. For all skeletal samples observed, at least one genetic marker was sequenced using the method of Tisthammer *et al*. (2017a). *P. evermanni* is genetically distinct from the *P. lobata* species complex, and therefore, all *P. evermanni* samples were positively identified.

Morphometric Analyses

Multivariate morphometric analyses were conducted to reveal micro-skeletal differences in the corallites of *P. lobata* from the nearshore and offshore sites of Maunalua Bay. An additional sample from the Kewalo basin was added for analytical purposes (better visualization) for conducting canonical discriminant analysis (CDA) (CDA does not produce a scatter biplot for two groups). A set of 19 numerical and seven descriptive characters were established in order to capture *Porites* corallite structural features, based on the previously published information as guidance (Brakel 1977; Veron & Pichon 1982; Jameson 1995; Ketchum & Bonilla 2001; Forsman *et al*. 2015) (Table 2, Fig. 4). Collected coral skeletal samples were bleached in 15-50% sodium hypochlorite, rinsed with fresh water, and dried. Digital images of corallites were produced using a stereomicroscope and 19 numerical characters were measured using ImageJ (Schneider *et al*. 2012) software. The seven descriptive characters were measured under a stereomicroscope. Measurements from 10 corallites per individual were taken. Principal coordinate analysis (PCO) was conducted to obtain an overall pattern of morphological variation using all 26 characters in PRIMER version 6 (Clarke & Gorley, 2006) and R version 3.3.1 (R Core Team 2016). The 19 numerical character data were standardized to variables, and the permutational multivariate analysis of variance (MANOVA) was performed to test the differences among the genotypes using the PERMANOVA function of PRIMER v6. CDA, which is a constraint ordination that maximizes differences between a priori defined groups, was used to test the discriminating power of morphometric characters, and to find characters with a significant conditional effect using MorphoTools (Koutecký 2014) in R. Forward selection of characters with non-parametric Monte Carlo permutation tests (1000 permutations) was used to

identify the characters with significant conditional effects. Classificatory discriminant analysis with cross-validation was conducted to obtain the posterior probabilities of classification into each group, as implemented in MorphoTools.

Genomic Analysis

a. Library preparation

High molecular weight genomic DNA was extracted using the Qiagen DNeasy® blood and tissue kit with modification. Extracted DNA was examined on 2% agarose gels to ensure sufficient quantities of DNA of over 2,500bp molecular weight. All samples were first cleaned up to eliminate small molecular weight DNA (< 100bp) using Agencourt AMpure XP beads (Beckman Coulter, Brea, CA), following the steps described in ezRAD Protocol modified from Toonen *et al*. (2013). Extracted DNA was quantified using a Qubit® fluorometer (Thermo Fisher Scientific, Waltham, MA) by measuring absorbance at λEx/λEm 485/530nm. DNA libraries were constructed using the Illumina TruSeqVR Nano DNA kit, based on the ezRAD Protocol described in details in Forsman *et al*. (2017). Briefly, all samples were adjusted to a concentration 1µg of DNA in 25µl prior to digestion. The samples were digested using the isoschizomers MboI and Sau3AI (New England BioLab, Ipswich, MA), cleaving at GATC sites. The digested samples were cleaned using Ampure XP beads, and quantified with a Qubit® fluorometer. Following end repair and size selection, samples were individually barcoded and pooled into a single library with a concentration of 1 mg/25 mL.

The DNA libraries were quality-checked with two steps (Agilent 2100 Bioanalyzer and qPCR), and sequenced on MiSeq® (Illumina, San Diego, CA) at the Evolutionary Genetics Core Facility at the Hawaii Institute of Marine Biology (HIMB), Kaneohe, HI, using a half lane. Raw Ilumina reads were sorted by barcodes, demultiplexed, and merged for paired reads using PEAR v. 0.9.6 (McLeod 1994) with the default parameters. Both ends of merged reads were trimmed for low quality (bases with more than a 1% chance of error were) using Geneious v.6.0.5 (Biomatters, San Francisco, CA).

b. Reference Assembly

mtDNA: Quality-filtered reads was assembled to the whole mitochondrial genome of *Porites okinawensis* (GenBank: NC015644) as a reference sequence, using the default parameters (medium/low sensitivity) of Geneious v.6.0.5, as well as BWA v.0.7.12 (Li & Durbin 2009) to ensure the assembly quality and base calls. Consensus sequences were called for each sample using the 0% majority option and N's were called if coverage was not greater than 2X).

SNPs: Coral holobiont DNA samples contain DNAs from their symbionts such as *Symbiodinium*, and other microbes. In order to separate the coral genomes from their symbionts, single nucleotide polymorphisms (SNPs) were obtained by aligning the reads to the *P. lobata* transcriptomic reference sequences. The *P. lobata* transcriptome reference sequences (http://comparative.reefgenomics.org/), which contain putative orthologous protein-coding sequences only from coral genomes, were concatenated with 200 bp of N's separating each transcript to form a pseudo genome. All libraries were then mapped to this reference sequence using BWA (Li 2013). Variants were called using Genome Analysis Tool Kit (McKenna *et al*. 2010) and FreeBayes (Garrison and Marth 2012) (See Forsman *et al*. 2017 for details). The resulting VCF files were further filtered using VCF tools (Danecek *et al*. 2011), and analyzed using the smartpca program of EIGENSOFT (Price *et al*. 2006). The holobiont metagenomic data were analyzed using pyRAD v.3.0.2 (Eaton, 2014), and the resulting phylogenetic trees were constructed using RAxML (Stamatakis 2006) as descried in Forsman *et al*. (2017).

c. Population Genomic Structure Analysis

Population genomic structure using the coral SNP loci was estimated using the *adegenet* package (Jombart & Ahmed 2011) in R. The grouping of the samples was also estimated using the *find.cluter* function in *adegenet*.

Morphological and Genetic Distance Comparison

A distance matrix of corallite measurements was created using the vegan package in R. Distance matrices based on Euclidian, Manhattan and Canberra distances were calculated for comparison. The genetic distance matrix was obtained from the 17,801 coral SNP loci using *adegenet*, as well as using the genpofad method of the *pofadinr* package (Joly *et al*. 2015) in R.

The genetic distance matrices obtained by the two methods showed a significant correlation in PRIMER, and therefore, only the results calculated using *pofadinr* were included in the results. The genetic distance was also calculated using the Histone2 sequences (H2, 1420 bp) (Tisthammer *et al*. 2017a) for the 17 samples. The obtained morphological and genetic distance matrices were tested for correlation using the Mantel test using the *ape* (Paradis *et al*. 2004) and *ade4* (Dray *et al*. 2007) packages in R, as well as in PRIMER using RELATE function.

RESULTS

Corallite Observation

Massive *Porites* species found in the main Hawaiian Islands include *P. lobata* and *P. evermanni*. The colony morphology of *P. evermanni* highly resembles that of *P. lobata*, and they are often difficult to distinguish in the field. Their corallite structures are distinct, and the prominent published key characters to distinguish *P. lobata* and *P. evermanni* are; 1) the height of pali with respect to corallite wall - *P. lobata* usually has eight relatively undeveloped pali that are shorter than the wall, while *P. evermanni* has eight tall, developed pali that come up to the wall, and 2) the thickness of septa and the wall - *P. evermanni* has much thicker septa and corallite wall than *P. lobata*, and the wall of *P. evermanni* has thicker ridges (Fig. 2). More than 100 corallites of massive *Porites* species form Hawaii were observed under a stereomicroscope, revealing a great amount of structural variation in both *P. lobata* and *P. evermanni* from the published keys.

a. *P. evermanni*:

The wall of Hawaiian *P. evermanni* samples ranged from the ‘typical’ thick wall with ridges to relatively thin wall, comparable to that of *P. lobata* (Fig. 5). The number of pali also ranged from five to eight, and the formation of the ventral triplet varied from having free margins, forming a trident, to being fused. Columella was observed in almost all corallites, but most were small, unlike as per the taxonomic description. One consistent feature observed was the vertical depths of corallites, which were extremely shallow, where the tips of pali and wall aligned horizontally on the same plane (referred to as ‘flat corallite’ hereafter).

b. *P. lobata*:

Hawaiian *P. lobata* samples also displayed variable numbers of pali, ranging from five to eight. The variability in the number of pali was also observed within a sample. Most corallites were moderately excavated with relatively undeveloped pali, forming a concave V- to U-shape, which represents 'typical' *P. lobata* corallite architecture (Fig. 6a). However, there were samples with flat corallites, in which the tips of pali and septal denticles aligned with the wall, resembling the corallites of *P. evermanni* (Fig. 6b). These samples were genetically confirmed as *P. lobata* (i.e. belonging to the *Porites* Clade I complex), and thus were not misidentified. The ventral triplet had free margins in the majority of observed samples, yet samples with a trident or a fused triplet were observed more frequently (~20% of samples) than expected (Fig. 6c & d). Some samples had highly developed pali, especially on the lateral pairs of septa (Fig. 6e & f). The diameter of pali was often greater for such tall, developed pali. A difference in pali development was among the most distinct characters observed between the nearshore and offshore *P. lobata* samples from Maunalua Bay; highly developed lateral pairs of pali were frequently observed in the nearshore samples, while none of the offshore samples showed such a feature. A columella was present in most samples examined. The shape of the columella ranged from rod-shaped to compressed flat-shaped (Fig. 6g), and the nearshore samples had more rod-shaped columella (83%) than the offshore samples (68%). Approximately 35% of the examined samples showed intra-colonial variation in the columella shape. The number of denticles observed also ranged from two to three, although the majority had two.

Colonies of *Porites lutea* strikingly resemble those of *P. lobata*, although *P. lutea* has not been reported in Hawaii. Some of the published key characters to distinguish *P. lutea* and *P. lobata* are; 1) the ventral triplet formation - the triplet of *P. lobata* has free margins, while the triplet of *P. lutea* is fused, or forms a trident, 2) the number of pali - *P. lobata* has eight while *P. lutea* has five pali, and 3) the height of pali with respect to the wall - *P. lutea* has well developed pali that come up to the wall, while *P. lobata* has relatively undeveloped pali that are shorter than the wall (Veron, 2000). Some samples from Maunalua Bay had skeletal characters similar to those of *P. lutea*, but genetic analysis showed that the samples belonged to the Clade I *P. lobata* complex. In the phylogenetic tree analysis by Forsman *et al*. (2009), the majority of the ITS sequences of *P. lutea* clustered separately from Clade I. However, some sequences identified as

P. lutea also clustered with Clade I. These samples could be misidentified from *P. lobata*, but further studies are needed to fully understand the genetic clade of *P. lutea*.

Morphometric Analysis

A total of 17 samples were used to assess the differences in corallite skeletal morphology between *P. lobata* from the nearshore site (nearshore genotype) and the offshore site (offshore genotype) in Maunalua Bay. One Kewalo sample was included to better visualize the canonical scores. All 26 assessed characters were used in the PCO, and all 19 numerical variables were used in the rest of the multivariate analyses, as none of the characters were highly correlated ($r < |0.95|$).

In order to assess whether 10 corallite measurements per sample was enough to capture the within-sample variation, the average coefficient of variation of each numerical character was calculated using five corallites and 10 corallites, and the values were then compared. The average coefficients of variation did not differ between the two methods (Wilcoxon Signed-Rank Test, P-value = 1), and therefore 10 measurements per sample was adequate to capture the within-sample variation.

PCO resulted in the first axis explaining 23.5% of and the second axis explaining 16.3% of the variance between the three locations (Fig. 7). The results of PERMANOVA revealed significant morphological differences between colonies from the three locations (pseudo-F[pF]= 7.6567, P = 0.0002, perm =5000), as well as between the nearshore and offshore genotypes (pF= 5.7713, P=0.0002, perm=5000). CDA revealed that more than half of the characters (11 out of 19) contributed significantly to define the morphological distinctiveness among the genotypes, rather than just a few characters influencing the differences (Table S1). The characters which contributed the most ($P \leqq 0.005$) were corallite spacing, ventral septum length, lateral septum length, columella diameter, ventral palus diameter, lateral palus diameter, ventral septa spacing, and ventral palus spacing. The forward selection procedure identified six characters with a significant conditional effect, which were, in the order of significance; ventral palus spacing, lateral palus diameter, corallite spacing, lateral septum length, ventral palus diameter, and ventral septum spacing (Fig. 8, Table S2). All of these characters had significant marginal effects (i.e. when a character is tested alone in the model). The Kewalo sample had almost no overlap of the canonical scores with other samples, while a portion of the canonical scores of the nearshore and

offshore genotypes overlapped (Fig. 9a). In CDA, the first axis explained 21.1% of the variance, and the second axis explained 19.0% of the variance. Kewalo and Maunalua Bay samples separated primarily along the first discriminant axis, while the nearshore and offshore genotypes within Maunalua Bay separated along the second discriminant axis (Fig. 9a). The canonical discriminant analysis, using the six characters identified as significant conditioning effects in the forward selection, showed that the pattern of canonical scores observed using 19 characters was preserved with the six characters, and the first and second axes still explained 19.2% and 14.6% of the variance respectively (Fig. 9b). CDA was also run using the averages of the 10 corallite measurements per individual sample, based on the six significant characters. The results also retained the pattern of canonical scores well (Fig. 9c) with the first and second axes explaining 38.9% and 32.7% respectively. The average values of these six characters revealed that corallite spacing was decreased in the nearshore samples, while lateral septum length, ventral palus diameter, ventral septum spacing, ventral palus spacing, lateral palus diameter were all increased in the nearshore samples compared to the offshore samples.

The classificatory discriminant analysis with cross-validation resulted in correct classification approximately 72% of the time for all samples. (Table 3, Fig. 10). The nearshore samples were correctly identified 74.4% of the time, while 67.1% of the offshore samples were correctly identified. The Kewalo sample was identified correctly 80% of the time.

Genomic Analysis

From nine holobiont *Porites* DNA samples, over nine million high-quality RAD-seq reads were obtained. The total merged reads per sample ranged from 586,847 to 2,396,522, with an average of 91.2% of reads being paired (Table 4). The mitochondrial genomes were assembled for each sample, covering 95.7% of the reference genome on average, with a mean depth of 12.2. The mitochondrial genome was also fully assembled using all *P. lobata* samples, and the consensus sequence was published as the first reported *P. lobata* mitochondrial genome in Tisthammer *et al*. (2016). Histone regions (>5,300-bp) and the ribosomal regions (28S) (8772-bp) were assembled almost fully (mapped 99.6%, and 99.9% on average respectively) for the nine samples. The de novo assembly statistics of the RAD reads are summarized in Table 4.

Together, with an additional three windward *P. lobata* samples, the reads from the 12 samples were mapped to the *P. lobata* transcriptome pseudo-reference sequence, which resulted in an average of ~299,700 mapped reads per sample, forming a total of ~87,800 clusters. Filtering the clusters to loci present in all samples resulted in 18,015 loci with a mean depth of 34.7(±23.0) for the 12 *Porites* samples, and 18,458 loci with a mean depth of 38.7(±23.2) for the nine leeward *Porites* samples. For population genomic analysis, the *P. evermanni* sample was removed, and filtering the clusters to loci present in all samples resulted in 17,850 loci with a mean depth of 33.3 (±21.6) in the 11 *P. lobata* samples, and 17,956 loci with a mean depth of 37.6 (±21.7) for the eight leeward *P. lobata* samples.

The assembled contigs were also mapped to *Acropora digitifera* genome sequences (Shinzato *et al* 2012, DDBJ accession number: BACK01000001 – BACK01053640) using BWA v.0.7.12 (Li & Durbin 2009). Less than 19% of reads were mapped sporadically to approximately 23,000 contigs of *A. digitifera,* due presumably to too divergent taxa. Therefore, no further mapping to Acropora genome was conducted (results not shown).

Tree/SNP Analysis:

The results of the PyRAD-RAxML tree analysis of holobionts showed all Maunalua Bay's nearshore samples to cluster together with strong bootstrap support (94%) (Fig 11a). One of the offshore samples (C16) and the Kewalo sample formed a sub-cluster to the nearshore sample group with strong bootstrap support (90%), while another offshore sample (C6) clustered together with the windward samples. The tree analysis highlighted a strong geographic signature of sampling locations (i.e. the leeward vs. windward-side of the island of Oahu) for *P. lobata* samples (90% support). Interestingly, the leeward and windward partitioning of the samples came out stronger than the partitioning between the two closely related *Porites* species, *P. lobata* and P. compressa. The detailed phylogenomic analysis results are presented in Forsman *et al*. (2017). *P. evermanni* samples formed a monophyletic cluster with strong bootstrap support, showing a clear distance from the *P. lobata* 'complex'.

The transcriptome aligned SNP loci were visualized using smartpca, which resulted in a strikingly similar grouping pattern to the holobiont tree by PyRAD-RAxML (Fig. 11b). Clear geographic separation was observed between the leeward and windward samples, with the

exception of one offshore sample (C6). The *P. evermanni* sample was separated by the axis 2 from the *P. lobata* samples in the PCA plot.

The population genomic structure of 11 *P. lobata* samples using coral SNPs (17801 loci) was analyzed using *adegenet*, which showed a significant F_{ST} value between the Maunalua Bay nearshore samples and the windward samples. The overall F_{ST} for the four locations was 0.031 (P = 0.01). The *find.cluster* analysis of the *adegenet* function resulted in two clusters: 1) all nearshore samples, K2 & C16, and 2) C6 & all windward samples. These clusters were congruent with the grouping found by the holobiont tree analysis (Fig. 11c).

Morphological and Genomic Distance Comparison

The morphological distance obtained from the 19 numerical characters and the genetic distance estimated from the 17,801 coral SNP loci showed a significant correlation between the nearshore and offshore *P. lobata* samples from Maunalua Bay (*Relate* in PRIMER: Rho = 0.641~0.667, P = 0.029~0.03, Mantel Test: r = 0.559~0.632, P = 0.030~0.046, n=8) (Fig. 12). The genetic distance matrix of 17 *P. lobata* was calculated using the unphased, approximately1400bp segment of the previously sequenced histone marker (Tisthammer *et al*. 2017a). The relationships between genetic distance and morphology were explored among the three locations. The results showed a significant, to a marginally significant, correlation, depending on the distance transformation methods used (Mantel Test: r = 0.357 ~ 0.397, P=0.049~0.065).

DISCUSSION

Coral systematics, built on skeletal morphology, are continually being challenged and revised as new genetic data become available (Fukami *et al*. 2008; Budd *et al*. 2012; Huang *et al*. 2014). When genetic markers can provide clear resolution to their evolutionary relationships, reconstructing phylogenies becomes rather straightforward. However, for certain taxa such as *Porites*, understanding their accurate phylogenetic relationships has been particularly difficult, since existing genetic data have not been able to resolve the species complexes, even with RAD-seq generated SNPs, (Forsman *et al*, 2017). High plasticity and/or variability in *Porites*'s

corallite morphology further adds to the confusion. Moreover, we lack knowledge on the degree of corallite morphological variability that exists within and between species, and how the environment and genotype affect such plasticity (Todd *et al*. 2004a). This study provided a new insight into the range of variation in corallite morphology of *P. lobata* and *P. evermanni*, as well as genetic influence on their variability. The results highlighted a need to establish clearer diagnostic morphological characters for *Porites* taxa. If only a handful of taxonomic experts can identify the species, this will not aid future research progress. Methods that require sophisticated technology, such as scanning electron microscopy or 3D reflex microscopy, are also not desirable, as most researchers will not have access to such instruments or resources to conduct expensive analysis. As in Forsman *et al*. (2015), our study showed that using a simple stereomicroscope and imaging software for morphometric analysis can be an efficient tool to capture character differences in *Porites* corallites.

Corallite Observation

The observation of a larger number of corallites revealed much greater variability in corallite morphology in both *P. lobata* and *P. evermanni* than expected. Since *P. lobata* and *P. evermanni* are genetically distinct, we were able to identify all *P. evermanni* samples with 100% certainty. *P. lobata*, on the other hand, belongs to the unresolved Clade I species complex (Forsman *et al*. 2009; Forsman *et al*. 2017), and can only be identified to the clade level. Therefore, there is a possibility that some samples might belong to a different species. Even though *P. lobata* is the only mounding massive species in Clade I in Hawaii, when the colonies are small, other growth forms, such as nodular or columnar, may look similar to massive form. The species in Clade I, with similar corallite structures to *P. lobata*, in Hawaii *include P. cf. duerdeni, P. pukoensis, P. cf. annae*, and *P. cf. studeri*. All of these species are either extremely rare, not confirmed as an independent species (*P. cf. duerdeni*), and/or have not been reported in the waters around the island of Oahu. Therefore, it is unlikely that our samples contained any of these species.

Assuming all Clade I samples assessed in our study were *P. lobata*, a high level of variation in corallite morphology existed, including key diagnostic characters, such as the number of pali. In the report by Ketchum and Bonilla (2001) on coral taxa from the Archipielago de Revillagigedo, Mexico, detailed variations in *P. lobata* corallite architecture were noted, such

as columella being compressed or rod-shaped, and the development state of pali. The authors classified the variation into three forms. All three forms were observed in our study. Additionally, the authors categorized the variants of massive *Porites* samples that did not match with any existing corallite descriptions as "*Porites* sp.1," which included samples having 5-8 pali with a fused to free ventral triplet. Some or all of their samples of *Porites* sp.1 could well be the variation of *P. lobata* we observed in our study. However, since no genetic analysis was conducted on their samples, we can only speculate at this point. The Eastern Tropical Pacific and the Hawaiian Islands represent a marginal habitat for reef corals, geographically apart from the central Pacific by thousands of kilometers (Baums *et al*. 2012; Hellberg *et al*. 2016). These isolated regions, with their low species diversity, offer an excellent opportunity to efficiently study *Porites* skeletal structures, since the uncertainty of species identification can be removed from the equation.

Morphometric Analysis

We assessed the adequacy of using 10 corallite measurements per sample by comparing coefficients of variation. Since there were no changes in the average coefficients of variation between using five and 10 measurements per sample, our previous assumption (that using 10 measurements per sample was sufficient to capture the 'within-sample' variability) was valid. This is not to be confused with intracolonial variability, since the majority of our observations were taken from one skeletal fragment per colony, with each fragment ranging in size from 1 to 16 cm^2. An ideal way to assess the intracolonial variations is to take skeletal samples from various parts of a colony, since the top and the bottom of a colony may show different skeletal characters. However, this is often not possible due to limited resources and/or restrictive collection permits. In terms of capturing the 'within-sample' variations, our analysis suggested that taking even five measurements per sample may be enough. This result will increase the efficiency of future morphometric studies, as taking multiple measurements from a small corallite is the most time-consuming part of the analysis.

The morphometric analysis of *P. lobata* corallites showed strong grouping based on geographic locations, which also corresponded to genetic distance. The six characters with a significant conditional effect, identified by the stepwise forward selection in CDA, were congruent with the characters that significantly contributed to defining the groups. These six

characters also retained the separation of canonical scores among the sites (Fig. 9b), suggesting that the number of characters to be measured can be substantially reduced in future morphometric studies of *P. lobata*. Three of the six key characters were associated with ventral triplet (ventral palus spacing, ventral palus diameter, and ventral septum spacing). Ventral triplet is one of the diagnostic characters for identifying *Porites* species, and is reported to 'usually have free margins' in *P. lobata* (Veron & Pichon 1982; Veron 2000). Our study revealed that the skeletal formation of the ventral triplet could vary substantially for *P. lobata*, with up to 20% of colonies having corallites with a fused triplet or a trident, indicating that ventral triplet may not be a reliable diagnostic character in species identification. Also, our results stress the importance of using the quantitative approach, as qualitative observations will unlikely be able to capture the subtle differences in morphology. The characters associated with lateral pali/septa were also important features in defining the groups in *P. lobata*. This was not surprising, since the most noticeable differences of *P. lobata* corallites (between the nearshore and offshore sites) were the prominent development of lateral pali.

'Corallite spacing' was another of the six key characters, which is a difficult feature to compare without a quantitative assessment. Weil (1992) reported corallite density (the number of corallites per area) as the most important distinguishing character in his discriminant analysis of *Porites* corallites. However, Jameson (1995) stated that corallite density is not a reliable character, since budding corallites would influence the number. Our results showed that corallite spacing, which is related to corallite density, is one of the key characters in defining the groups. Jameson (1995) did measure corallite spacing in his study, but the corallite spacing was not one of the five characters identified as important in his discriminant analysis.) Certain environmental stressors, such as sedimentation, are also known to influence corallite density (Mwachireya & McClanahan 2015). We, therefore recommend corallite spacing as a useful diagnostic character.

Genetic Basis for Corallite Morphology

The genomic data of eight *P. lobata* samples (from the leeward side of the island of Oahu [Maunalua Bay and Kewalo Basin]) were originally assessed to understand the genetic basis for the observed corallite morphological variability, rather than geographical grouping. However, quantitative morphometric analysis revealed a strong geographic signature in corallite morphology, and strikingly similar results were found from the genomic analysis. The result was

especially pronounced when the windward samples were included in the analysis (Fig.11). Surprisingly, the geographic grouping was stronger than grouping between the species of *P. lobata* and P. compressa. Detailed results of the phylogenomic analysis of the Hawaiian *Porites* samples are summarized in Forsman *et al*. (2017), and will not be discussed here.

The significant correlation found between the morphological and genetic distances (Fig. 12) suggests corallite architecture is potentially largely determined genetically in *P. lobata*. This is congruent with previous studies, which concluded that much of the observed corallite variation in *Porites* species was genetically based (Brakel 1977; Weil 1992; Forsman *et al*. 2015). Nearshore samples used in our analysis were genetically and morphologically closer than the two offshore samples (Fig. S1). Since the number of samples used in the analysis was limited, further studies will be needed to better understand the exact nature of the relationship between the genetic and morphological distances. Certain coral species are known to exhibit high phenotypic plasticity in corallite morphology. As pointed out in Todd (2008), phenotypic plasticity and intraspecific variation are not the same, though they are often used interchangeably, causing confusion and misunderstanding. Our study focused on intraspecific variation of corallite morphology; whether, or how much, these corals would exhibit plasticity in a different environment was beyond the scope of this research. Based on the strong genetic basis for corallite architecture, it is unlikely that corallite morphology will drastically change in the *P. lobata* samples used in our study.

So, does the corallite structure have adaptive values? We can speculate from previous studies that the unique corallite structure of the nearshore genotype is not by coincidence. For example, light and water movement are known to induce changes in corallite morphology, and sedimentation also likely plays a role (Todd, 2008). The coral fragments transplanted to the shallow water site (with greater light intensity and higher total suspended sediment concentration), showed increased calice size, skeletal topology, and fragment rugosity in Favia speciosa (Todd *et al*. 2004a; b). The authors concluded that these induced changes likely had an adaptive value, since the increase in calice size correlates to the sediment shedding capacity in many coral species (Stafford-Smith & Ormond, 1992). The shape of calice also appeared to affect the sedimentation shedding ability (Riegl 1995). In contrast, the Maunalua Bay nearshore site has considerably lower light intensity (Tisthammer *et al*. 2017b) and higher total suspended sediment concentration (Presto *et al*. 2012) than the offshore site. Therefore, it is possible that

the corallite morphology of the nearshore corals is beneficial for surviving in such an environment. The nearshore corals overall had shallower corallites and much more pronounced pali than the offshore corals. These traits may help prevent the accumulation of sediments and/or facilitate the removal of sediments, which may reduce the energy required to shed sediments, and/or help polyps extend under limited light.

CONCLUSIONS

Our results indicate a strong genetic effect in determining corallite morphology of *P. lobata*. Our previous studies have shown the molecular and physiological response differences between the nearshore genotype and offshore genotype of *P. lobata* from Maunalua Bay, suggesting the nearshore corals are genetically adapted to their environment. The distinct morphological characters seen in the nearshore *P. lobata*, therefore, also suggest that the corallite characters observed may have an adaptive value. The high level of variation in skeletal morphology observed in *P. lobata* and *P. evermanni* in our study spells out the need for further understanding of the extent of skeletal variability and plasticity in *Porites* species, as well as establishing a new classification system that integrates morphological data and genetic information.

ACKNOWLEDGEMENTS

We thank for the support provided by Z. Forsman and A. Amend. We also appreciate Illumina, Inc. for providing the reagents and supplies for sequencing. Coral samples were collected under Department of Land and Natural Resources permit SAP 2013-26 and 2015-06. Following people assisted in collecting coral samples: M. Stiber, V. Sindorf, F. Seneca, J. Murphy, J. Martinez, A. Lyman, K. Richmond, V. Hölzer, N. Spies, and A. Irvine..

REFERENCES

Ahrens D, Fujisawa T, Krammer H-J *et al.* (2016) Rarity and Incomplete Sampling in DNA-Based Species Delimitation. *Systematic Biology*, **65**, 478–494.

Arrigoni R, Berumen ML, Chen CA *et al.* (2016) Species delimitation in the reef coral genera *Echinophyllia* and *Oxypora* (Scleractinia, Lobophylliidae) with a description of two new species. *Molecular Phylogenetics and Evolution*, **105**, 146-159.

Baums IB, Boulay JN, polato NR, Hellberg ME (2012) No gene flow across the Eastern Pacific Barrier in the reef-building coral Porites lobata. *Molecular Ecology*, **21**, 5418–5433.

Baums IB, Miller MW, Hellberg ME (2005) Regionally isolated populations of an imperiled Caribbean coral, *Acropora palmata*. *Molecular Ecology*, **14**, 1377–1390.

Bosch TCG, Miller DJ (2016) Corals. In: *The Holobiont Imperative: Perspectives from Early Emerging Animals*, pp. 99–111. Springer, Vienna.

Brainard RE, Birkeland C, Eakin CM, McElhany P, Miller MW, Patterson M, and Piniak GA (2011) Status review report of 82 candidate coral species petitioned under the U.S. Endangered Species Act. U.S. Dep. Commer., NOAA Tech. Memo., NOAA-TM-NMFS-PIFSC-27, 530 p. + 1 Appendix.

Brakel WH (1977) Corallite variation in Porites and the species problem in corals. *Proceedings of Third International Coral Reef Symposium*, 457–462.

Budd AF, Fukami H, SMITH ND, Knowlton N (2012) Taxonomic classification of the reef coral family Mussidae (Cnidaria: Anthozoa: Scleractinia). *Zoological Journal of the Linnean Society*, **166**, 465–529.

Campbell NA (1996) *Biology*. Benjamin/Cummings Publishing Company, Menlo Park, California.

Carpenter KE, Abrar M, Aeby G *et al.* (2008) One-third of reef-building corals face elevated extinction risk from climate change and local impacts. *Science*, **321**, 560–563.

Clarke KR, Gorley RN (2006) PRIMER v6: User Manual/Tutorial. PRIMER-E, Plymouth, 192pp.

de Queiroz K (1998) The general lineage concept of species, species criteria, and the process of speciation: a conceptual unification and terminological recommendations. In: *Endless forms: species and speciation* (eds Howard DJ, Berlocher SH), pp. 57–75. Oxford University Press on Demand.

de Queiroz K (2007) Species Concepts and Species Delimitation. *Systematic Biology*, **56**, 879–886.

Danecek P, Auton A, Abecasis G, Albers CA, Banks E, DePristo MA, Handsaker RE, Lunter G, Marth GT, Sherry ST, McVean G, Durbin R (2011) The variant call format and VCF tools. *Bioinformatics* **27**, 2156–8.

Dray S, Dufour AB, Chessel D (2007) The ade4 package-II: Two-table and K-table methods. *R news*, **7**, 47–52.

Dunn CP (2003) Keeping taxonomy based in morphology. *TRENDS in Ecology and Evolution* **18**, 270–271.

Eaton DAR (2014) PyRAD: Assembly of de novo RADseq loci for phylogenetic analyses. *Bioinformatics* **30**:1844–1849.

Eytan RI, Hayes M, Arbour-Reily P, Miller M, Hellberg ME (2009) Nuclear sequences reveal mid-range isolation of an imperilled deep-water coral population. *Molecular Ecology*, **18**, 2375–2389.

Forsman ZH, Barshis DJ, Hunter CL, Toonen RJ (2009) Shape-shifting corals: molecular markers show morphology is evolutionarily plastic in Porites. *BMC Evolutionary Biology*, **9**, 45.

Forsman ZH, Wellington GM, Fox GE, Toonen RJ (2015) Clues to unraveling the coral species problem: distinguishing species from geographic variation in Poritesacross the Pacific with molecular markers and microskeletal traits. *PeerJ*, **3**, e751.

Forsman ZH, Knapp ISS, Tisthammer KH, Eaton DAR, Belcaid M, Toonen RJ (2017) Coral hybridization or phenotypic variation? Genomic data reveal gene flow between *Porites lobata* and *P. Compressa. Molecular Phylogenetics & Evolution* http://dx.doi.org/10.1016/j.ympev.2017.03.023.

Fukami H, Budd AF, Levitan DR *et al.* (2004a) Geographic differences in species boundaries among members of the *Montastraea annularis* complex based on molecular and morphological markers. *Evolution*, **58**, 324–337.

Fukami H, Budd AF, Paulay G, Solé-Cava A, Chen CA (2004b) Conventional taxonomy obscures deep divergence between Pacific and Atlantic corals. *Nature*, **427**, 832–835.

Fukami H, Chen CA, Budd AF *et al.* (2008) Mitochondrial and nuclear genes suggest that stony corals are monophyletic but most families of stony corals are not (Order Scleractinia, Class Anthozoa, Phylum Cnidaria). *PLoS ONE*, **3**, e3222.

Garrison E, Marth G (2012) Haplotype-based variant detection from short-read sequencing. arXiv Prepr. arXiv1207.3907 9

Hellberg ME, Prada C, Tan MH, Forsman ZH, Baums IB (2016) Getting a grip at the edge: recolonization and introgression in eastern Pacific *Porites* corals. *Journal of Biogeography*.

Huang DW, Sherman BT, Lempicki RA (2009) Bioinformatics enrichment tools: paths toward the comprehensive functional analysis of large gene lists. *Nucleic Acids Research*, **37**, 1–13.

Huang D, Benzoni F, Fukami H *et al.* (2014) Taxonomic classification of the reef coral families Merulinidae, Montastraeidae, and Diploastraeidae (Cnidaria: Anthozoa: Scleractinia). *Zoological Journal of the Linnean Society*, **171**, 277–355.

Jameson SC (1995) Morphometric analysis of the Poritidae (Anthozoa: Scleractinia) off Belize. In:, pp. 1591–1596.

Joly S, Bryant DJ, Lockhart PJ (2015) *Flexible methods for estimating genetic distances from nucleotide data*. Methods in Ecology and Evolution.

Jombart T, Ahmed I (2011) adegenet 1.3-1: new tools for the analysis of genome-wide SNP data. *Bioinformatics*, **27**, 3070–3071.

Ketchum JT, Bonilla HR (2001) Taxonomía y distribución de los corales hermatípicos (Scleractinia) del Archipiélago de Revillagigedo, México. *Revista de Biología Tropical*, **49**, 803–848.

Knowlton N (2000) Molecular genetic analyses of species boundaries in the sea. *Hydrobiologia*, **420**, 73–90.

Koutecký P (2014) MorphoTools: a set of R functions for morphometric analysis. *Plant Systematics and Evolution*, **301**, 1115–1121.

Li H, Durbin R (2009) Fast and accurate short read alignment with Burrows-Wheeler transform. *Bioinformatics* **25**:1754–1760.

McKenna A, Hanna M, Banks E, Sivachenko A, Cibulskis K, Kernytsky A, Garimella K, Altshuler D, Gabriel S, Daly M, DePristo MA (2010) The Genome Analysis Toolkit: A MapReduce framework for analyzing next-generation DNA sequencing data. *Genome Research* **20**, 1297–1303.

Miller DJ, van Oppen MJ (2003) A "fair go"* for coral hybridization. *Molecular Ecology*, **12**, 805–807.

Mwachireya SA, McClanahan TR, Hartwick BE, *et al* (2015) Growth and corallite characteristics of Kenyan scleractinian corals under the influence of sediment discharge. *International Journal of Biodoversoty and Conservation,* **7**:364–377.

Paradis E, Claude J, Strimmer K (2004) APE: Analyses of Phylogenetics and Evolution in R language. *Bioinformatics*, **20**, 289–290.

Pinzón JH, Sampayo E, Cox E *et al.* (2013) Blind to morphology: genetics identifies several widespread ecologically common species and few endemics among Indo-Pacific cauliflower corals (*Pocillopora*, Scleractinia). *Journal of Biogeography*, **40**, 1595–1608.

Prada C, DeBiasse MB, Neigel JE *et al.* (2014) Genetic species delineation among branching Caribbean Porites corals. *Coral Reefs*, **33**, 1019–1030.

Presto KM, Storlazzi CD, Logan JB, Reiss TE, Rosenberger KJ (2012) *Coastal Circulation and Potential Coral-larval Dispersal in Maunalua Bay, Oahu, Hawaii -Measurements of waves, Currents, Temperature, and salinity June-September 2010*. U.S. Geological Survey Open-File Report 2012-1040.

Price AL, Patterson NJ, Plenge RM *et al.* (2006) Principal components analysis corrects for stratification in genome-wide association studies. *Nature Genetics*, **38**, 904–909.

R Core Team. 2016. A Language and Environment for Statistical Computing. R Foundation for Statistical Computing, Vienna, Austria. https://www.R-project.org.

Richards ZT, Miller DJ, Wallace CC (2013) Molecular phylogenetics of geographically restricted Acropora species: Implications for threatened species conservation. *Molecular Phylogenetics and Evolution*, **69**, 837–851.

Riegl B (1995) Effects of sand deposition on scleractinian and alcyonacean corals. *Marine Biology*, **121**, 517-526.

Schneider CA, Rasband WS, Eliceiri KW (2012) NIH Image to ImageJ: 25 years of image analysis. *Nature Methods*, **9**, 671–675.

Selkoe KA, Gaggiotti OE, Treml EA *et al.* (2016) The DNA of coral reef biodiversity: predicting and protecting genetic diversity of reef assemblages. *Proceedings of the Royal Society B: Biological Sciences*, **283**, 20160354.

Stafford-Smith MG, Ormond R (1992) Sediment-rejection mechanisms of 42 species of Australian scleractinian corals. *Australian Journal of Marine and Freshwater Research*, **43**: 583–705.

Stamatakis A (2006) RAxML-VI-HPC: maximum likelihood-based phylogenetic analyses with thousands of taxa and mixed models. Bioinformatics 22:2688–90.

Stat M, Baker AC, Bourne DG *et al.* (2012) Molecular Delineation of Species in the Coral Holobiont. In: *Advances in Marine Biology*, pp. 1–65. Elsevier Ltd.

Stefani F, Benzoni F, Yang SY *et al.* (2011) Comparison of morphological and genetic analyses reveals cryptic divergence and morphological plasticity in *Stylophora* (Cnidaria, Scleractinia). *Coral Reefs*, **30**, 1033–1049.

Tautz D, Arctander P, Minelli A, Thomas RH (2003) A plea for DNA taxonomy. *Trends in Ecology & Evolution*, **18**, 70–74.

Tisthammer KKH, Forsman ZZH, Sindorf VL, Massey TL, Bielecki CR, Toonen RJR (2016) The complete mitochondrial genome of the lobe coral *Porites lobata* (Anthozoa:Scleractinia) sequenced using ezRAD. *Mitochondrial DNA Part B*, **1**, 1–3.

Tisthammer, K, Forsman Z, Richmond R (2017a) Isolation by adaption? Genetic structure is stronger across habitats than islands in the coral Porites lobata from Oahu and Maui. Manuscript in preparation.

Tisthammer, K, Seneca, F, Richmond R (2017b) Local adaptation of the lobe coral, *Porites lobata*, to reduced water quality. Manuscript in preparation.

Todd PA (2008) Morphological plasticity in scleractinian corals. *Biological Reviews*, **83**, 315–337.

Todd PA, Ladle RJ, Lewin-Koh N (2004a) Genotype× environment interactions in transplanted clones of the massive corals Favia speciosa and Diploastrea heliopora. *Marine ecology Progress Series*, **271**, 167–182.

Todd PA, Sidle RC, Lewin-Koh NJI (2004b) An aquarium experiment for identifying the physical factors inducing morphological change in two massive scleractinian corals. *Journal of experimental marine biology and ecology*, **299**, 97–113.

Toonen RJ, Puritz JB, Forsman ZH, Whitney JL, Fernandez-Silva I, Andrews KR, Bird CE (2013) ezRAD: a simplified method for genomic genotyping in non-model organisms. *PeerJ*, **1**, e203.

Valentini A, Pompanon F, Taberlet P (2009) DNA barcoding for ecologists. *Trends in Ecology & Evolution*, **24**, 110–117.

van Oppen MJ, Willis BL, Miller DJ (1999) Atypically low rate of cytochrome b evolution in the scleractinian coral genus *Acropora*. *Proceedings of the Royal Society B: Biological Sciences*, **266**, 179–183.

Veron JEN (1995) *Corals in Space and Time:The Biogeography and Evolution of the Scleractinia*. Cornell University Press, Ithaca, NY.

Veron JEN (2000) *Corals of the World* (MG Stafford-Smith, Ed,). Australian Institute of Marine Science, Townsville, Australia.

Veron JEN (2013) Overview of the taxonomy of zooxanthellate Scleractinia. *Zoological Journal of the Linnean Society*, **169**, 485–508.

Veron JEN, Pichon M (1982) *Scleractinia of Eastern Australia Part IV Family Poritidae*. Australian Institute of Marine Science and Australian National University Press, Miami, FL.

Vollmer SV, Palumbi SR (2002) Hybridization and the evolution of reef coral diversity. *Science*, **296**, 2023–2025.

Warner PA, van Oppen MJH, Willis BL (2015) Unexpected cryptic species diversity in the widespread coral Seriatopora hystrixmasks spatial-genetic patterns of connectivity. *Molecular Ecology*, **24**, 2993–3008.

Weil E (1992) Genetic and Morphological Variation in Caribbean and Eastern Paci c Porites (Anthozoa, Scleractinia). *Proc. of the Seventh International Coral Reef Symposium*, **2**, 643–656.

Willis BL, van Oppen M, Miller DJ, Vollmer SV (2006) The role of hybridization in the evolution of reef corals. *Annual Review of Ecology, Evolution, and Systematics*, **37**, 489–517.

Yang Z, Rannala B (2012) Molecular phylogenetics: principles and practice. *Nature Reviews Genetics*, **13**, 303–314.

Table 1. *Porites* sample information used in morphometric and genomic analyses.

Sample ID	Species	Location	Analysis	SRA or Genbank#
C6	*P. lobata*	O	M,G	SAMN06648852
C16	*P. lobata*	O	M,G	SAMN06648853
B3	*P. lobata*	O	M	KY502366
B7	*P. lobata*	O	M	KY502286
B9	*P. lobata*	O	M	KY502368
B10	*P. lobata*	O	M	KY502690
B11	*P. lobata*	O	M	KY502370
M2	*P. lobata*	N	M,G	SAMN06648857
M7	*P. lobata*	N	M,G	SAMN06648858
M12	*P. lobata*	N	M,G	SAMN06648859
N1	*P. lobata*	N	M,G	SAMN06648855
N3	*P. lobata*	N	M,G	SAMN06648856
N4	*P. lobata*	N	M	KY502357
N6	*P. lobata*	N	M	KY502358
N12	*P. lobata*	N	M	KY502362
N17	*P. lobata*	N	M	KY502364
K1	*P. evermanni*	K	G	SAMN06648867
K2	*P. lobata*	K	M,G	SAMN06648854

Abbreviations
O Offshore, Maunalua Bay
N Nearshore, Maunalua Bay
K Kewalo Basin
M Morphometrics
G Genomics

Table 2. Corallite characters of Porites samples measured for morphometric analysis. N= numerical characters, and D = descriptive characters.

	Characters	Type	Description
1	Corallite diameter (length)	N	Length parallel to dorso-ventral axis
2	Corallite diameter (width)	N	Length perpendicular to dorso-ventral axis
3	Corallite spacing	N	Average linear distance between centers of nearest and farthest neighboring corallites
4	Dorsal septum length	N	Linear distance from dorsal septum tip to inner theca margin
5	Ventral septum length	N	Linear distance from ventral septum tip to inner theca margin
6	Lateral septum length	N	Average of four linear distances from lateral septum tip to inner theca margin
7	Columella diameter	N	Average of maximum and minimum diameters of columella
8	Ventral palus diameter	N	Average diameters of ventral pali
9	Lateral palus diameter	N	Average of maximum and minimum diameters of lateral pali
10	Dorsal palus diameter	N	Diameter of dorsal palus
11	Fossa length	N	Distance measured across corallite center from middle ventral palus to dorsal palus
12	Fossa width	N	Average of distances measured across corallite center from a lateral palus to a diagonal lateral palus
13	Lateral septal spacing	N	Average of distances between lateral septa at thecal margin
14	Ventral septal spacing	N	Average of distances between ventral septa at thecal margin
15	Ventral pali spacing	N	Average of distances between ventral pali
16	Dorsal pali spacing	N	Average of distances between dorsal palus to a neighboring lateral plus
17	Lateral septa thickness	N	Average of cross-distances of lateral septa at midpoint
18	Dorsal septa thickness	N	Cross-distances of dorsal septum at midpoint
19	Ventral septa thickness	N	Average of cross-distances of lateral septa at midpoint
20	Number of pali	D	Number of pali per corallite
21	Lateral pali height	D	Degree of pronunciation of lateral pali (1 = not pronounced, 2=slightly pronounced, 3=moderately pronounced, 4=highly pronounced)
22	Triplet form	D	1=separated, 2=fused, 3=trident
23	Wall height	D	Pali to wall height: 1=High walls, tips of pali are much lower than wall, 2=Walls are slightly higher than pali, 3=Pali come up to the wall height
24	Corallite shape	D	3=round, 4=diamond/square/rectangle, 5=pentagon, 6=hexagon
25	Number of denticles	D	Average number of denticles per septa
26	Columella shape	D	0=not visible/none, 1=rod shape, 2=compressed

Table 3. Results of cross-validated classificatory discriminant analysis of 17 P. lobata corallites using the six morphological characters identified as discriminant variables in the forward selection process. Showing the N=Nearshore, O=Offshore, and K=Kewalo.

	N	O	K	% correct
Nearshore	66	20	4	73.3%
Offshore	21	43	6	61.4%
Kewalo	1	1	8	80%
Total			170	68.8%

Table 4. Summary of RAD read assembly statistics for nine *Porites* samples from the leeward side of Oahu.

Sample ID	Total reads	# reads used for assembly	% assembled	Total assembled contigs	N50	Contigs >100bp	Contigs >1000bp
C6	1,286,689	753,494	58.56	209,541	222	203,183	253
C16	1,122,131	719,383	64.11	206,918	443	206,422	2,573
K1	727,557	563,247	77.42	150,279	753	150,269	21,105
K2	586,847	337,579	57.52	107,587	434	107,487	593
N1	969,672	639,548	65.96	198,615	491	198,608	3,607
N3	615,094	378,919	61.60	107,726	425	107,608	999
M2	1,225,490	862,400	70.37	245,092	459	244,952	4,086
M7	1,203,255	883,406	73.42	256,857	444	256,733	2,760
M12	2,396,522	2,018,645	84.23	443,517	395	443,281	3,537
Ave.	1,125,917	795,180	68.13	214,015	452	213,171	4,390

Figure 1 *Porites lobata* corallites, live (a), and skeletal structure (b)

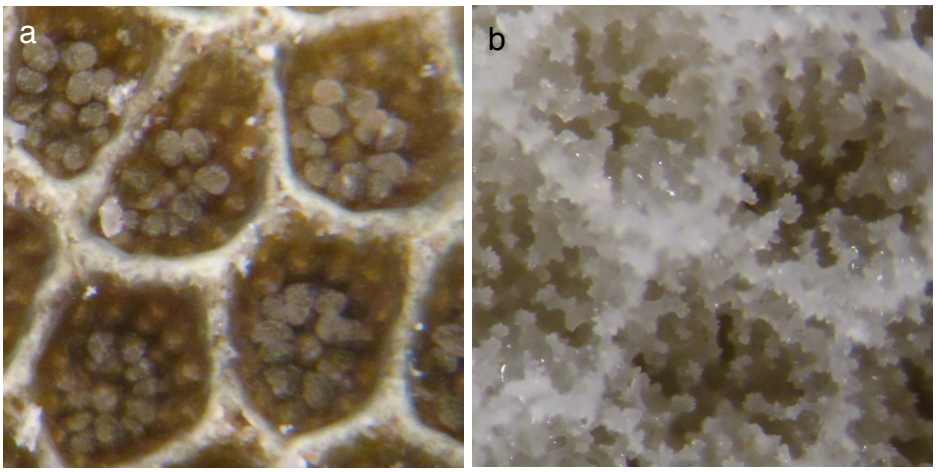

Figure 2. Map of coral sampling locations

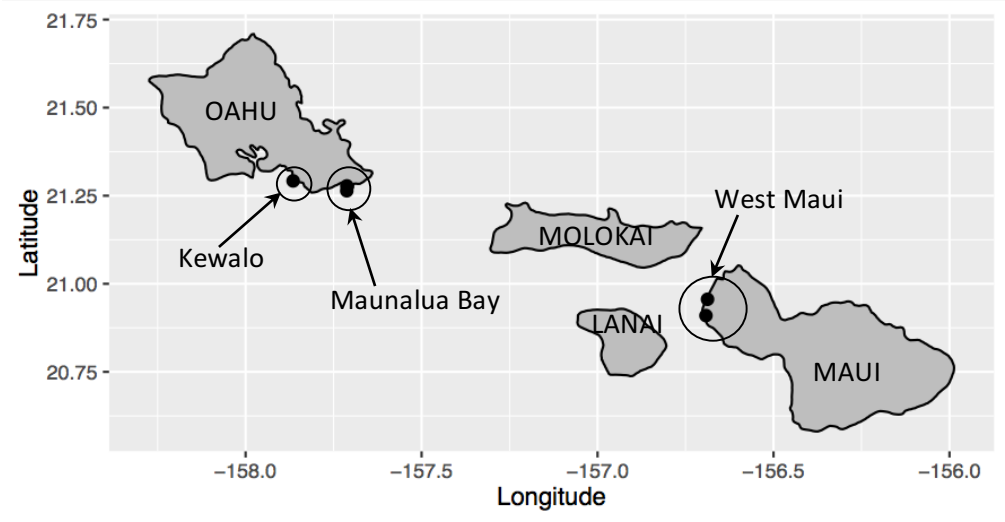

Figure 3. Examples of the published description of P. lobata and P. evermanni corallite skeletal structure. The figures are obtained from the Australian Institute of Marine Science (AIMS) website (http://coral.aims.gov.au/factsheet.jsp?speciesCode=0319 and http://coral.aims.gov.au/factsheet.jsp?speciesCode=0393from).

Porites lobata

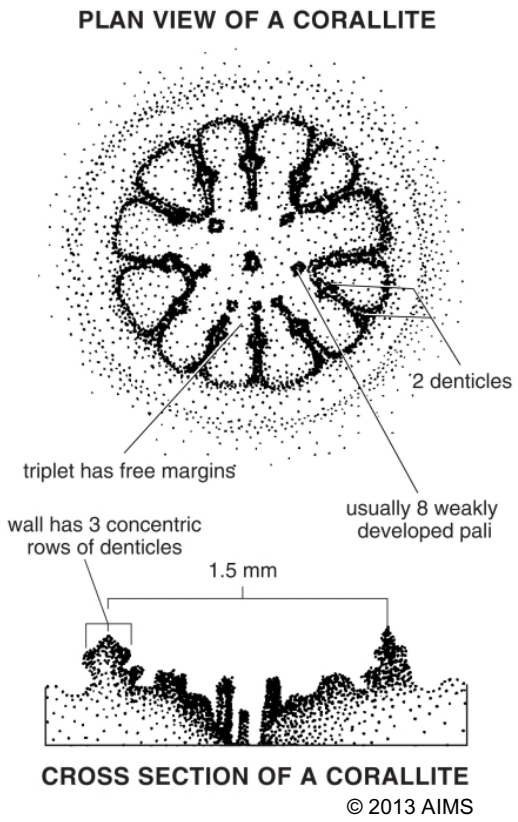

Porites evermanni

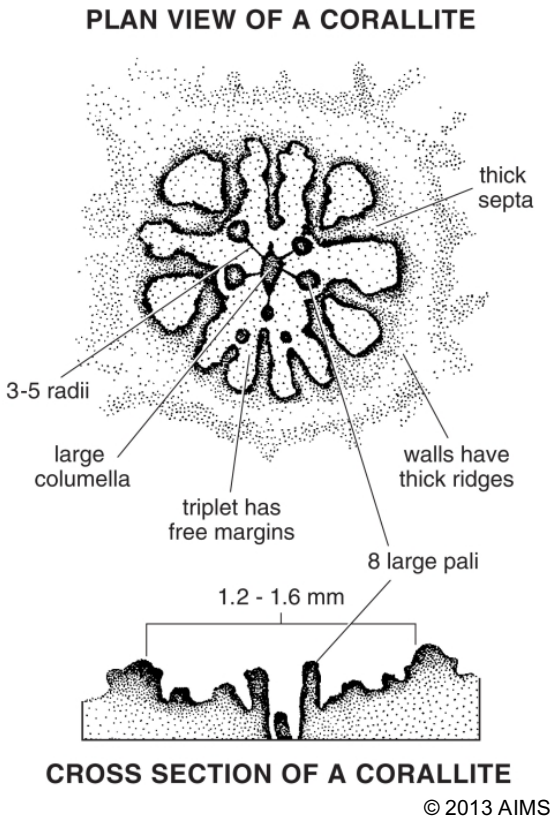

Figure 4. Diagram of examples of measurement locations of P. lobata corallite listed on Table 2.

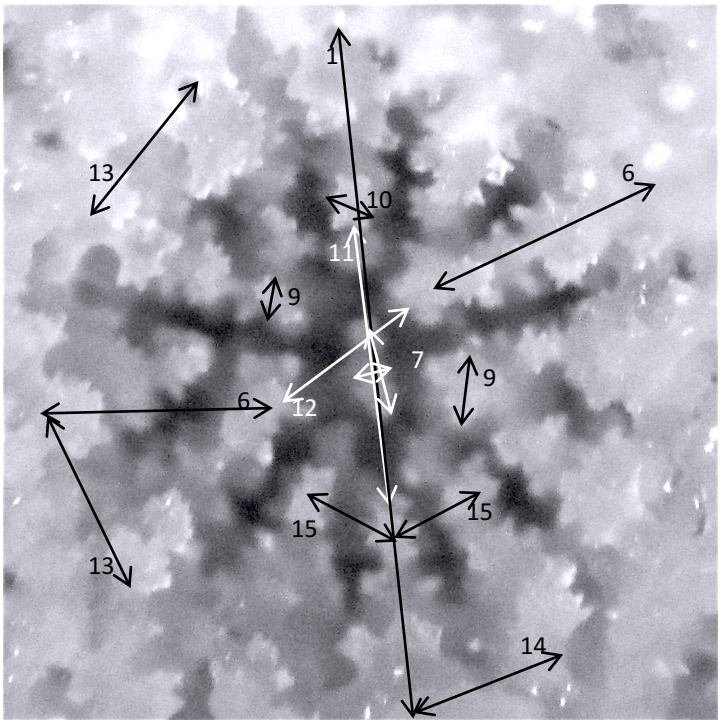

Figure 5. Images of P. evermanni corallites with typical thick wall (a), and thin wall (b).

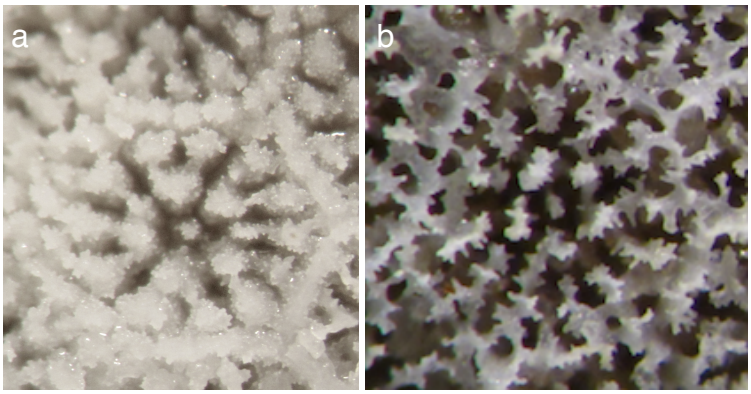

Figure 6. Images of *P. lobata* corallites; a) 'typical' corallite structure (represents the offshore site of Maunalua Bay), b) flat corallite variation (shallow calice), c) reduced number of pali (5~6), d) ventral triplet forming a trident, e & f) tall, pronounced lateral pali (represent the nearshore site of Maunalua Bay), g) compressed columella.

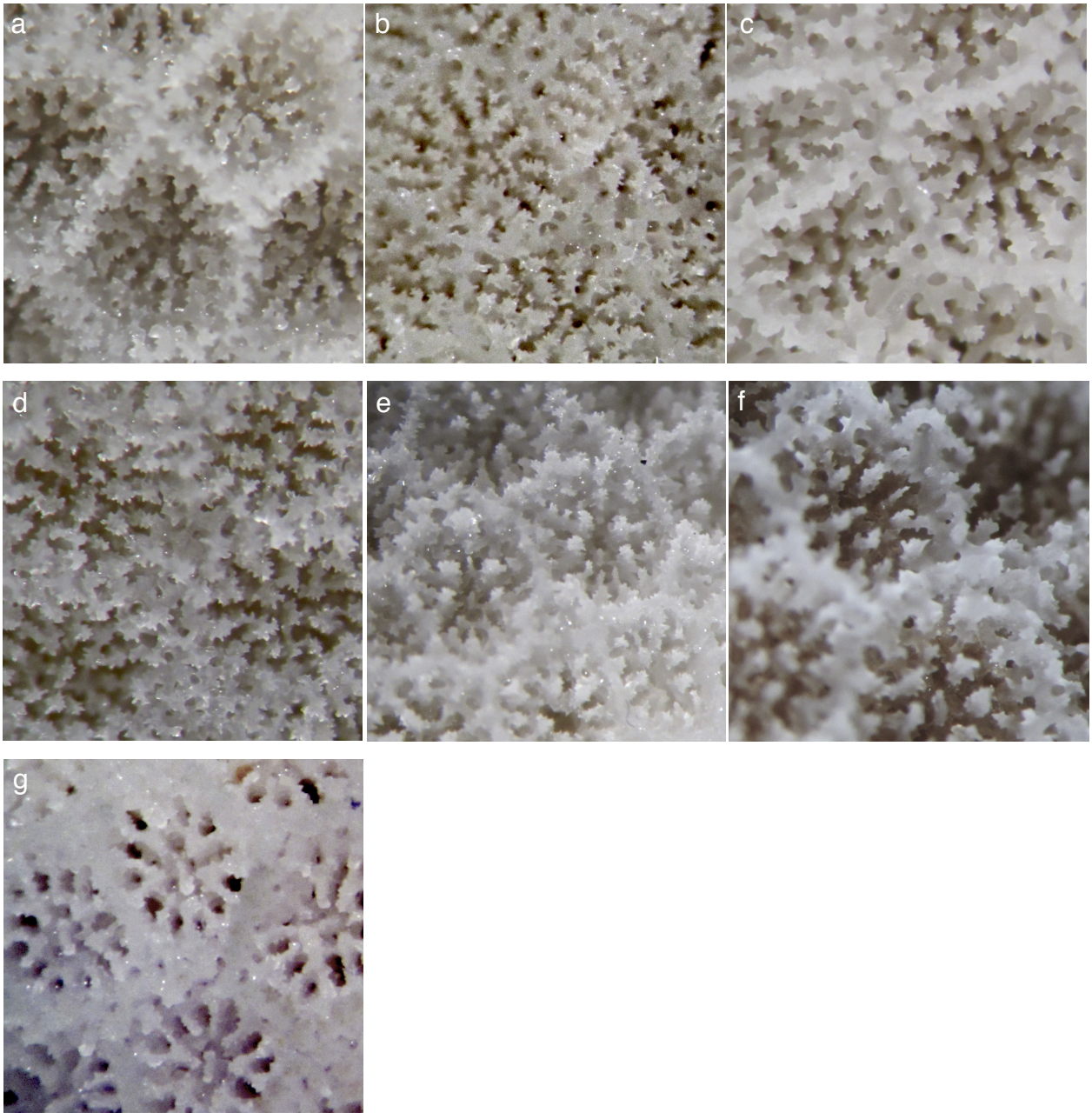

Figure 7. Results of PCO based on 26 morphological characters of 17 *P. lobata* corallites. The first and second ordination axes are displayed.

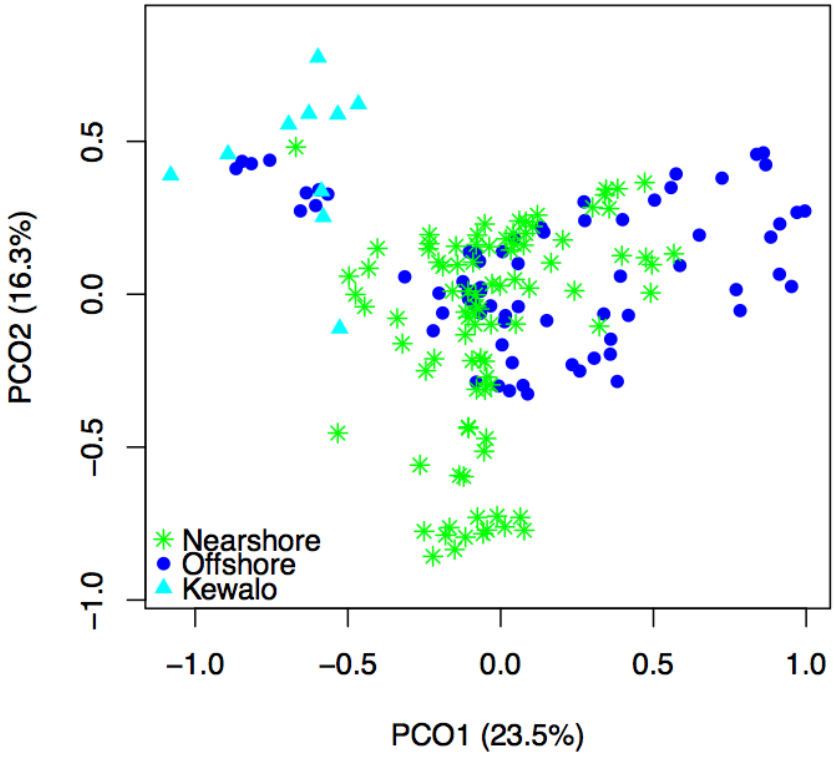

Figure 8. *P. lobata* corallite picture (a) and schematic diagram (b) showing the six characters with a significant conditional effect identified in the forward selection of CDA. 1:ventral palus spacing, 2: lateral palus diameter, 3: corallite spacing, 4: lateral septum length, 5: ventral palus diameter, and 6: ventral septum spacing (See detailed descriptions in Table 2, Table S2).

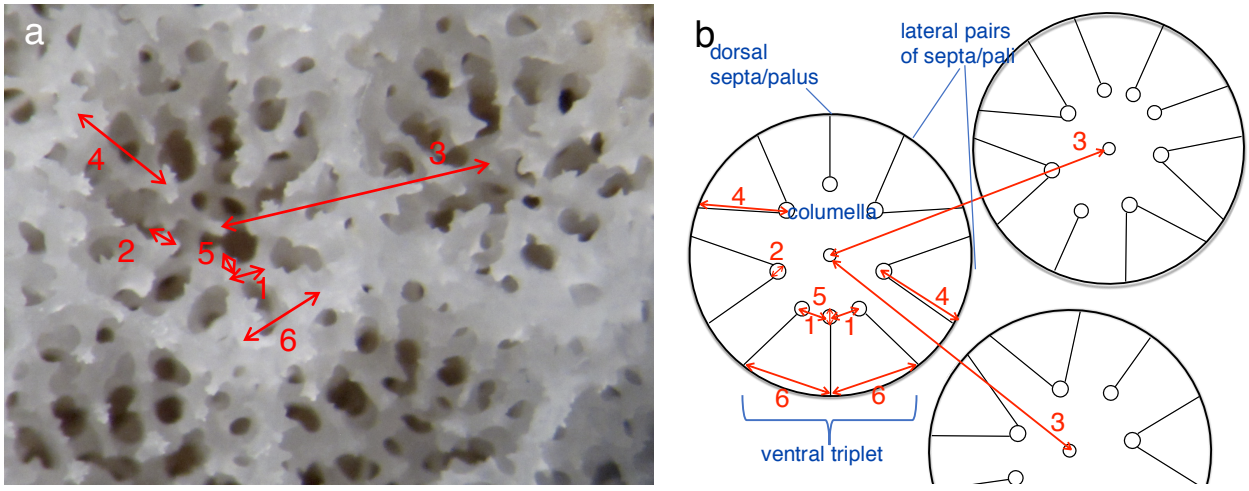

Results of CDA using 19 morphological characters of 17 *P. lobata* corallites (a), using the six characters identified in the forward selection process (b), and using the six characters based on the average character values per individuals . The first and second discriminant axes are displayed, which explained 21.1% and 19.0% in (a), 19.25 and 14.6% in (b), and 38.9% and 32.7% in (c).

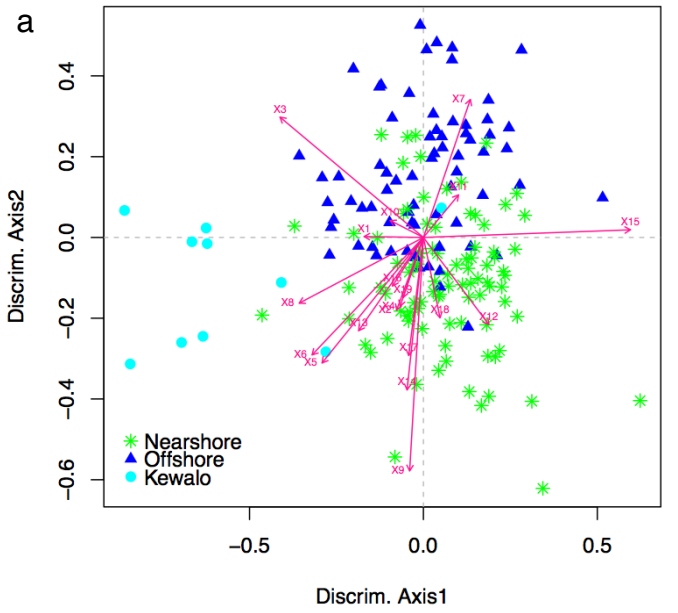

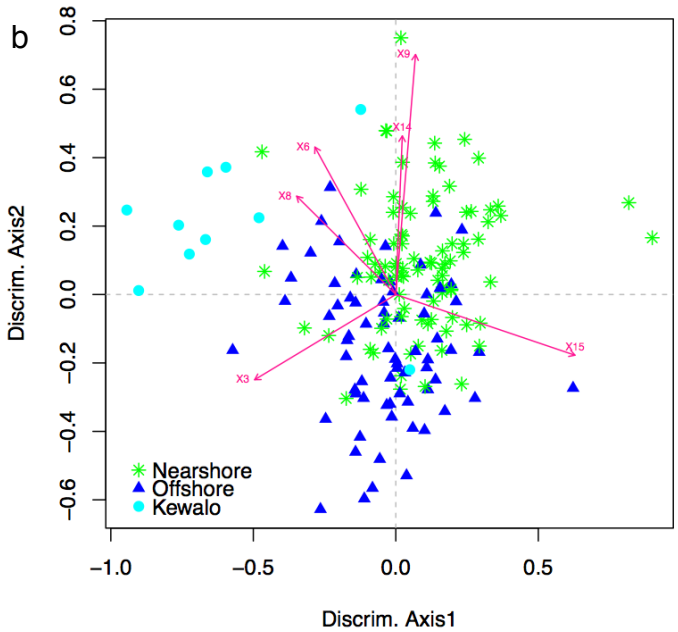

C

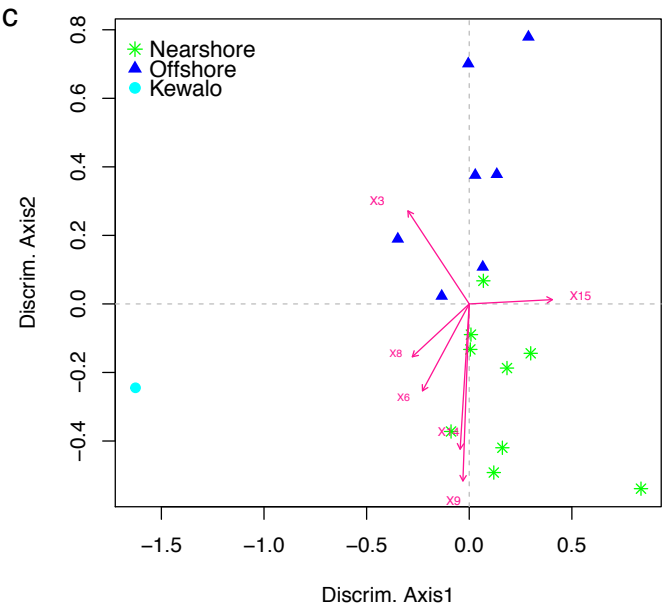
Nearshore
Offshore
Kewalo
X3
X15
X8
X6
X4
X9
Discrim. Axis2
Discrim. Axis1
0.8
0.6
0.4
0.2
0.0
−0.2
−0.4
−1.5
−1.0
−0.5
0.0
0.5

Figure 10. Results of classificatory discriminant analysis of 17 P. lobata corallites based on six morphological characters identified in the forward selection of discriminant analysis. Table 3 shows the

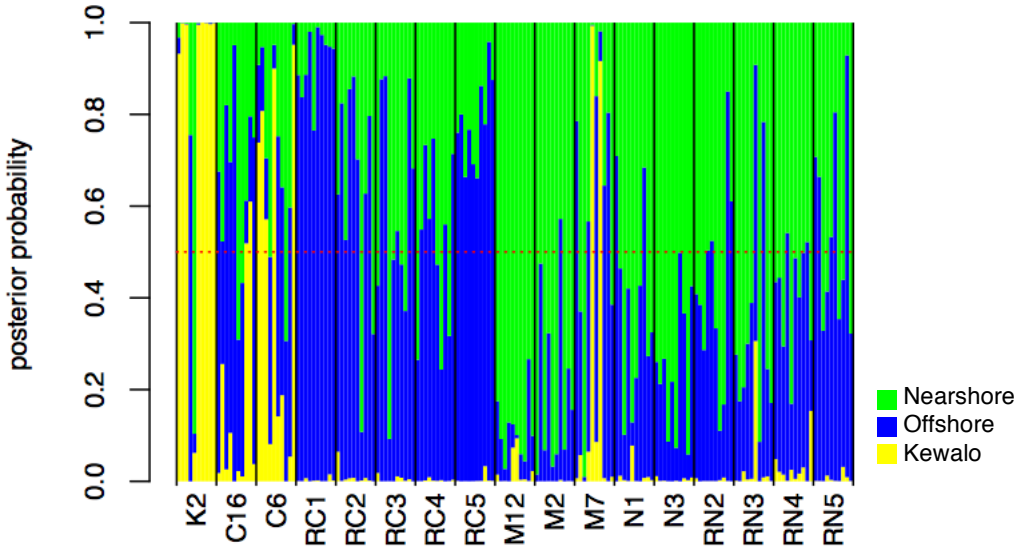

Figure 11. Results of genomic analysis of *Porites* samples. a) A tree generated from the holobiont data by RAxML (21 *Porites* samples), b) a PCA scatter plot of transcriptome aligned coral SNPs from smartpca analysis (12 *Porites* samples), and c) a PCA scatter plot for *P. lobata* populations generated by *adegenet*, with two clusters identified (pink dotted line circles) by the *find.cluster* analysis. Colors denotes the sample locations (green = Nearshore, Maunalua Bay blue = Offshore, Maunalua Bay, brown = Kewalo, light blue=the windward site of Oahu).

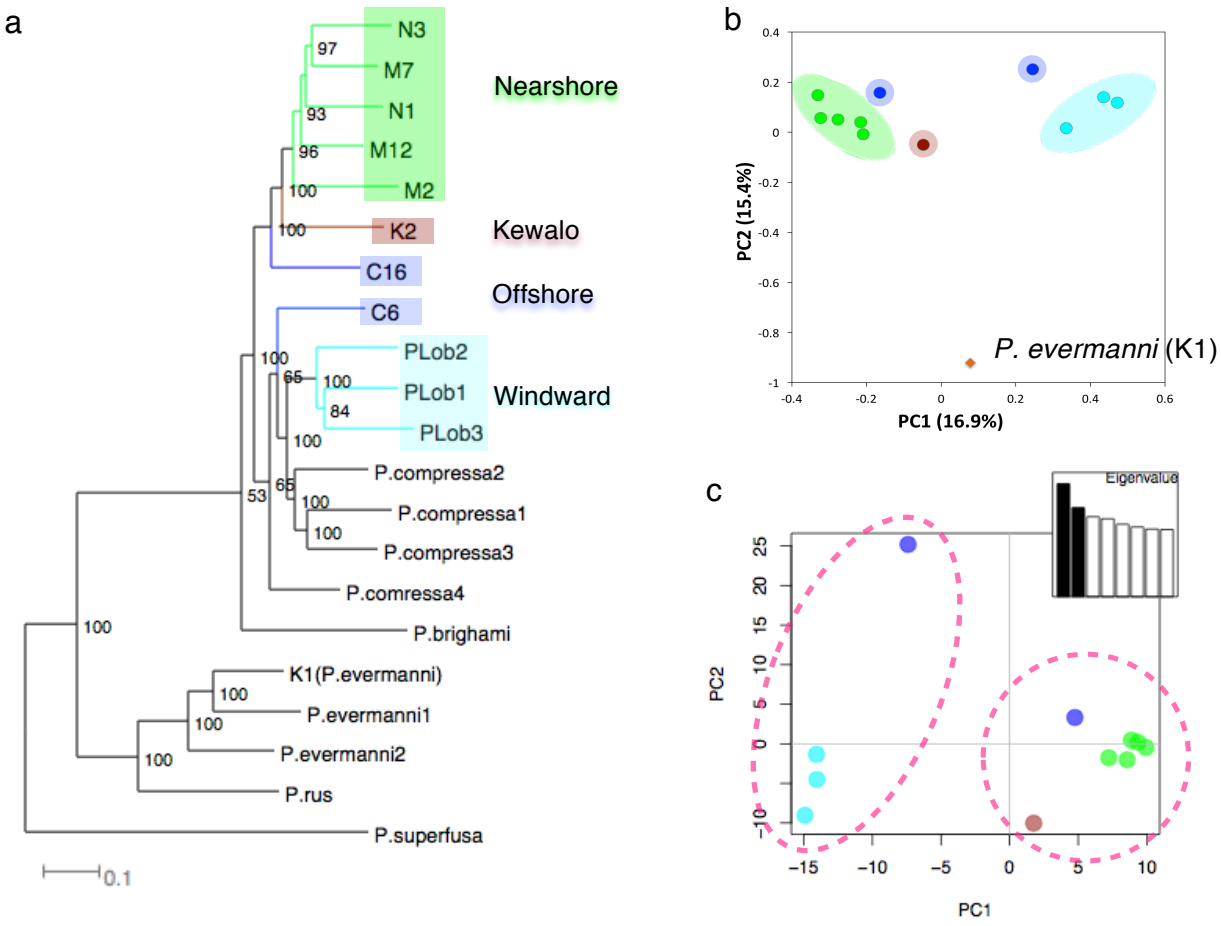

Figure 12. Relationship between *P. lobata* corallite morphology and genetics. The morphological distance matrix was obtained using the Euclidian method based on 19 characters, and the genetic distance matrix was calculated using the *genpofad* method based on 17,801 SNP loci of coral host.

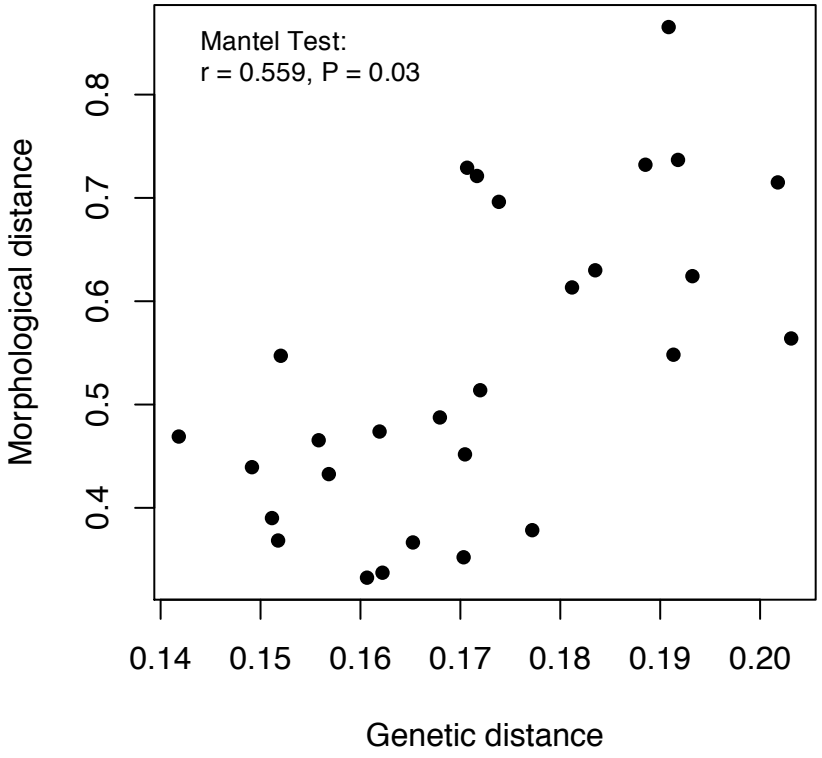

Table S1. Morphological characters of P. lobata corallites with significant marginal effects. P = significance level based on 1000 permutations.

Characters	F	P
Corallite spacing	13.77	0.005
Septum length (ventral)	9.59	0.005
Septum length (lateral)	10.00	0.005
Columella diameter	6.81	0.005
Ventral palus diameter	8.72	0.005
Lateral palus diameter	15.62	0.005
Ventral septa spacing	7.13	0.005
Ventral palus spacing	19.31	0.005
Lateral septa spacing	4.73	0.01
Fossa width	4.43	0.015
Lateral septa thickness	4.38	0.02

Table S2. Morphological characters of *P. lobata* corallites with a significant conditional effect identified in the forward selection process of discriminant analyses (in order of significance). P = significance level based on 1000 permutations, Pseudo-F = the ratio of constrained and unconstrained total Inertia, each divided by their respective ranks (df =1 for all data), obtained from the *ordistep* function .

Characters	Pseudo-F	P
Ventral palus spacing	19.31	0.005
Lateral palus diameter	15.62	0.005
Corallite spacing	13.77	0.005
Septum length (lateral)	9.997	0.005
Ventral palus diameter	9.588	0.005
Ventral septa spacing	8.718	0.005

Figure S1. The relationship between *P. lobata* corallite morphology and genetics, as in Figure 12, with individual points labeled to show which pairs of samples were compared.